

AMERICAN UNIVERSITY OF BEIRUT

MULTISCALE INVESTIGATION OF THE IMPACT OF
FILLER ON ASPHALT CONCRETE BEHAVIOR

By

JALAL ANTOUNE KARAZIWAN

A thesis
submitted in partial fulfillment of the requirements
for the degree of Master of Engineering
to the Department of Civil and Environmental Engineering
of the Faculty of Engineering and Architecture
at the American University of Beirut

Beirut, Lebanon
April 2016

AMERICAN UNIVERSITY OF BEIRUT


MULTISCALE INVESTIGATION OF THE IMPACT OF
FILLER ON ASPHALT CONCRETE BEHAVIOR

by
JALAL ANTOUNE KARAZIWAN

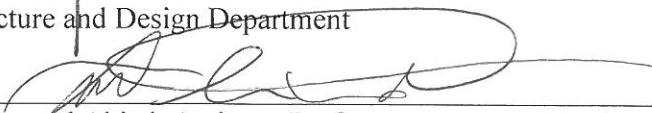
Approved by:



Dr. Ghassan Riad Chehab, Associate Professor Advisor
Civil and Environmental Engineering Department



Dr. Aram Yeretizian, Assistant Professor Member of Committee
Architecture and Design Department



Dr. Mohamad Abiad, Assistant Professor Member of Committee
Nutrition and Food Science Department

Date of thesis defense: April 21, 2016

AMERICAN UNIVERSITY OF BEIRUT

THESIS, DISSERTATION, PROJECT RELEASE FORM

Student Name: Karaziwan Jalal Antoine
Last First Middle

Master's Thesis Dissertation Master's Project Doctoral

I authorize the American University of Beirut to: (a) reproduce hard or electronic copies of my thesis, dissertation, or project; (b) include such copies in the archives and digital repositories of the University; and (c) make freely available such copies to third parties for research or educational purposes.

I authorize the American University of Beirut, **three years after the date of submitting my thesis, dissertation, or project**, to: (a) reproduce hard or electronic copies of it; (b) include such copies in the archives and digital repositories of the University; and (c) make freely available such copies to third parties for research or educational purposes.



Signature

10/5/2016

Date

ACKNOWLEDGMENTS

First of all, I would like to gratefully and sincerely thank my advisor, Professor Ghassan Chehab for his continuous guidance, understanding, patience, and help throughout the past two years of my graduate studies at AUB. Next, I would like to express my gratitude Professor Mohamad Abiad, and Professor Aram Yeretzian for providing me with their helpful guidance and insights and for the time they spent by serving on my committee.

Next, a special thank you for Mr. Helmi El-Khatib, the manager of the Civil Engineering Labs at AUB, for his help, support, and never ending guidance.

I want to thank Ms. Dima Al Hassanieh and Mr. Hussein Kassem for their continuous help in the lab work and for their valuable friendship. The help and technical assistance provided by the staff and graduate students at the Central Research Science Laboratory, Rheology lab, and the Structures and Materials lab at AUB, is highly appreciated especially that by Mr. Abdel Rahman Sheikh and Bashir Asyala and Jamil Bashir.

The encouragement, patience, sacrifices and care of my parents and my sister Jasmin, got me where I am now. Thanks to all their efforts and all their love; for that I will be indebted forever. Finally, thanks to all my friends who has been there for supporting, helping, and encouraging me.

AN ABSTRACT OF THE THESIS OF

Jalal Antoun Karaziwan for Master of Engineering
Major: Materials and Pavement Engineering

Title: Multiscale investigation of the impact of filler on Asphalt Concrete Behavior

This study evaluates the effect of different types of natural and by-product filler properties on asphalt mastics. Seven types of fillers, namely; Gabbro, Basalt, Limestone Lebanon, Limestone Qatar, Lime, Hydrated Cement, and Recycled Concrete Aggregate were blended with one type of binder. Extensive laboratory testing is considered, including filler characterization (surface analyzer, scanning electron microscope, X-ray diffraction, methylene blue value, etc.) and rheological testing of mastic (dynamic shear rheometer, multiple stress creep recovery, rotational viscometer). Furthermore, the asphalt mixes with different fillers were evaluated for moisture damage by ultra sound accelerated condition test which is energy based test evaluates the mix performance under moisture conditions. Finally, a statistical analysis was conducted to investigate the correlation between the filler properties and mastics performance. Furthermore, comparison between the filler properties and their mastics was conducted using Tukey post hoc analysis. The study results reveal that lime as filler significantly affect the resistance of moisture damage and rutting and fatigue cracking, in addition, the recycled concrete aggregate filler shows a higher performance compared to natural filler therefore, as a consequence, it is a sustainable and cost effective replacement solution. The prediction models for $|G^*|$ and J_{nr} show good agreement with testing data. Also, this study illustrates the considerable influence of the methylene blue value as indicator for mastics performance.

CONTENTS

ACKNOWLEDGEMENTS	v
ABSTRACT.....	vi
LIST OF ILLUSTRATIONS.....	x
LIST OF TABLES.....	xii

Chapter

1. INTRODUCTION.....	1
1.1.Problem Statement	1
1.2.Research Needs	1
1.3.Research Objectives and Significance.....	2
2. LITERATURE REVIEW	4
2.1.Introduction.....	4
2.2. The Functions of Filler in Mastic Performance	5
2.3. The Effect of Mastic in Mix Performance	7
2.4. Using of Recycled Concrete Aggregate	9
3. METHODOLOGY AND SCOPE OF RESEARCH.....	12
3.1. Material Used.....	12
3.1.2. Fillers Used	12
3.2. Filler Characterization.....	13

3.2.1. BET.....	13
3.2.2 Scanning Electron Microscope (SEM).....	13
3.2.3. Methylene blue value.....	16
3.2.4. X-ray Diffraction (XRD).....	16
3.2.5. Hydrometer.....	17
3.3. Mastic Testing.....	17
3.3.1. Linearity.....	17
3.3.2. Complex Shear Modulus Test.....	17
3.3.2. Multiple Stress Creep Recovery (MSCR).....	18
3.3.3. Rotational Viscometer:.....	18
3.4. Advanced Testing:.....	18
3.4.1. Modified Dynamic Shear Rheometer:.....	18
3.4.2. UAMC Ultrasonic Accelerated Moisture Conditioning.....	22
4. RESULTS AND ANALYSIS.....	27
4.1. Filler Characterization.....	27
4.1.1. BET.....	27
4.1.2. Scanning Electron Microscope (SEM).....	30
4.1.3. X-ray Diffraction.....	38
4.1.4. Hydrometer.....	40
4.1.5. Methylene Blue Value.....	41
4.2. Mastic Characterization.....	Error! Bookmark not defined.
4.2.1. Viscosity.....	42
4.2.2. Linearity.....	44
4.2.3. Complex Shear Modulus and Phase Angle.....	45
4.2.4. Multiple Stress Creep and Recovery (MSCR).....	47
4.3. Advanced Testing.....	50
4.3.1. Ultrasound Accelerated Moisture Conditioning.....	50

4.4. Analysis of Mastic Performance Vs. Filler Properties	54
4.4.1. Mineral Filler	54
4.4.2. Complex Modulus	57
4.4.3. Multiple Stress Creep Recovery:	63
4.4.4 Rotational Viscometer:.....	67
5. CONCLUSIONS AND FUTURE WORK	71
5.1. Conclusions.....	71
5.2. Recommendations and future work:.....	72
REFERENCES	74
Appendix	
A. EXPERIMENTAL PROCEDURES.....	76
B. PHOTOGRAPHS	79
C. RAW DATA.....	85

ILLUSTRATIONS

Figure	Page
1 User interface of ImageJ.....	16
2 Discs for MDSR RCA,RAP,Limestone (from the left).....	21
3 Example of limestone disc and disposal plate.	21
4 Schematic representation of the UAMC setup.....	23
5 Sample in the ultrasound water bath.	25
6 Sample submerged in water.....	25
7 Material lost on the bottom of ultrasound bath.	26
8 Conditioned sample after the UAMC testing.	26
9 TukeyHSD graph for surface area results.....	29
10 TukeyHSD graph for pore size results	30
11 SEM image of Basalt.....	31
12 SEM image of Gabbro.....	31
13 SEM image of Limestone Qatar.....	31
14 SEM image of Limestone Lebanon.	31
15 SEM image of Hydrated Cement.	32
16 SEM image of Lime.	32
17 SEM image for RCA.	32
18 SEM image for Gabbro.	33
19 SEM image for Basalt.	33
20 SEM image for Limestone Lebanon.	33
21 SEM image for Limestone Qatar.	33
22 SEM image for Hydrated Cement.	34
23 SEM image for Lime.	34
24 SEM image for RCA.	34
25 Example of image analysis.	35
26 Example of image analysis.	36
27 Figure 9 TukeyHSD graph for solidity results.....	37
28 TukeyHSD graph for circularity results	38
29 X-ray diffraction for the fillers	39
30 Fillers particle size distribution.....	40
31 Hydrometer analysis for different fillers	40
32 TukeyHSD graph for percentage finer than 15micron results	41
33 Viscosity versus Temperature for Different fillers.	43
34 TukeyHSD graph for rotational viscosity results at 135°	44
35 Linearity for filler.....	44
36 Values of $ G^* /\sin\delta$ versus Temperature for fillers.	45
37 TukeyHSD graph for DSR results at 52°C.....	46
38 TukeyHSD graph for DSR results at 76°C.....	47
39 Jnr results for fillers.	48

40 TukeyHSD graph for Jnr0.1 results	49
41 TukeyHSD graph for Jnr 3.2 results.....	50
42 UAMC testing results.....	51
43 TukeyHSD graph for UAMC results ,2hrs	52
44 $ G^* $ & $ G^* _{re}$ for Gabbro.	59
45 Log complex modulus vs temperature.	60
46 MBV linearity transformation.	60
47 Scatter plots for $ G^* _{at 64}$ vs filler properties	62
48 Scatter plots for Jnr0.1vs filler properties.....	65
49 Scatter plots for Jnr3.2vs filler properties.....	66
50 Scatter plots for RV 135 vs filler properties	69
51 Scatter plots for RV 165 vs filler properties	70

TABLES

Table	Page
1 Experimental Plan for Evaluating MDSR Test.....	20
2 Description of mixes and number of replicates for UAMC testing	24
3 Average value of the surface area and total pore size for different types of fillers investigated in this study	28
4 Average values of image analysis	36
5 Average Methylene Blue Value.....	42
6 Energy dissipated.....	51
7 Recommended filler properties.....	53
9 Controlled and response variables involved in this study	54
10 Average Properties of fillers	55
11 Correlation matrix for the properties of fillers.....	56
12 Average $ G^* $ and $ G^* _{re}$ for the filler	57
13 Correlation Matrix between Mastic Complex Modulus and Filler properties	58
14 Stepwise regression models for $ G^* $	61
15 Average values of J_{nr} & $J_{nr re}$ for different fillers	63
16 Correlation Matrix between J_{nr} 0.1&3.2 and Filler properties	63
17 Stepwise regression models for J_{nr}	64
18 Average RV & RV_{re} for Mastics.....	67
19 Correlation Matrix between Rational Viscosity and Filler properties.....	68

I dedicate this work to my parents

CHAPTER 1

INTRODUCTION

1.1. Problem Statement

Filler material, the fraction of fine aggregate passing No. 200 (75 μm) sieve, has commonly been used in asphalt mixtures and played an important role in the behavior of the asphalt mixture and the performance of the asphalt pavement (Zeng & Wu, 2008). This filler has a significant effect on stabilizing the asphalt concrete by filling the voids between the aggregates, and improving the consistency of the binder that cements the aggregates together. Furthermore, it can improve the workability, moisture sensitivity, stiffness and ageing characteristics of asphalt concrete.

Numerous studies have indicated that the addition of mineral filler to an asphalt binder increases the stiffness of the binder. The stiffening ratio and change in rheological properties have attracted researchers to report data and model the changes due to physical and sometimes mineralogical nature of fillers.

Hence, a proper understanding of the role of filler in asphalt mixture is needed to aid in predicting the performance of mastics and preventing the pavement from failing in early phases especially due to moisture damage.

1.2. Research Needs

Asphalt concrete is a composite material whose properties are sensitive to the quality, quantity, and/or distribution of its components being asphalt binder, aggregates, and air voids. The different portions of aggregates composed of coarse aggregates, fine

aggregates, and filler will be mixed together at given proportions with asphalt binder to produce a designed asphalt mixture.

In spite of the small proportion it represents in the mix being 3-6% of total the weight of the mix, the filler material has a critical importance in the performance of the designed asphalt concrete mix. Moreover, mineral filler has not been extensively investigated in the literature, in contrast of coarse and fine aggregates. Thus, there is a need to identify the effect of the type of filler material in an asphalt mixture. This research will investigate the use of different fillers in asphalt mixes and their different impact on the mastics properties.

1.3. Research Objectives and Significance

The research study herein focuses on characterizing the different properties of several types of fillers: Basalt (B), Gabbro (G), Limestone brought from Lebanese quarries (LL), Limestone brought from local quarries in Qatar (LQ), Recycled Concrete Aggregate (RCA), Hydrated Cement (HC), Lime (L). These fillers will then be investigated to study their influence in asphalt mixes performance, especially in moisture sensitivity failure. Thus, this research will explain the macro scale behavior of asphalt concrete mixes with different types of fillers.

These objectives will be achieved by completing the following set of tasks:

- Task one: Characterizing the different filler properties by Hydrometer analysis, Scanning Electron Microscope (SEM), Brunauer-Emmett-Teller (BET), X-ray Diffraction (XRD), Methylene Blue Value (MBV).
- Task two: Testing the rheology of mastics (Filler + Binder) in terms of complex shear modulus and by Multiple Stress Creep Recovery test (MSCR) by using

Dynamic Shear Rheometer (DSR) and dynamic viscosity using Rotational Viscometer.

- Task three: Assessing the effect of the investigated fillers on the mix design of asphalt concrete and testing the moisture sensitivity of these by performing Ultrasound accelerated moisture conditioning (UAMC) and modified dynamic shear rheometer.
- Task four: Statistical analysis of the filler characterization results with that of the mastic in order to determine filler properties that are sensitive to the mix's performance.

CHAPTER 2

LITERATURE REVIEW

2.1. Introduction

Filler is those material passing the 75 μm sieve in a mix. The two most important properties of mineral filler are geometry (size, shape, angularity) and composition.

Mineral fillers which are used in the pavement industry can be divided into two groups namely;

- Natural fillers: Andesite, Basalt, Caliche, Dolomite, Gabbro, Granite, and Limestone.
- By-product fillers: Fly ash, Slag, and Hydrated Lime (NCHRP 9-45).

However, the interaction between asphalt binder and filler is affected by a variety of chemical compounds such as calcite, quartz. The two main phenomenon of these interaction are the reactivity (calcium compound and water solubility) and the harmful fines (active clay content and organic content) (Bahia, Faheem, & Hintz, 2011).

The effect of filler on the properties of asphalt concrete has been studied by several researchers since the beginning of the 19th century. Two fundamental theories have emerged regarding the function of the filler: 1) Filler theory and 2) Mastic theory (Al-Abdulwahhab, 1981).

1) **Filler Theory**

The Filler theory assumes that “The filler serves to fill voids in the mineral aggregates and thereby creates a denser mix”. This theory holds that each particle of the

filler is individually coated with asphalt and that such coated particles, either discrete or attached to an aggregate particle, serves to fill the voids in between the aggregate.

2) **Mastic Theory**

The Mastic theory indicates that asphalt and filler combine together to form a mastic which fills voids and binds aggregate particles together into a dense mass. In this case, filler is in colloidal suspension.

2.2. The Functions of Filler in Mastic Performance:

Asphalt mastics are composite materials with asphalt binder and filler dispersed within it. Because the mineral filler fraction has a much higher surface area than the coarser aggregates in the mixtures, the physiochemical interaction between bitumen and fillers may be an important parameter in the mixture performance. The long-term performance of asphalt concrete mixes might be significantly affected by various properties of the filler including: particle size, filler gradation, surface texture, adsorption intensity, chemical composition, and particle's shape.

Many studies have continuously reported the effect of mineral filler on various properties of bitumen-filler mastics. One of the earliest studies to postulate the effect of filler on asphaltic materials is that conducted by Clifford Richardson in the beginning of 20th century (Richardson, 1905) which reported that certain types of fillers such as silica, limestone dust, and Portland cement adsorb relatively thicker film of asphalt. In 1912, Einstein studied the stiffness effect of fillers on composite matrices in which a coefficient was developed as an indicator of the rate of increase in stiffness of the matrix due to the incorporation of filler particles (Einstein, 1956)

Following the study conducted by Einstein, the stiffening effect of filler to the asphaltic materials had been the focus of many specialists in the asphalt field. In 1930, Traxler reported the important parameters in fillers with regard to their potential for stiffening the asphaltic materials. According to this study, size and size distribution of filler particles are the fundamental filler parameters as they affect the void content of filler. Also, this study considered the surface area of filler particles and their shape as the influential parameters governing the stiffening effect of filler to the asphaltic materials (Traxler, 1961).

In 1947, P. J. Rigden developed a new theory named the “fractional voids concept” which is the void volume in dry compacted fines. He considered the asphalt required to fill the voids in a dry compacted bed as “fixed asphalt,” while asphalt in excess of that amount was defined as “free asphalt”. According to the Rigden theory, the only factor affecting the viscosity of the filler-asphalt system is the fractional voids in filler. He has reported that other characteristics of fillers, and also asphalt properties are of less significant with regard to the viscosity of filler-asphalt system (Rigden, 1947).

Furthermore, Kallas and Krieger found out that a decrease in asphalt content to compensate for increasing densities may lead to greater pavement brittleness and a decline in pavement durability (Kallas & Krieger, 1960). Later, Kallas and Krieger they found that all mineral fillers, regardless of type of concentration, increase stability or strength properties of compacted asphalt paving mixtures when added up to a certain limit. They found that by changing the concentration of filler, stability increased and optimum asphalt content decreased; however, as more filler is added, these tend to reverse (kallas and puzinski). They also noted that in several instances finer fillers caused lower mixture viscosity than the coarser fillers at the same concentration level

Another study by Tunnicliff described the importance of filler particle size distribution as the main properties of filler affecting the filler-asphalt system. This study reported that there is a gradient of stiffening effect, which has a bigger value at the surface of the particle size, and becomes weaker with distance from the surface (Tunnicliff, 1962). In addition, Little and Petersen have reported the potential of hydrated lime filler to decrease the phase angle (δ), and thus improving resistance of mastic against loading. In this research, bitumen with different ageing condition was mixed with limestone and hydrated lime filler at the fixed concentration of 20%. Rheological results showed a significant increase in resistance to loading for mastics prepared with aged bitumen and hydrated lime (Little & Petersen, 2005).

Many other studies have also been performed to better understand the linear viscoelastic analysis of bituminous binders using a rheometer (Delaporte, Di Benedetto, Chaverot, & Gauthier, 2007; Yusoff, Shaw, & Airey, 2011). However, in 2010, Faheem and Bahia introduced a conceptual model for the filler stiffening effect on mastic. They postulated that the filler stiffening effect varies depending on the filler mineralogy and the concentration in the mastic (Faheem & Bahia, 2010). According to their study, the change in stiffness ($|G^*|$) as a function of the increase in filler concentration can be divided into two regions: diluted and concentrated regions.

2.3. The Effect of Mastic in Mix Performance:

To understand the properties of asphalt mixtures and their resistance to environmentally induced failure mechanisms, it is paramount to study not only asphalt binder and the asphalt mixture but also the mastic itself.

The asphalt mastic, or the combination of the asphalt binder and mineral filler in an asphalt paving mixture, has long been known to influence the overall performance of asphalt paving mixtures. The behavior of the asphalt mastic influences nearly every aspect of asphalt mixture design, construction, and performance. In the design of asphaltic paving mixtures, the mastic influences the lubrication of the larger aggregate particles and thus affects voids in the mineral aggregate, compaction characteristics, and optimum asphalt content. During construction of asphalt concrete pavements, the mastic must have enough stiffness to prevent drain-down, or the downward migration of the mastic mainly due to gravitational forces during storage and handling. This is particularly important in open- or gap graded mixtures, such as stone mastic asphalt (SMA) mixtures. Finally, the stiffness of the mastic affects the ability of the mixture to resist permanent deformation at higher temperatures and/or slow speeds, influences stress distribution and fatigue resistance at intermediate temperatures, and influences stress development and fracture resistance at low temperatures.

NCHRP Project 9-45 studied the effect of mastic on different parameters in asphalt mixtures. The researchers found that the viscosity of mastic related significantly to compatibility and mixture rutting resistance.

The most common mechanical properties used to characterize the mastics are:

- Complex shear modulus ($|G^*|$):

The sample's total resistance to deformation when repeatedly sheared.

- Phase angle (δ):

The lag between the applied shear stress and the resulting shear strain.

Purely elastic material: $\delta = 0$ degrees.

Purely viscous material: $\delta = 90$ degrees.

In order to resist rutting, an asphalt binder should be stiff (it should not deform too much) and it should be elastic (it should be able to return to its original shape after load deformation). Therefore, the complex shear modulus elastic portion, $|G^*|/\sin\delta$, should be large and according to AASHTO M320 the $|G^*|/\sin\delta > 1$ for binder at performance grade (PG) temperature. Moreover, in order to resist fatigue cracking, an asphalt binder should be elastic (able to dissipate energy by rebounding and not cracking) but not too stiff (excessively stiff substances will crack rather than deform-then-rebound). Therefore, the complex shear modulus viscous portion, $|G^*|\sin\delta$, should be a minimum.

2.4. Using of Recycled Concrete Aggregate

The increase in construction activities over the past two decades has resulted in an increase in the amounts of generated waste and a shortage in natural resources. This expansion in construction, combined with shortages in landfill space (particularly in urban areas), has proved to be a major threat to the environment and the atmosphere.

Lebanon, like many developing countries, has suffered from increased volume of construction and demolition waste, and shortage of natural aggregate resources.

Since the early 1980's, the recycling and re-usage processes have become more common in most developing countries, and authorities have been fighting to implement reasonable and safe recycling measures in the construction industry. This is why, in developing countries, the major part of the waste materials meets the technical properties for reuse after being appropriately processed.

In the past ten years, Lebanon witnessed a wide development campaign in the construction field. There is an increasing pressure on the construction industry to reduce

costs and improve the quality of our environment. But the fact is that both of these goals can be achieved at the same time. Although construction and demolition constitute are a major source of waste in terms of volume and weight, their management and recycling efforts have not yet seen the light in Lebanon.

Therefore, looking at the natural resources, one must think of ways to ensure that these resources do not deplete. Hence, the need to consider aspects like recycling is essential especially in the construction sector.

The effective utilization of waste cement concrete is to gain recycled concrete aggregate (RCA), which can be reused in Portland Cement Concrete or Asphalt Concrete.

Most investigations focus on the coarse proportion of RCA. To use RCA in Portland Cement Concrete and asphalt mixes have been reviewed and discussed (Mills-Beale & You, 2010; Paravithana & Mohajerani, 2006; Rahal, 2007). However, the production of RCA is accompanied with a large amount of fine aggregates (<1.18 mm) and powders, which will cause detrimental effects on the fresh and hardened properties of concrete, and thus cannot be reused in concrete cursorily (Hansen, 2004; Poon, Qiao, & Chan, 2006) . The fine waste is mainly composed of cement mortar and aggregates, these are which remained unused (Wong, Sun, & Lai, 2007) and buried in suburbs usually, consequently worsen environmental pollution.

However, the reuse of fine waste aggregates has been reported as granular road materials and substitutive aggregates in asphalt mixture.

Park reported that both coarse and fine RCA can be used as base and sub-base materials in pavement (Park, 2003).

Poon et al. investigated the influence on the self-cementing properties of using fine RCA powder (<0.6 mm) for sub-base. They concluded that the self-cementing

property was determined by the un-hydrated cement in waste cement mortar, effect of which can be neglected on the performance of the overall sub-base materials prepared with RCA (Poon et al., 2006).

Wong et al. investigated the feasibility of using fine waste concrete aggregates (<3 mm) as partial substitution granite aggregates in asphalt mixes and the conclusion was affirmative. However, it is noted that the optimum asphalt content was 1.2% higher than that of conventional mixture with fine waste aggregates was 45% of fine granite aggregates(Wong et al., 2007).

Therefore, it is uneconomical to use fine recycled aggregates as substitutive aggregates. Based on the previous researches, to find more effective and reliable ways for reusing the fine waste aggregates is crucial, and thus enlarging the application of construction and demolition waste and environment friendly.

CHAPTER 3

METHODOLOGY AND SCOPE OF RESEARCH

The following section presents the materials used for conducting this study, an explanation of the BET, XRD, SEM, and MBV methods used to obtain the micro properties of the fillers as well as the DSR, MSCR, Rotational Viscometer and Modified DSR to obtain the performance of the mastic. Finally, UAMC was conducted to obtain the performance of the mixes with different fillers.

3.1. Material Used

The natural aggregates used in the asphalt mixtures consist of Limestone aggregates from Lebanon. The bulk specific gravity of the aggregate, G_{sb} , and the absorption are required for volumetric calculation of compacted asphalt concrete. Testing is done according to ASTM C127-12 and C128-12 respectively.

The asphalt binder was obtained from ARACO, a local asphalt concrete plant. It is unmodified asphalt which is commonly used in all mixtures and regions in Lebanon. The mixing and compaction temperatures used were 150°C and 140 °C respectively based on the viscosity result. Asphalt binder properties are studied by conducting complex shear modulus according to ASTM D7175-08. Moreover, the non-recoverable strain is calculated from the multiple stress creep and recovery test according to ASTM D7405.

3.1.2 Fillers Used

The different fillers used were obtained from Qatar and Lebanon. Gabbro (G) and limestone (LQ) filler were brought from Qatar, while Basalt (B) and Limestone (LL)

filler were brought from Lebanon, in addition to Lime (L) and Hydrated Cement (HC) and Recycled Concrete Aggregate (RCA). The recycled concrete filler was obtained by crushing and sizing bulks of crushed Portland cement concrete taken from a 50 year-old demolished building in Beirut. All the used fillers are passing the #200 sieve.

3.2. Filler Characterization

3.2.1. BET

The BET method is the most widely used procedure for the determination of the surface area of solid materials and involves the use of the BET equation.

$$\frac{1}{W\left(\frac{P}{P_0}\right)-1} = \frac{1}{W_m C} + \frac{C-1}{W_m C} \left(\frac{P}{P_0}\right) \quad (1)$$

where W is the weight of gas adsorbed at a relative pressure; $\frac{P}{P_0}$, and W_m is the weight of adsorbate constituting a monolayer of surface coverage. The term C , the BET C constant, is related to the energy of adsorption in the first adsorbed layer and consequently its value is an indication of the magnitude of the adsorbent/adsorbate interactions.

3.2.2. Scanning Electron Microscope (SEM)

The Morphology of the filler surface was studied using SEM. In the images produced by SEM, the electron beam interacts with atoms in the sample in order to produce signals that contain information about the surface relief of the aggregate. Specimens are imaged with a beam of electrons, but instead of the electrons being transmitted through the specimen, the beam is "scanned" across, creating an image of the surface of the sample, with exceptional depth of field. This image is achieved via the

detection of "secondary" electrons that are released from the specimen as a result of it being scanned by very high energy "primary" electrons (i.e. those emitted from the electron "gun" in the SEM).

SEM shows the true texture of each sample, without confusing it with the appearance of colors, which allows one to quantitatively measure and comparatively evaluate aggregates from different sources.

The samples are mounted on a stub of metal with adhesive, coated with 40-60 nm of metal such as Gold/Palladium and then observed in the microscope, we use in this study "TESCAN, VEGA 3 LMU with OXFORD EDX detector (INCA XMAW20)". Moreover, in this study, shape properties of the fillers were compared using image analysis by determining the shape characteristics of aggregates such as aspect ratio, roundness, shape factor, and sphericity.

To properly characterize the form of an aggregate particle, Circularity, Aspect ratio, Roundness, Solidity, Ferit's micron were proposed as imaging indexes for the SEM images.

Circularity:

Circularity compares the perimeter of an equivalent circle to the perimeter of the particle. An equivalent circle has the same area as the particle. Because angularity and texture influence the perimeter of a particle, it follows that form factor not only influenced by particle form but also reflects angularity and texture as well. Circularity has been used to describe surface irregularity and is defined as follow:

$$\mathbf{Circularity} = 4\pi \frac{[Area]}{[Perimeter]^2} \quad (2)$$

With a value of 1.0 indicating a perfect circle. As the value approaches 0.0, it indicates an increasingly elongated shape.

Aspect Ratio:

The aspect ratio of the particle's fitted ellipse.

$$\mathbf{AR} = \frac{\mathbf{Major\ Axis}}{\mathbf{Minor\ Axis}} \quad (3)$$

Roundness:

$$\mathbf{Roundness} = 4 \frac{[\mathbf{Area}]}{\pi[\mathbf{Major\ Axis}]^2} \quad (4)$$

This is a shape factor that has a minimum value of 1 for a circle and larger values for shapes having a higher ratio of perimeter (P) to area (A), longer or thinner shapes, or objects having rough edges.

Solidity:

Solidity is the ratio of area of the 2-dimensional projection of the aggregate particle to the convex area. The convex area can be defined as the area enclosed by an imaginary "string" wrapped around the object. Solidity has values in the range 0 to 1. A low solidity towards 0 indicates a rough particle edge. A high solidity of 1 indicates a smooth particle edge

$$\mathbf{Solidity} = \frac{\mathbf{Area}}{\mathbf{Convex\ Area}} \quad (5)$$

Feret's diameter:

The longest distance between any two points along the selection boundary, also known as maximum caliper. We used in this study Image J software which is an open source image processing program designed for scientific multidimensional images, Figure 1 shows the user interface of this software. Multiple steps were followed in analysis the images you can find it in Appendix (A).

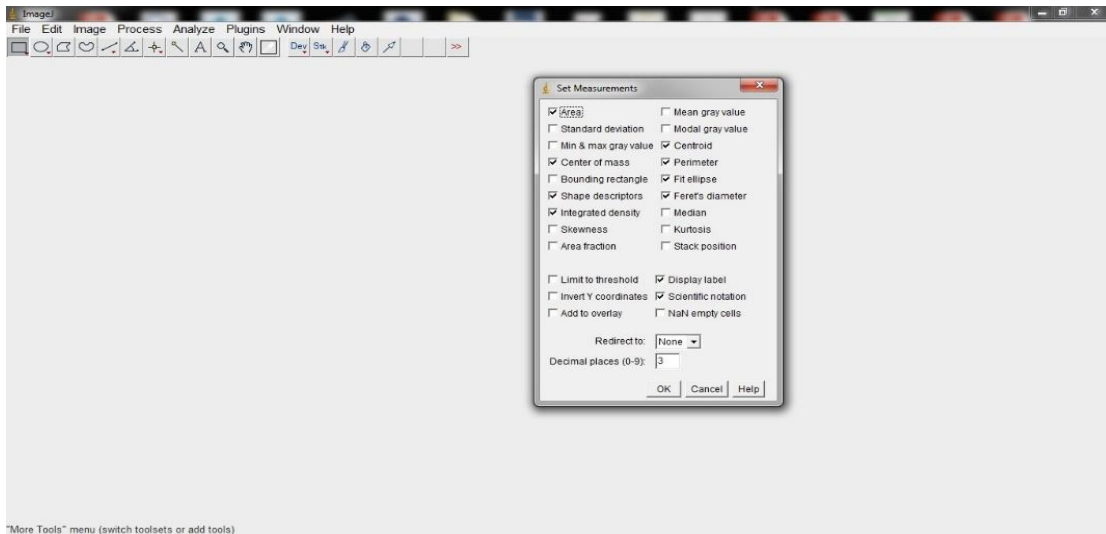


Figure 1 User interface of ImageJ

3.2.3. Methylene blue value:

The presence of clay particles in the fine aggregate portion of asphalt mixes may induce stripping in the mix when exposed to water or moisture. This test undertaken for determining the plastic fines in the fine aggregate, which may induce stripping in asphalt concrete mixtures according to Nevada test method T503A testing procedure.

3.2.4. X-ray Diffraction (XRD):

X-ray diffraction (XRD) analysis was used to characterize the crystallographic structure of fillers. “XRD D8 ADVANCE BRUKER” was used in this study. In addition, ORIGIN software was used for the analysis of results and the comparison of the intensity peaks compounds for different fillers.

3.2.5. Hydrometer

The hydrometer method for the analysis of the particle size distribution of fillers that were used according to ASTM D422. This method is simple method that requires inexpensive equipment and basic technical expertise.

3.3. Mastic Testing

In order to better understand the behavior of the mix, the rheological properties of the mastic were studied. Two replicates were used to determine the mechanical properties of the different mastics. The sample used had a diameter of 25mm and a thickness of 1mm. All mastics were produced at a 1:1 mixing ratio of filler to binder by mass. This blending concentration corresponds to the typical filler concentration in asphalt mixes. In addition, the NCHRP project 9-45 conducted at the University of Wisconsin-Madison proposed this concentration in its work plan as the testing filler to binder ratio to study the filler effect on asphalt binder.

3.3.1. Linearity

A linearity check was first performed on all mastics in order to confirm linear viscoelastic behavior. Linearity tests were performed at 64° C with 10 rad/s angular frequency, strain ranging from 2% to 16% and 2% increment.

3.3.2. Complex Shear Modulus test

After confirming the mastics linear viscoelastic behavior, oscillatory test was conducted in order to determine the dynamic shear modulus ($|G^*|$) and the phase angle(δ) in order to analyze the rutting factor ($|G^*|/\sin \delta$) and performance grade, the DSR test was conducted according to ASTM 7175-08. The tests were conducted under 52,58,64,70 and 76° C with 12% strain and angular frequency ranging from 100 to 0.1

rad/sec. To identify the performance grade, values of $(|G^*|/\sin \delta)$ should exceed 1 at 10 rad/sec.

3.3.2. Multiple Stress Creep Recovery (MSCR)

The MSCR tests were conducted following ASTM D7405. The temperature used for the Mastics were those identified at the performance grade. Stress levels of 100 Pa and 3200 Pa were used with creep time of 1 second and recovery time of 9 seconds, repeated 10 times each.

3.3.3. Rotational Viscometer

The viscosity tests were conducted following ASTM D 4402. The temperature ranged from 120°C-180°C at increments of 15 °C. The viscosity results indicate the ease of mixing and compaction temperature.

3.4. Advanced Testing

3.4.1. Modified Dynamic Shear Rheometer:

Most of the techniques used today to evaluate practically moisture damage in asphalt pavements are involved on compacted asphalt mixes. These tests generally simulate field conditions, and provide a performance-related parameter of moisture effects by applying mechanical techniques. No test of the compacted mixtures, however, can isolate the fundamental and rheological properties of the asphalt-aggregate bond, which hinder proper understanding and quantification of the moisture damage phenomenon. To avoid these complications and improve the evaluation of asphalt-aggregate interfacial properties in moist situations, this study proposes a new experimental method used by Bahia et al. (Cho & Bahia, 2010). In this method,

dynamic shear rheometer was used to measure asphalt-aggregate interfacial properties. A degree of moisture damage relating to the interfacial properties was then quantified using linear viscoelastic concepts to propose a meaningful parameter, called wet to dry yield shear stress ratio.

The experimental design is based on modification of the standard DSR test. Cored disks 25 mm in diameter and 5 mm thick are used as the substrates for adhering asphalts. The disks are glued on the DSR metal spindle and the base metal plate as shown in Figure 3. The disks and asphalt binder simulate the asphalt-aggregate interface in asphalt mixtures. A water cup that was fabricated specially for the DSR is used to allow continuous water access to the interface. Stress sweep facilitates measuring the changes in the rheological properties of the asphalt as it responds to gradually increasing stress conditions. Using the DSR in this study has many advantages, such as loading rate control, precise film thickness, and temperature control. Most importantly, it allows a fundamental study of moisture effects where the effects of moisture are isolated and not confounded by mixture voids, variable film thickness, and different sizes of aggregates. Super Glue –Putty Epoxy was used to bond cored rock disks to the upper spindle and the bottom plate of DSR. The epoxy's temperature range is -10 to 135 °C. For water conditioning of the interface between a rock disk and asphalt binder, a plastic water cup was fabricated whose dimension is 50 mm in inner diameter and 60 mm outer diameter, and 27 mm outer in height and 20 mm inner. In order to clean the used epoxy with heat in an oven, a disposal spindle was used, whose cylinder part can easily be screwed in and out of the shaft part but is secure enough screwed in.

MATERIALS AND EQUIPMENT

Three types of discs were selected: 1) Limestone aggregate - 2) Recycled Asphalt Pavement- 3) Recycled Concrete Aggregate . The Limestone aggregate was selected because it simulates what is typically used in Lebanon roadways, the Recycled Asphalt Pavement was selected to simulate the overlay process, finally, Recycled Concrete Aggregate was selected to investigate the failure of coarse recycled concrete aggregate in moisture damage. Seven different mastics were selected for testing with similar Performance Grades (PG 64-10). Table 1 shows the overall testing plan used for conducting the DSR moisture damage test in this research. The variables for this research are discs types and mastics types.

Table 1 Experimental Plan for Evaluating MDSR Test

Testing Task	Material Variables		Number of Replicates
	Contact Material	Type of Mastic	
T1	Limestone	Binder -control	3
T2	Recycled Concrete Aggregate	Binder -Control	3
T3	Recycled Asphalt Pavement	Binder-Control	3
T4	Limestone	Gabbro+Binder	3
T5	Recycled Concrete Aggregate	Gabbro+Binder	3
T6	Recycled Asphalt Pavement	Gabbro+Binder	3
T7	Limestone	Basalt+Binder	3
T8	Recycled Concrete Aggregate	Basalt+Binder	3
T9	Recycled Asphalt Pavement	Basalt+Binder	3
T10	Limestone	LL+Binder	3

T11	Recycled Concrete Aggregate	LL+Binder	3
T12	Recycled Asphalt Pavement	LL+Binder	3
T13	Limestone	LQ+Binder	3
T14	Recycled Concrete Aggregate	LQ+Binder	3
T15	Recycled Asphalt Pavement	LQ+Binder	3
T16	Limestone	Hydrated Cement + Binder	3
T17	Recycled Concrete Aggregate	Hydrated Cement + Binder	3
T18	Recycled Asphalt Pavement	Hydrated Cement + Binder	3
T19	Limestone	RCA + Binder	3
T20	Recycled Concrete Aggregate	RCA + Binder	3
T21	Recycled Asphalt Pavement	RCA + Binder	3
T22	Limestone	Lime + Binder	3
T23	Recycled Concrete Aggregate	Lime + Binder	3
T24	Recycled Asphalt Pavement	Lime + Binder	3



**Figure 2 Discs for MDSR
RCA,RAP,Limestone (from the left).**



**Figure 3 Example of limestone disc and
disposal plate.**

3.4.2. UAMC Ultrasonic Accelerated Moisture Conditioning

Ultrasonic accelerated moisture conditioning (UAMC) was used by several researchers as a quantitative analysis to evaluate the moisture sensitivity of asphalt concrete mixture (McCann, Anderson-Sprecher, Thomas, & Huang, 2006). This method was used in this study to assess the effect of different filler types. UAMC is accomplished by containing a loose sample of asphalt concrete on a sieve in 60°C water bath while subjecting the sample to ultrasonic energy. As the asphalt strips from the surface of the aggregate, small particles of the mix are released and drop through the sieve. The percent of material lost from the sample is recorded for five hours and plotted with respect to conditioning time. The slope of a linear regression function that is fit to the data represents the rate at which the small particles are released as the asphalt recedes along the surface of the aggregate. Seven mixes with seven different filler types were subjected to UAMC and replicate samples were used.

Test objectives:

- 1) To test if a relationship exists between loss of material and the time of asphalt mix sample is subjected to ultrasonic conditioning for the same mix gradation with different filler and asphalt content.
- 2) To determine if a correlation exists between test results obtained using the UAMC procedure and other moisture damage test or indicator.

Test hypothesis:

The loss of material is proportional to the length of time an asphalt concrete sample is subjected to ultrasonic conditioning. Ultrasonic conditioning will recognize the effect of different types of fillers on moisture damage.

Experimental Design:

The experimental design is based on modification of McCann et al experiment. A typical asphalt concrete loose mix was prepared in accordance with AASHTO T209, after that we sieved the loose mix and we prepared a sample with the same gradation of the mix from size 12.5 to # 16.

Materials and Equipment:

- Ultrasonic bath (sonication)
- Balance with accuracy 0.01 gr
- #16 sieve mesh (1.16mm)
- Syringe and water heater
- Tabletop with hook
- Distilled water
- Vacuum oven

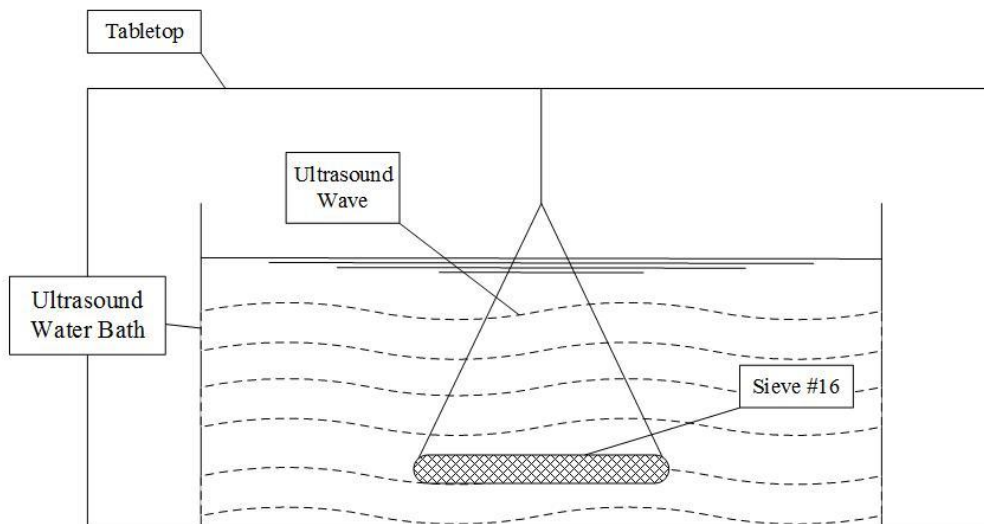


Figure 4 Schematic representation of the UAMC setup

Experimental Plan for Evaluating UAMC Experiment:

One gradation for the seven loose asphalt concrete mixes was used with seven different filler types, furthermore, the optimum asphalt content was determined by mixing and compacting trial asphalt concrete specimens using the Superpave gyratory compactor (SGC). The variables incorporated in this experiment were filler type and asphalt content.

Table 2 Description of mixes and number of replicates for UAMC testing

Testing Task	Materials Variables		Number of Replicates
	Filler Type	Asphalt Content	
T1	G	3.85	2
T2	B	3.85	2
T3	LL	3.9	2
T4	LQ	3.9	2
T5	L	4.3	2
T6	HC	4.1	2
T7	RCA	3.95	2

Description of UAMC testing protocol:

As we know, the ultrasonic intensity distribution inside an ultrasonic bath is not homogeneous. However, simple, rapid methods have been adopted to locate the position that has the highest intensity of sonication. The aluminum foil test is the easiest method that can be applied in the laboratory. Using a series of aluminum foil sheets the most intense zones of sonication inside the bath can be quite accurately identified. As

consequence of cavitation, the aluminum foils are perforated. The maximum perforation occurs at maximum intensity. Obviously, the sieve should be located at the point where the maximum sonochemical effect achieved.

After that, the sample was obtained from a loose mix following the format of AASHTO T248 and preparation of the loose mix was in accordance with AASHTO T-209 and cured the sample for 2 hours at 149° C, the sample was removed from the oven and stored at room temperature until the sample cooled to room temperature and then, was sieved on number 16# sieve the sample and placed in a glass dish containing distilled water. The submerged sample will be placed in a vacuum oven to maintain the 60 °C temperature and degassed at – 0.8 bar for 15 minutes. After that the sample will be removed from the oven and the syringe will be used for expelling the retained air bubbles on the sample.



Figure 5 Sample in the ultrasound water bath.



Figure 6 Sample submerged in water.

The sample will be transferred to the sieve that is already in water bath and make sure to keep the water level over the sample to avoid the formation of air bubbles again. Each replicate consists of four samples that were conditioned for (2,3,4 and5) hours



Figure 8 Conditioned sample after the UAMC testing.



Figure 7 Material lost on the bottom of ultrasound bath.

CHAPTER 4

RESULTS AND ANALYSIS

In this chapter, the results of the conducted tests will be presented to characterize the different materials used in this study, namely; asphalt binder, aggregates, filler and mastic (filler + asphalt). As mentioned previously, several types of experiments were conducted on the various types of fillers; furthermore, statistical analysis was conducted in order to investigate the effect of filler on the mix performance.

4.1 Filler Characterization:

4.1.1 BET:

The surface area for each type of fillers is calculated based on the BET testing as presented in (The results show that lime, RCA and hydrated cement have the highest surface area while LQ has the lowest. Moreover, the basalt shows a big surface area when compared to natural filler (**Error! Not a valid bookmark self-reference.**)). The BET results reveal that some fillers might require more asphalt binder to be coated and fill the filler's voids than others due to the difference of the surface area between one type of filler and the another. This finding was confirmed when the optimum asphalt contents of mixes with different types of fillers were investigated.

Table 3). The results show that lime, RCA and hydrated cement have the highest surface area while LQ has the lowest. Moreover, the basalt shows a big surface area when compared to natural filler (**Error! Not a valid bookmark self-reference.**). The BET results reveal that some fillers might require more asphalt binder to be coated

and fill the filler's voids than others due to the difference of the surface area between one type of filler and the another. This finding was confirmed when the optimum asphalt contents of mixes with different types of fillers were investigated.

Table 3. Average value of the surface area and total pore size for different types of fillers investigated in this study

<u>Filler</u> <u>Type</u>	<u>Surface</u> <u>area (m²/g)</u>	<u>Total pore</u> <u>volume (cc/g)</u>
L	8.11	0.0341
HC	9.80	0.0412
G	4.70	0.0228
LL	4.59	0.0181
LQ	2.81	0.014
B	10.81	0.0315
RCA	11.47	0.0554

A one-way analysis of variance (ANOVA) was conducted to check if there is any significant difference in the surface area and pore size between the different types of filler. This is coupled with conducting the TukeyHSD post hoc test to rank the fillers based on their surface area and pore volume. As shown in Figure 10 and Figure 9 , The mean difference used as criteria to compare the filler combination as the mean difference has low value as the combination studied do not differ significantly. For example, LL-LQ, LL-G, RCA-HC and HC-L filler combinations have the lowest mean difference and their non-statistical difference between their values. Moreover, a

conclusion has been drawn by comparing the two figures that the pore size volume and surface area are very similar, in addition the surface area increasing coupled with pore volume increasing as a result the pore volume size is the responsible for the increasing the surface area. Finally, the surface area and pore size values divide the filler into two groups, natural filler with low surface except Basalt and pore size value and by-product filler with high values.

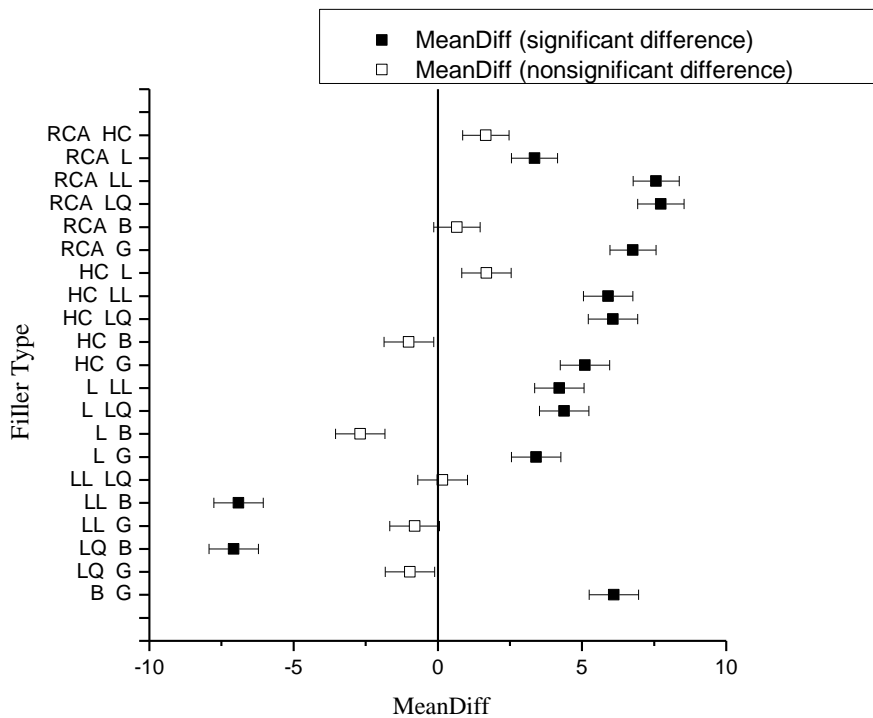


Figure 9 TukeyHSD graph for surface area results

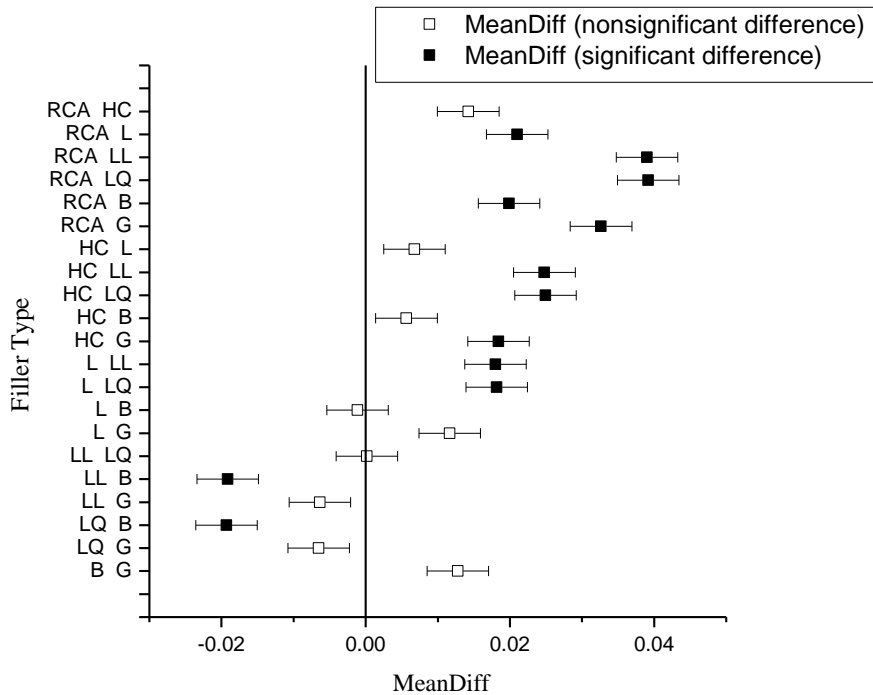


Figure 10 TukeyHSD graph for pore size results

4.1.2 Scanning Electron Microscope (SEM)

The results stated in BET can be revealed in the microscopic images of all the fillers. As shown in (Figure 11, Figure 12), the SEM images clearly illustrates that the surface of the Gabbro and Basalt is smooth while that of RCA, Hydrated cement are much rougher and include more pores thus leading to higher surface area.

In addition, the SEM images shown in Figure 21 and Figure 13 for the Limestone Qatar show the presence of fiber on the surface of aggregate which represent of Halloysite clay that affect the moisture damage of the Limestone Qatar filler mix.

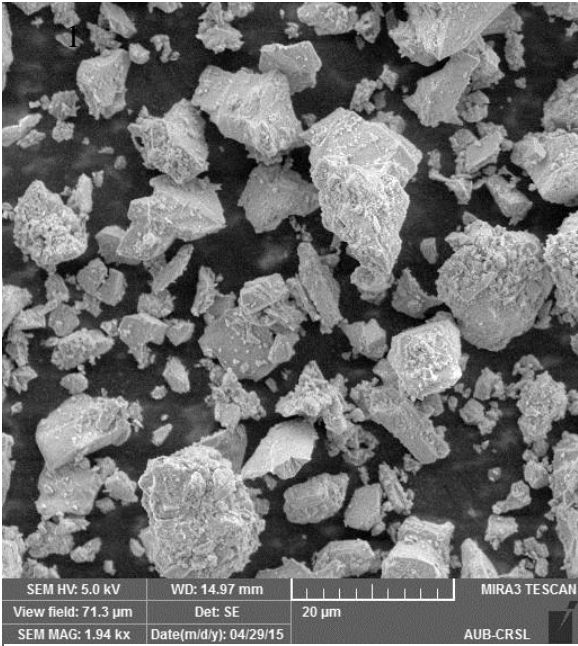


Figure 11 SEM image of Basalt.

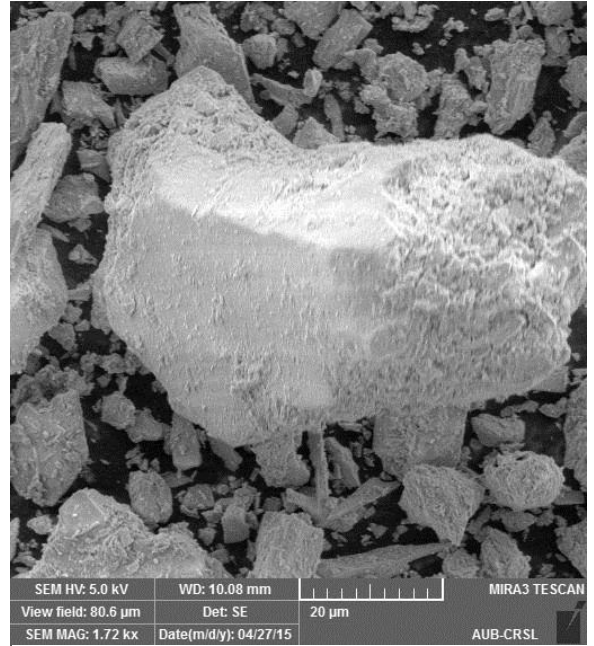


Figure 12 SEM image of Gabbro.

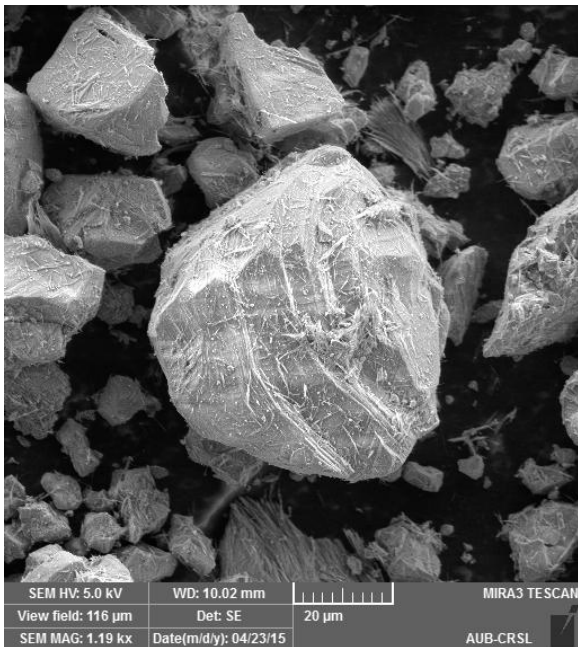


Figure 13 SEM image of Limestone Qatar.

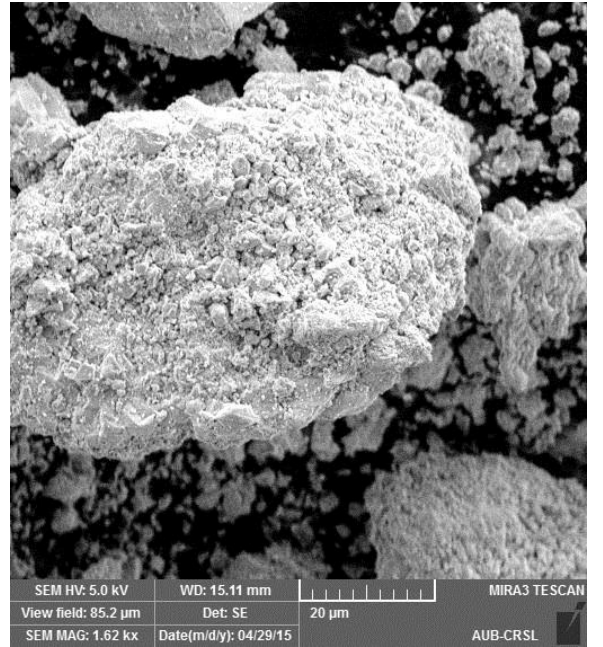


Figure 14 SEM image of Limestone Lebanon.

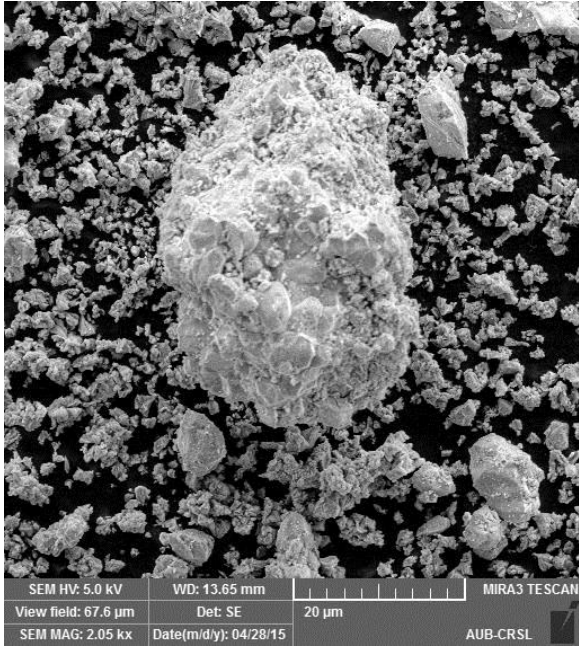


Figure 16 SEM image of Lime.

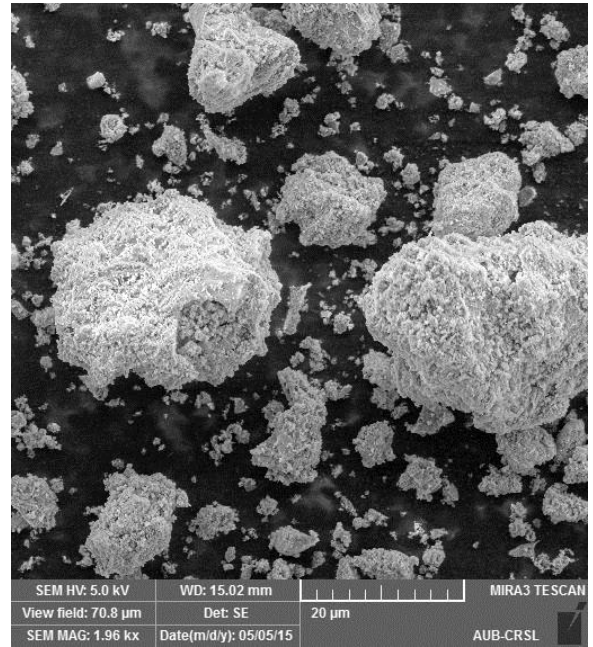


Figure 15 SEM image of Hydrated Cement.

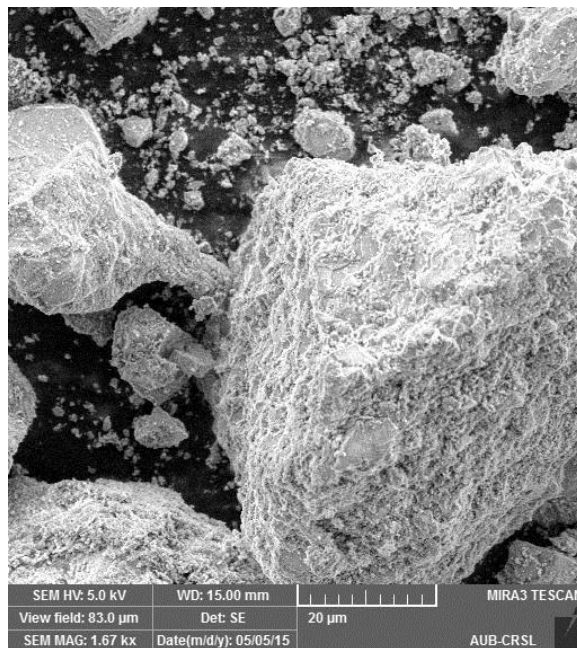


Figure 17 SEM image for RCA.

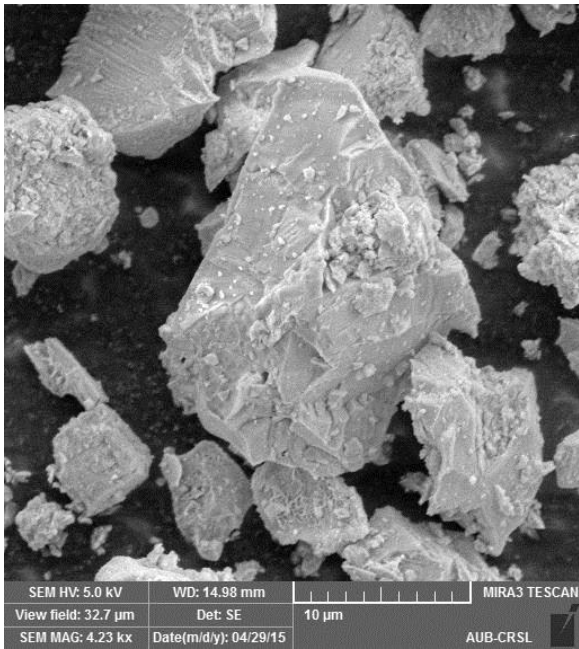


Figure 19 SEM image for Basalt.



Figure 18 SEM image for Gabbro.

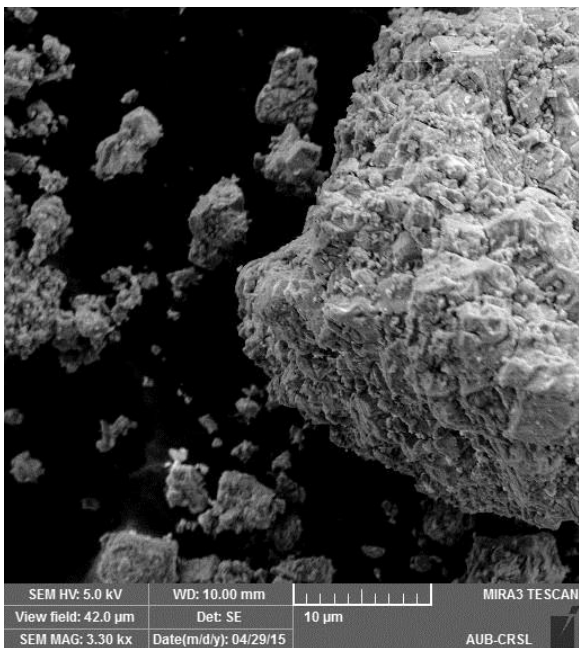


Figure 20 SEM image for Limestone Lebanon.

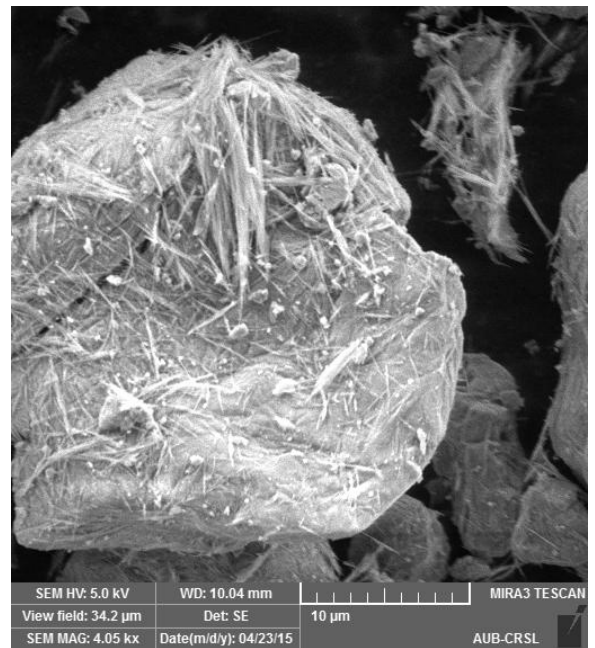


Figure 21 SEM image for Limestone Qatar.

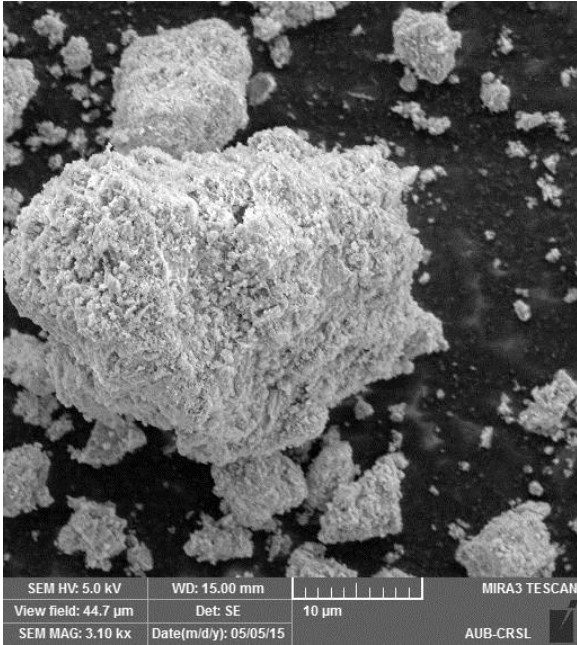


Figure 22 SEM image for Hydrated Cement.

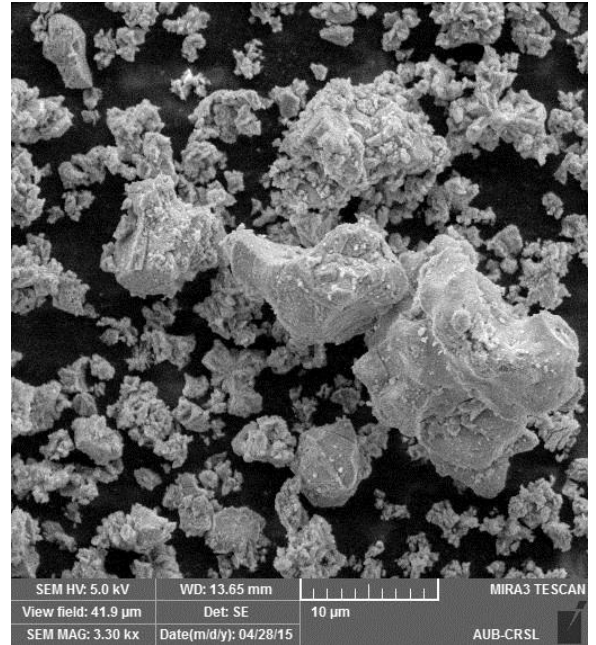


Figure 23 SEM image for Lime.

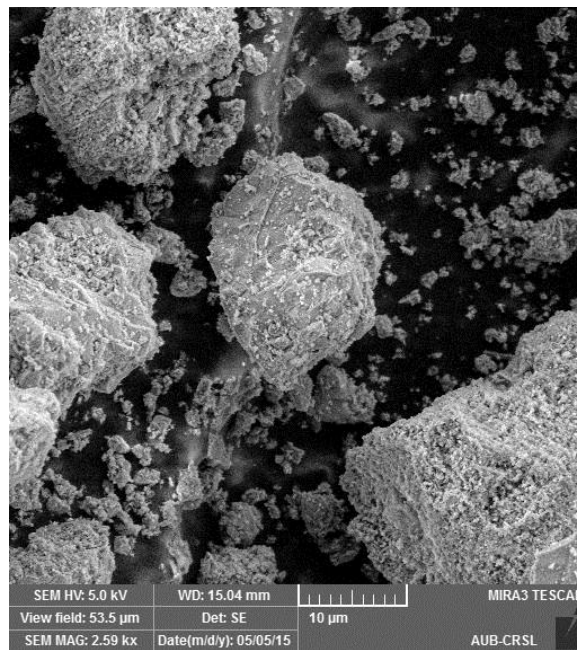


Figure 24 SEM image for RCA.

From the images in the figures above, the difference in surface texture between the different fillers can be observed. Gabbro and Basalt have a smoother surface texture than other samples. The dominant difference between RCA, Hydrated cement and other fillers is the presence of the smaller particles on the surface of the grains.

Particle shape analysis was carried out using some shape properties of aggregate. The average values for each shape properties are listed in

Table 4. The results showed that there exist distinct morphological characteristics for different filler aggregate shapes (i.e., AR, Roundness, Circularity,...etc.). These shape indices give us a conception of the packing behavior for the different filler types which related to Rigden Voids experiment that have a high correlation with asphalt mastics performance as has been stated in the literature.

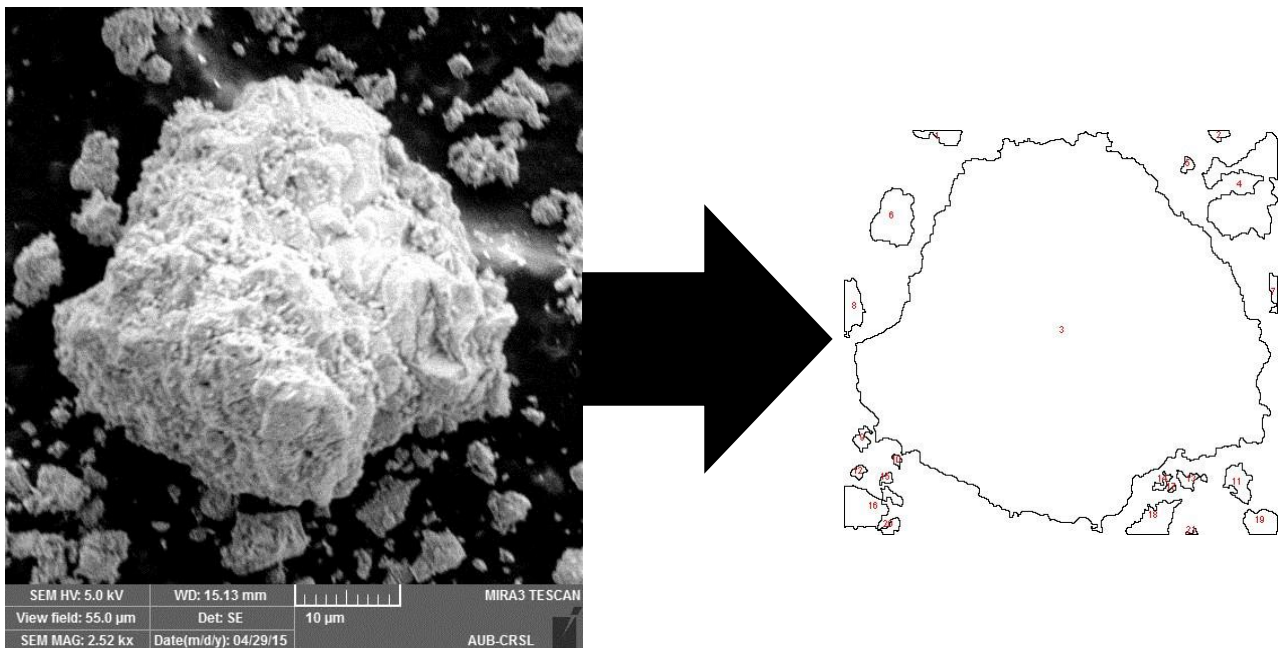


Figure 25 Example of image analysis.

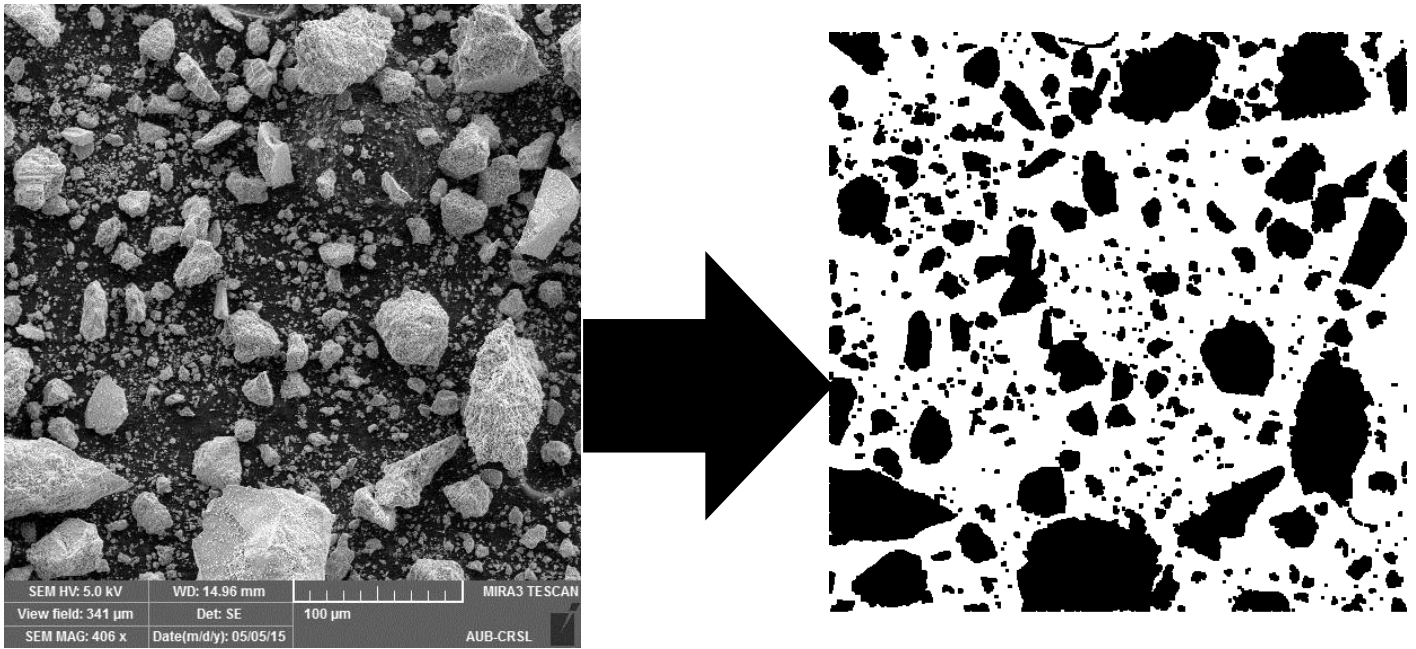


Figure 26 Example of image analysis.

Table 4 Average values of image analysis

<u>Filler type</u>	<u>Circ.</u>	<u>Ar</u>	<u>Round</u>	<u>Maximum Aggregate Size (micron)</u>
B	0.453	1.501	0.673	91.29
G	0.486	1.419	0.712	73.71
LQ	0.598	1.149	0.872	85.49
LL	0.450	1.366	0.773	76.34
L	0.346	1.503	0.690	17.53
RCA	0.300	1.244	0.822	94.78
HC	0.362	1.319	0.759	70.99

One-way ANOVA for the shape indices shows non-significant differences for aspect ratio and roundness, in contrast, the solidity and circularity show significant difference so we can use them as shape descriptor for filler properties.

TukeyHSD was conducted for both solidity and circularity as shown in Figure 27 and Figure 28. The circularity and solidity results show clearly difference between the natural filler and byproduct filler. The natural filler has smooth edge while the byproduct filler has rough edge, in addition the shape of natural filler is more close to circle than byproduct filler.

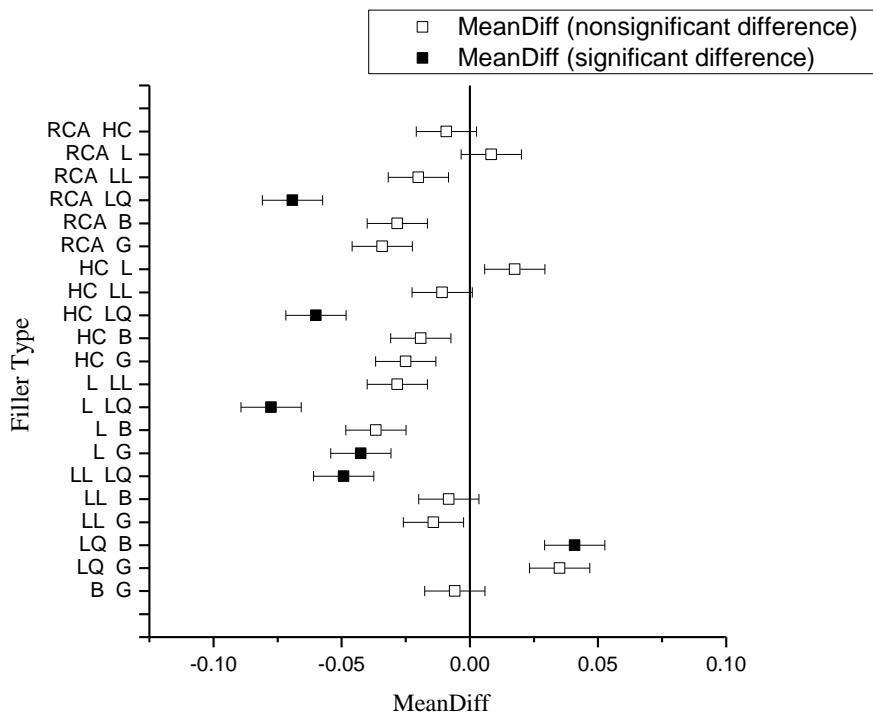


Figure 27 Figure 9 TukeyHSD graph for solidity results

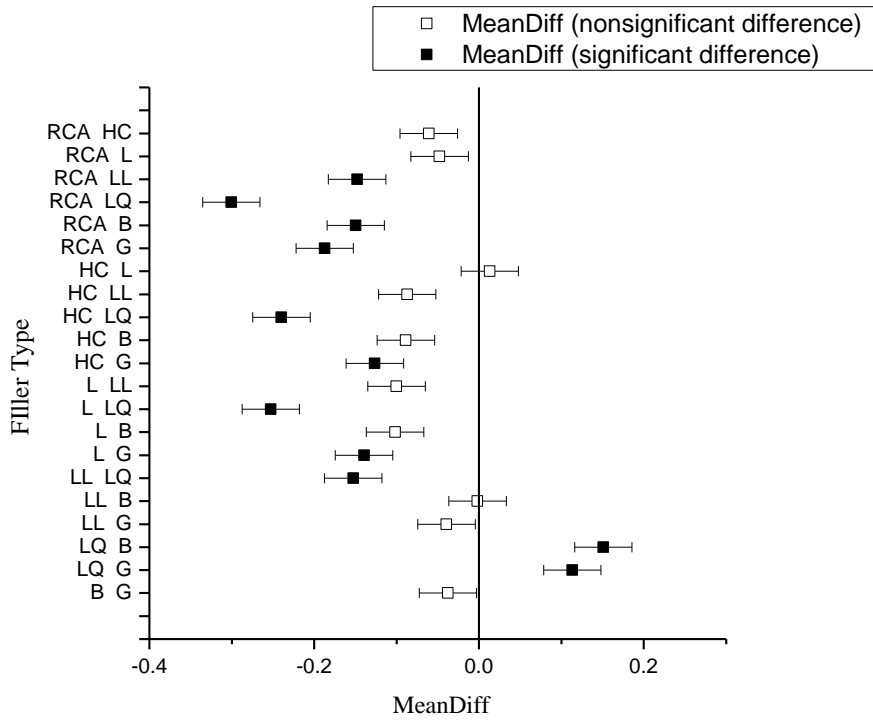


Figure 28 TukeyHSD graph for circularity results

4.1.3 X-ray Diffraction

Figure 29 shows the chemical and mineralogical composition of the seven tested fillers from the XRD test results. As shown in Figure 29, Limestone Qatar, and Limestone Lebanon, Lime, Hydrated Cement and Recycled Concrete Aggregate show calcite in their mineralogical composition.

In the case of Hydrated Cement and RCA, Calcite and Silica were found in their composition, which is an indication that RCA is mainly composed from hydrated cement. Therefore, because the quartz usually has a poor adhesion with the binder (Bagampadde, 2004), it is expected that the adhesion of RCA filler with the bitumen is not satisfactory. Conversely, the Basalt and Gabbro contain other mineralogical compounds like Sodium and Magnesium.

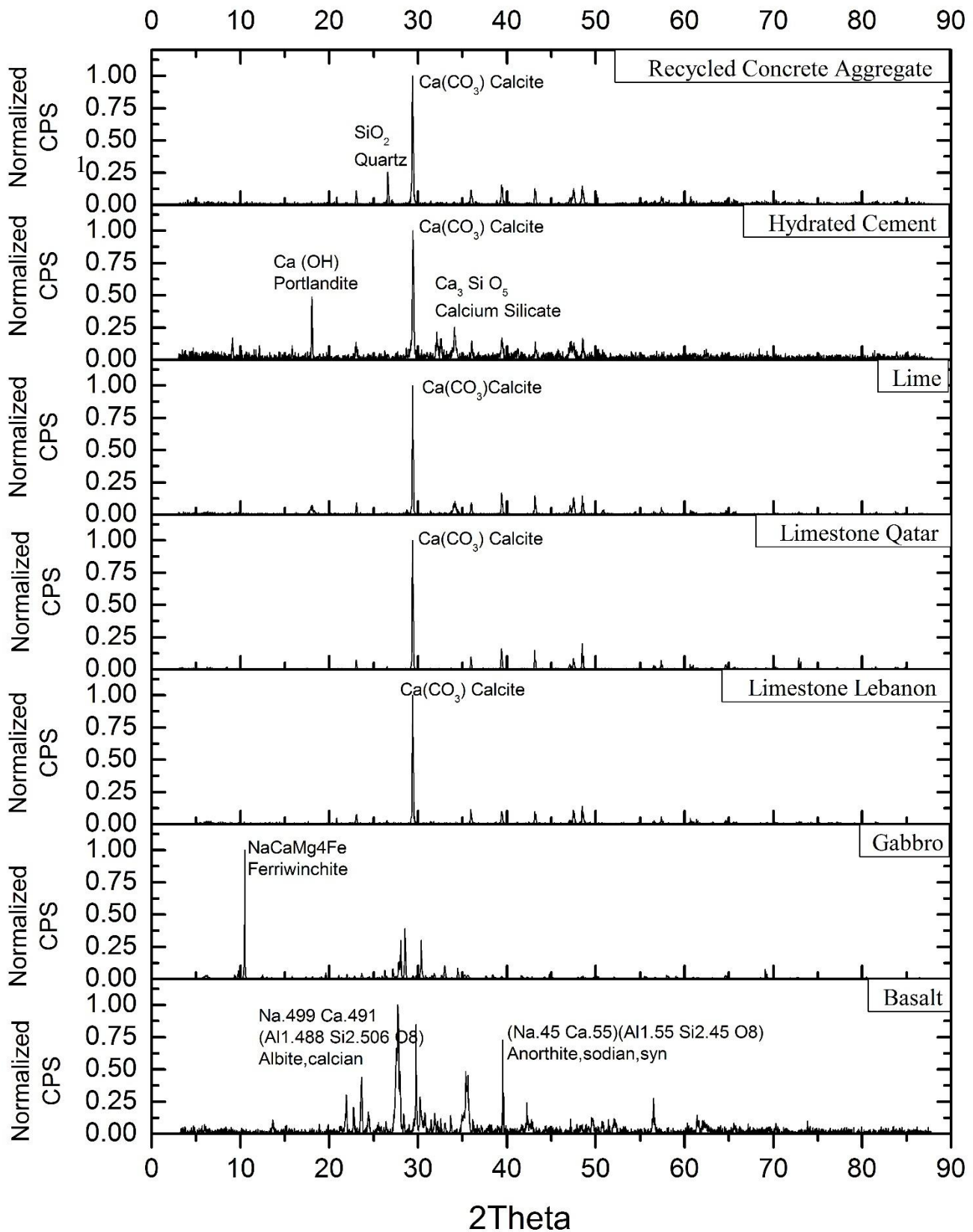


Figure 29 X-ray diffraction for the fillers

4.1.4 Hydrometer

Hydrometer analysis was conducted on the fillers. Figure 30 shows the gradation curve for the seven tested fillers. As shown in Figure 30 that all the natural fillers and RCA were continuously graded, while Lime and hydrated cement show a discontinuity between sizes from 0.015 mm to 0.6 mm. Thereby, the lime was the finest filler while limestone Qatar was the coarsest filler.

To determine which filler size differ than the other Tukey post hoc was conducted on the percentage finer that of 15 micron for each filler type. As shown in Figure 32, the results show that B, G, LL, LQ and RCA have almost the same percentage of particles finer than 15 micron. However, L and HC particles are finer and significantly differ than other types of filler.

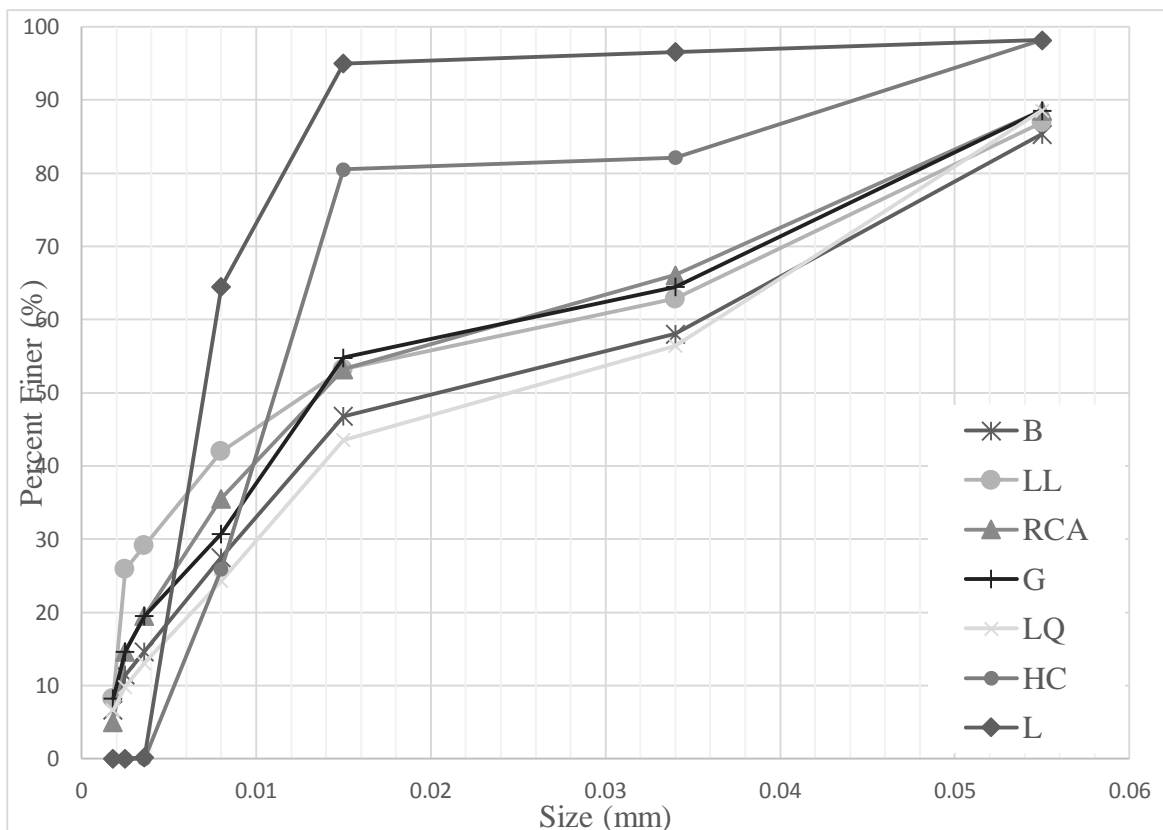


Figure 31 Hydrometer analysis for different fillers

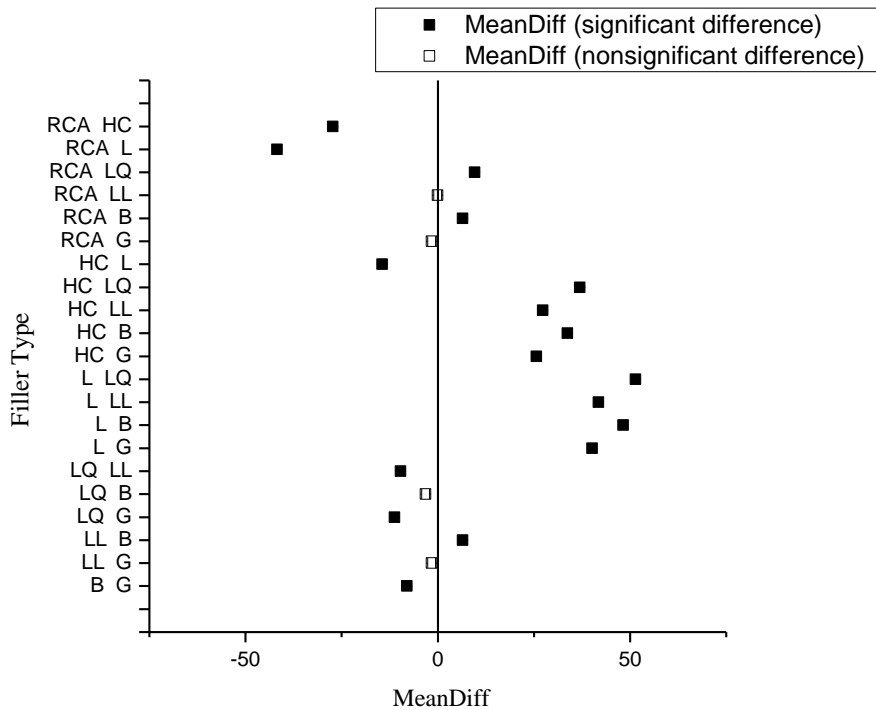


Figure 32 TukeyHSD graph for percentage finer than 15micron results

4.1.5 Methylene Blue Value (MBV)

As mentioned earlier, the methylene blue test determines the amount and nature of potentially detrimental material, such as clay and organic material that may be present in an aggregate. The MBV was measured by using a modified “AASHTO TP57” procedure and reported as milligrams of methylene blue per gram of filler (EN 13043). Methylene blue value were determined as shown in Table 5.

In all cases, the methylene blue values are near the lower limit of the methylene blue values range of the most common fillers (0-20) (Lesueur, Petit, & Ritter, 2013), indicating that there are no detrimental fines. The Table 5 shows the average values of MBV for the different filler types.

Table 5 Average Methylene Blue Value

<u>Filler Type</u>	RCA	LQ	LL	G	B	HC	L
<u>Methylene Blue Value(MBV)</u>	0.5	0.75	2.75	7	9	0.5	0.3

4.2 Mastic Characterization

4.2.1 Viscosity

As an indicator of the workability of the mastic which reflects on the constructability mix, viscosities of the different mastics were measured at different temperatures. It is the norm that the viscosity of a binder decreases with the increase in temperature; this is also applicable to mastics in which the binder softens with rising temperatures.

The average apparent viscosity of the binder dropped down from 0.76 Pa.s to 0.06 Pa.s between 115°C and 195°C. These values increased to 4.77 Pa.s and 0.21 Pa.s upon adding the lime and RCA filler. These results reflect the fact that the filler stiffens the asphalt binder in a mix.

Furthermore, for mastic containing only filler RCA, the viscosity increases by about two times than that of the mastic with limestone filler solely.

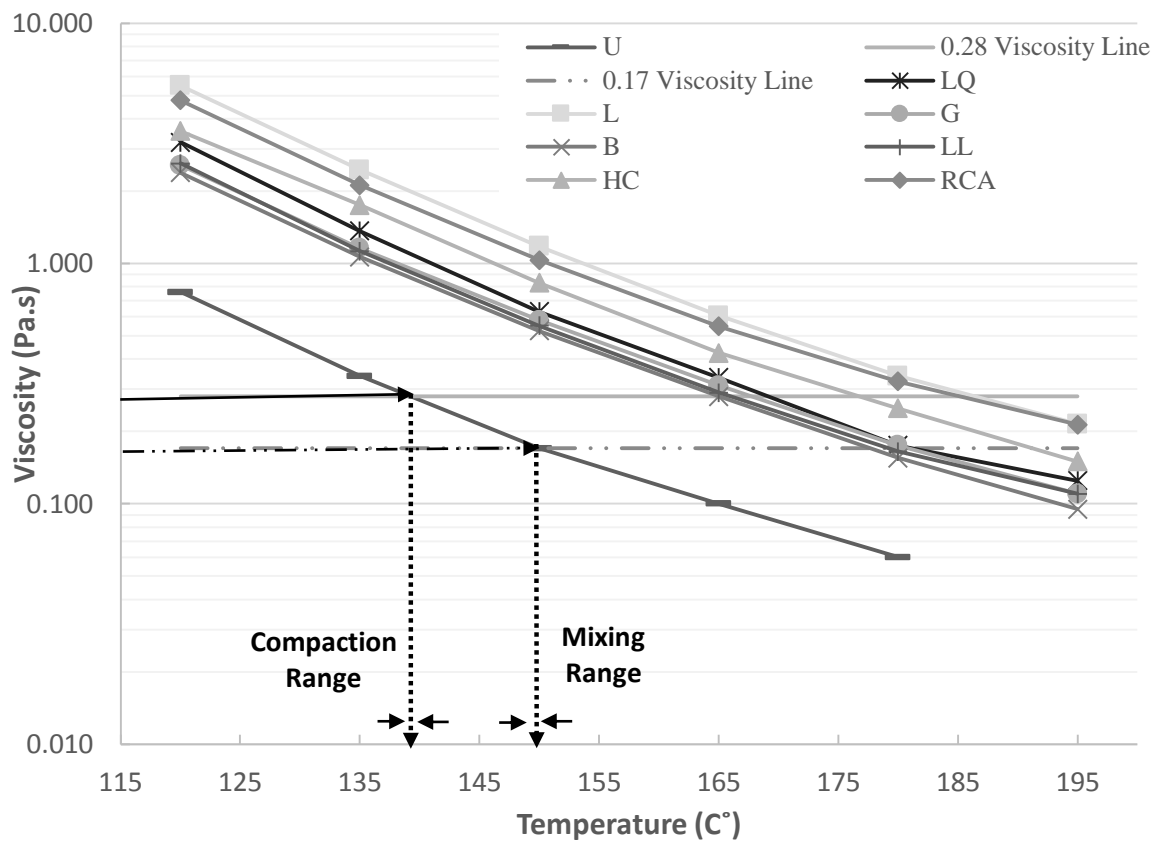


Figure 33 Viscosity versus Temperature for Different fillers.

TukeyHSD analysis was conducted in order to investigate the difference between the multiple mastic types. As we can see in the below that all the fillers have significantly change the viscosity of the binder but in different percentage. No significant difference was found between the effect of natural filler on mastic viscosity in other word all natural filler increases the viscosity in the same rate. Moreover, RCA and HC have also the same effect on mastic viscosity. In addition, Lime has the most significant effect on the mastic viscosity. As a result, some considerations should be adopted when using byproduct filler, especially Lime, since it increases the viscosity of mastic significantly than other natural filler. Finally, we can see two different groups in terms of viscosity namely; the natural with low viscosity and byproduct filler with high viscosity.

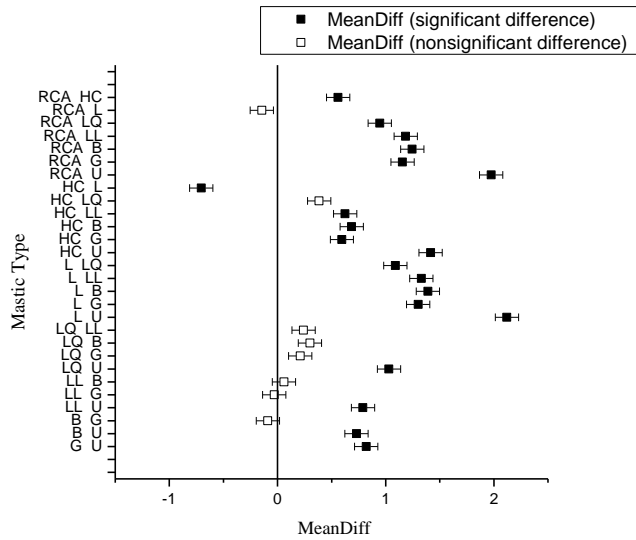


Figure 34 TukeyHSD graph for rotational viscosity results at 135°

4.2.2 Linearity

To confirm linearity, the percentage difference of the dynamic shear modulus (G^*) between 2% and 12% oscillation strains was calculated. All the binders were noticed to retain linearity where the binders belonged in the linear visco-elastic range as shown in Figure 35.

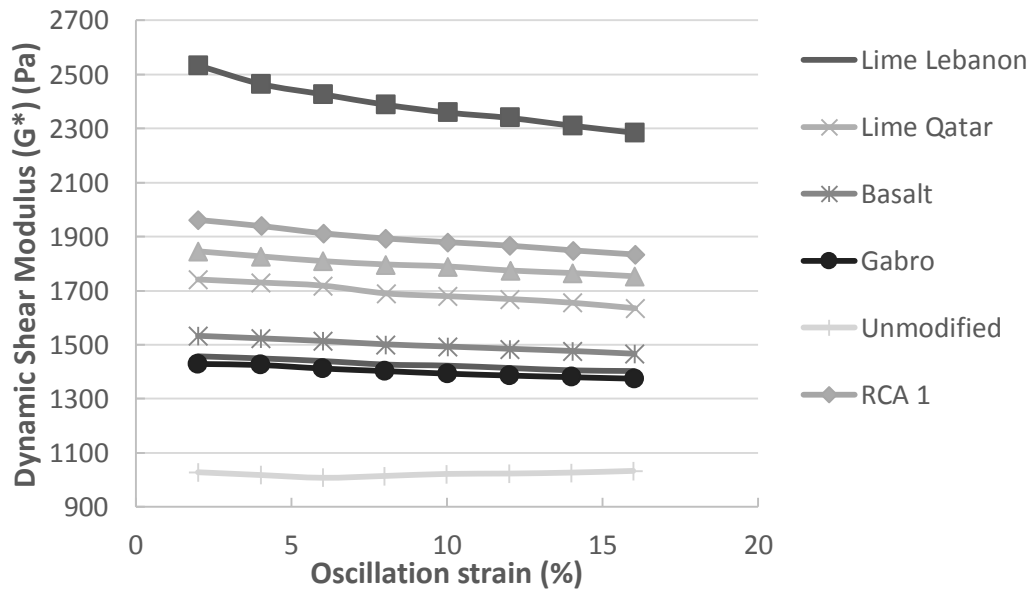


Figure 35 Linearity for filler.

4.2.3 Complex Shear Modulus and Phase Angle

G^* is used as an indicator for the stiffness of the mastic and its resistance to shear deformation under various loads. The results obtained for $G^*/\sin\delta$ at 10 rad/sec present a trend similar to that of the measured viscosity with respect to the replacement of the limestone filler by RCA filler. The $G^*/\sin\delta$ figure for a temperature range between 52°C and 76°C is shifted up by a factor of 3.5 when the filler used was lime. At low temperatures of 64°C, the $G^*/\sin\delta$ value is high where it can be explained that the binder is stiff and thus the effect of the filler is more dominant, but this way is inverted as the temperature increases where the binder softens, hence it controls the properties of the mastic at high temperatures rather than the filler itself.

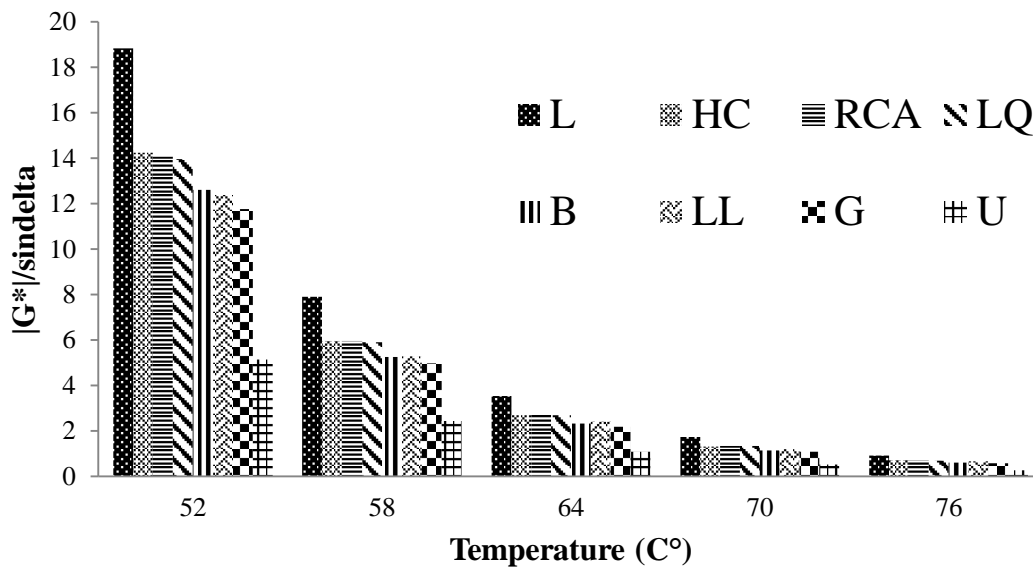


Figure 36 Values of $|G^*|/\sin\delta$ versus Temperature for fillers.

Figure 36 shows $|G^*|/\sin\delta$ at different temperatures for the seven mastics prepared. Taking $|G^*|$ and δ individually shows that the increase in value of $|G^*|/\sin\delta$ upon addition of filler is explained by the stiffening of the binder body where $|G^*|$ is significantly increased.

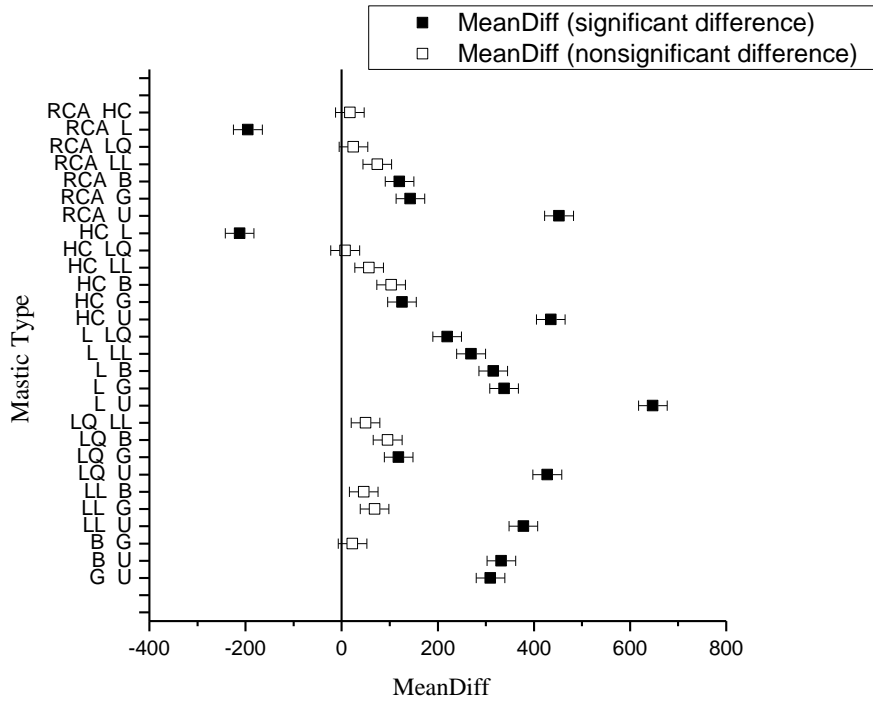


Figure 38 TukeyHSD graph for DSR results at 76°C

4.2.4 Multiple Stress Creep and Recovery (MSCR)

Another measure considered to study the reactivity of the filler with the binder is the non-recoverable creep compliance (J_{nr}) measured in DSR with parallel plate geometry by the multiple stress creep recovery test. This test method determines the presence of elastic response in the studied mastics where the creep portion of the test lasts for 1 second followed by a 9 seconds period of recovery for 10 consecutive cycles for each of the stress levels used: 0.1 kPa and 3.2 kPa at 64°C.

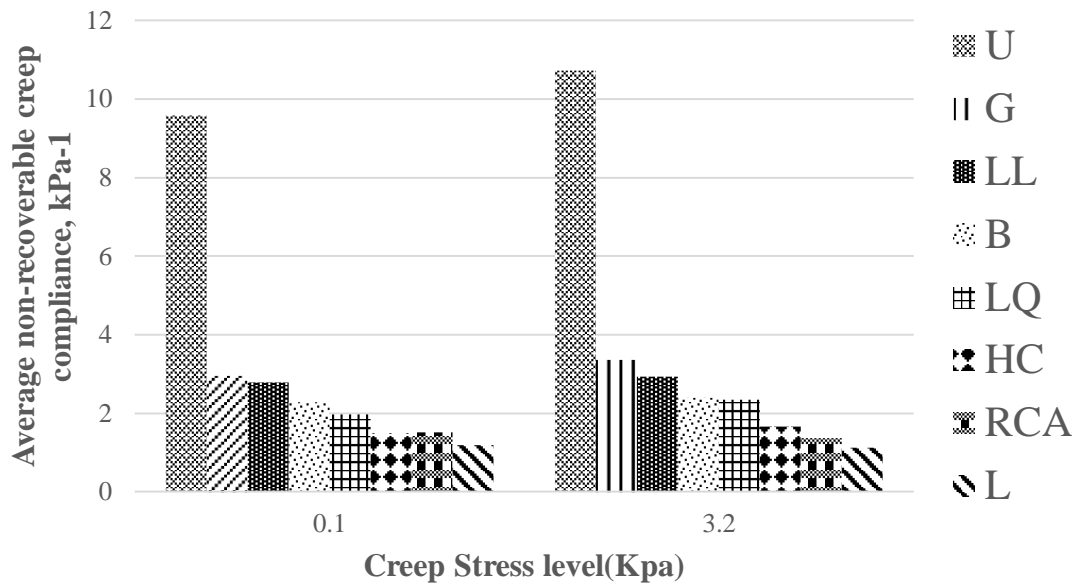


Figure 39 Jnr results for fillers.

The Jnr at 0.1 kPa can be considered as an indicator of the properties in the linear viscoelastic region; while, the Jnr at 3.2 kPa will be taken as an indicator of rutting susceptibility.

The results for Jnr at 0.1 kPa are observed to be similar to those of $|G^*|/\sin\delta$ where Jnr at 0.1 kPa dropped from 9.58 kPa-1 to 1.19 kPa-1 when the mastic contains lime which is approximately a drop by a factor of 8.

The trend of Jnr at 3.2 kPa is similar to that at 0.1 kPa; knowing that Jnr at 3.2 kPa is always higher than that at 0.1 kPa because the higher level of stress leads to more damage in the mastic. But, it is remarkable here that filling the binder reduced the Jnr by a factor of 9.5 times for lime implying that the filler plays a significant role in providing more resistance to permanent deformation.

For the case of mastic with only RCA filler, Jnr at 3.2 kPa is approximately the same as that at 0.1 kPa taking two replicates into consideration. This shows that RCA as a filler is able to stiffen the binder enough so that it will have high rutting resistance. So, this

mastic is stiff enough and it has the same behavior at low and high stress levels where it is still in the linear viscoelastic range unlike other types of mastics presented in this study. Based on this, RCA can be recommended as filler for asphalt concrete mixes that will be placed in hot conditions with slow traffic in order to resist the ability of these mixes to rut.

TukeyHSD analysis was conducted in order to investigate the difference between the multiple mastic types. As we can see in the Figure 40 and Figure 41 that all the fillers have significantly decrease the Jnr for the binder but in different percentage. No significant difference was found between the effect of filler on mastic Jnr expect for LL and G, in other word all the filler decreases Jnr in the same rate expect LL and G. In addition, Lime has the most significant effect on the mastic resistance.

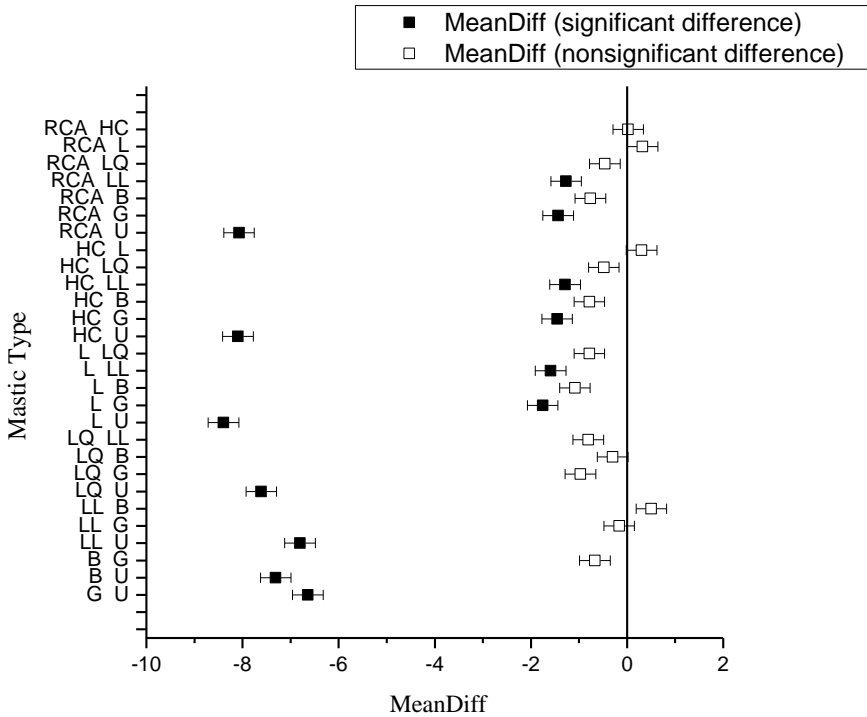


Figure 40 TukeyHSD graph for $Jnr_{0.1}$ results

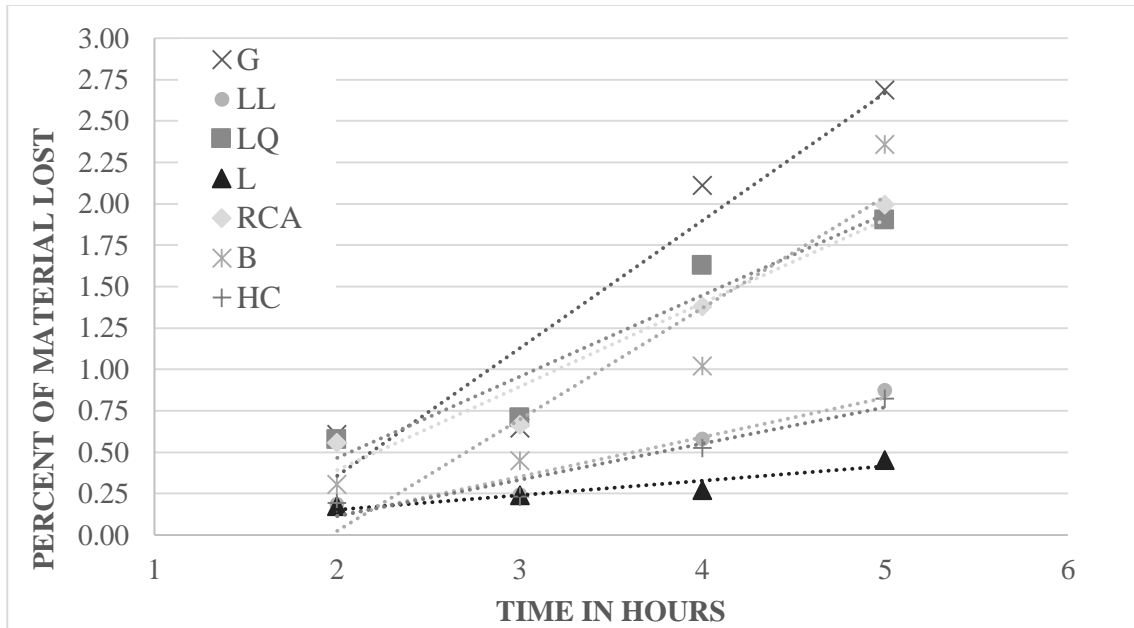


Figure 42 UAMC testing results

The amount of energy dissipated (E) during conditioning was determined calorimetrically, thus the amount of energy needed for stripping the asphalt from the binder was determined by using UAMC.

E is calculated according to:

$$E = \frac{P \times t}{V}$$

Where P is the power output(W), t is the sonication time (s) and V is the volume of the suspension (cm³).

Table 6 Energy dissipated

Conditioning time (hours)	Energy dissipated (Jcm ⁻³)
2	72
3	108
4	144
5	180

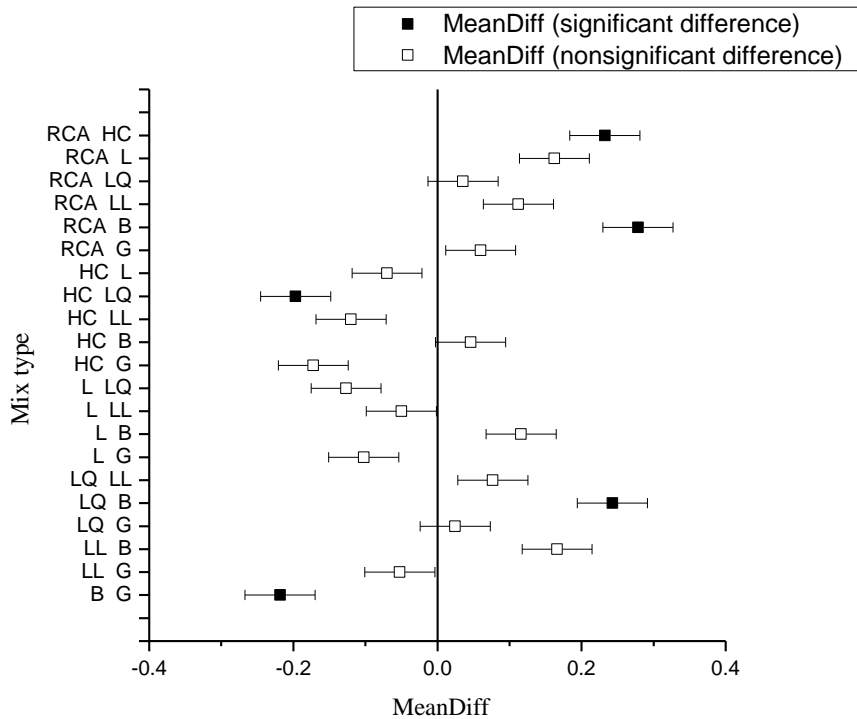


Figure 43 TukeyHSD graph for UAMC results ,2hrs

The one-way ANOVA for UAMC results at different conditioning times confirm that the ultrasonic accelerated moisture conditioning can distinguish between the mixes with different types of fillers. Moreover, TukeyHSD post hoc analysis shows that the UAMC experiment can distinguish between mix with multiple filler types. For 2 and 3 hours conditioning non-significant differences were found expect for Gabbro and Basalt mixes. In contrast the 4 and 5 hours conditioning show a significant difference between all the mixes.

In summary, after studying the different filler properties and its effect on the mastic and mix performance, recommended filler properties were selected for choosing the suitable filler for our design as shown in Table 7. Lime was the best filler but it has high viscosity and LQ was the best filler between the natural filler but it failed in

moisture resistance, as a result the LL was the best filler which has a reasonable performance in viscosity and moisture damage and rutting and fatigue resistance. As a results, Lebanese limestone was selected as benchmark for comparing the different filler

Table 7 Recommended filler properties

Test	Acceptance range	Recommended Value	Remark	Method
BET-Surface area (m2/gr)	3.7-11.5	3.9	The higher the surface the higher viscosity and complex shear modulus	BET method
Bet-Pore Size (cc/gr)	0.0162-0.0554	0.0162	The higher pore volume the higher viscosity and complex shear modulus	BET method
Hydrometer-%finer than 15 Micron	43-94	53	The finer the filler the higher viscosity and complex shear modulus	ASTM 422
Hydrometer-%finer than 30 Micron	56-96	63	The finer the filler the higher viscosity and complex shear modulus	ASTM 422
SEM-solidity	0.87-0.91	0.90	The less solidity the higher viscosity and complex shear modulus	SEM image analysis
SEM-Circularity	0.30-0.60	0.45	The less circularity the higher viscosity and complex shear modulus	SEM image analysis

4.4 Analysis of Mastic Performance Vs. Filler Properties:

4.4.1 Mineral Filler

The fillers were tested to determine the value of their unique properties. Table 8 Table 8 Controlled and response variables involved in this study shows the measured properties of the mineral and by-product filler used in this study. The seven selected filler for testing demonstrate a wide range for each of the properties identified as important for the stiffening and adhesion effect.

Table 8 Controlled and response variables involved in this study

	Filler Properties	Binder Properties	Mastic Properties
<u>Controlled Variable</u>	1) Filler Source <ul style="list-style-type: none"> • G • B • LQ • LL • L • HC • RCA 	PG 64-10	1 to 1 in weight filler concentration
<u>Dependent Variable</u>	1-Surface Area 2-Pore Volume 3-MBV 4-Hydrometer 5-Shape indexes	1-Complex Shear Modulus 2-Multiple Stress Creep Recovery 3-Rotational Viscosity	1-Complex Shear Modulus 2-Multiple Stress Creep Recovery 3-Rotational Viscosity

Table 9 Average Properties of fillers

	G	B	LL	HC	LQ	RCA	L
Surface Area	4.70	10.81	4.59	9.80	2.81	11.47	8.11
Pore volume	0.0228	0.0315	0.0180	0.0412	0.0140	0.0554	0.0341
MBV	7	9.1	2.75	0.5	0.75	0.5	0.25
% Passing 15 micron	54.81	46.78	53.21	80.5	43.57	53.21	94.96
% Passing 34 micron	64.45	58	62.85	82.12	56.42	66.02	96.57
Circ.	0.486	0.453	0.45	0.362	0.598	0.3	0.346
Ar	1.419	1.501	1.366	1.319	1.149	1.244	1.503
Round	0.712	0.673	0.773	0.759	0.872	0.822	0.69
Solidity	0.915	0.905	0.898	0.887	0.95	0.878	0.871
Maximum Aggregate Size	73.71	91.29	76.34	70.99	85.49	94.78	17.53

In order to establish the relationship between different filler properties, Table 9 shows the inter-correlation between the different filler properties. These correlation coefficients are used to select the properties that can independently represent characteristic of the fillers. The selected independent properties will be used in developing the final form of the prediction models.

Table 10 Correlation matrix for the properties of fillers

	Surface Area	Pore. volume	MBV	% Passing 15 micron	% Passing 34 micron	Circ.	Ar	Roundness	Solidity	Maximum Aggregate Size
Surface Area	1.000	0.895	0.039	0.277	0.294	-0.796	0.298	-0.347	-0.710	0.071
Pore Volume	0.895	1.000	-0.268	0.336	0.375	-0.887	0.025	-0.069	-0.744	0.040
MBV	0.039	-0.268	1.000	-0.465	-0.495	0.324	0.551	-0.599	0.253	0.334
% Passing 15 micron	0.277	0.336	-0.465	1.000	0.995	-0.599	0.412	-0.410	-0.683	-0.871
% Passing 34 micron	0.294	0.375	-0.495	0.995	1.000	-0.630	0.396	-0.385	-0.707	-0.880
Circ.	-0.796	-0.887	0.324	-0.599	-0.630	1.000	-0.289	0.280	0.965	0.292
Ar	0.298	0.025	0.551	0.412	0.396	-0.289	1.000	-0.982	-0.478	-0.506
Roundness	-0.347	-0.069	-0.599	-0.410	-0.385	0.280	-0.982	1.000	0.443	0.448
Solidity	-0.710	-0.744	0.253	-0.683	-0.707	0.965	-0.478	0.443	1.000	0.452
Maximum Aggregate Size	0.071	0.040	0.334	-0.871	-0.880	0.292	-0.506	0.448	0.452	1.000

As shown in Table 10 , all measured properties weakly correlate with the MBV, as a results MBV can be used as predictor variable, moreover the percentage finer that 15 and 34 micron strongly correlate with solidity and maximum aggregate size but unexpectedly, there not correlate with surface area nor pore volume, on the other hand the surface area and pore volume are strongly correlated, as a result a conclusion can be drawn that the surface area is affected by the pore volume and not by filler gradation.

4.4.2 Complex Modulus

The complex shear modulus ($|G^*|$) values of the mastic were measured using DSR. The ANOVA analysis shows that the filler type has statistically significant influence ($p\text{-value} < 0.05$) on the $|G^*|$ result. The measured values of the $|G^*|$ of the mastics were then divided by the value of $|G^*|$ measured for the unfilled binder to determine the complex modulus ratio or ($|G^*|_{re}$) so we can get a better indication for the influence of the filler on the Mastic properties.

Table 11 Average $|G^*|$ and $|G^*|_{re}$ for the filler

	$ G^* _{52}$	$ G^* _{RE52}$	$ G^* _{58}$	$ G^* _{re58}$	$ G^* _{64}$	$ G^* _{re64}$	$ G^* _{70}$	$ G^* _{re70}$	$ G^* _{76}$	$ G^* _{re76}$
G	11737.30	2.30	4951.96	2.05	2176.16	2.02	1065.18	2.04	570.61	2.18
B	12585.80	2.47	5234.17	2.16	2304.13	2.14	1121.21	2.15	593.19	2.27
LL	12370.15	2.42	5261.84	2.17	2398.03	2.22	1188.87	2.27	639.21	2.45
HC	14225.90	2.79	5934.80	2.45	2684.47	2.49	1298.18	2.48	696.22	2.67
LQ	13914.50	2.73	5889.48	2.43	2693.43	2.50	1315.19	2.52	688.91	2.64
RCA	14050.65	2.75	5945.67	2.46	2700.06	2.50	1333.46	2.55	713.38	2.73
L	18792.45	3.68	7875.96	3.25	3513.60	3.26	1730.65	3.31	908.51	3.48

The Pearson correlation test was conducted to analyze the relationship between mastic complex modulus and filler properties.

Table 12 presents the correlation matrix between Mastic $|G^*|$ and filler properties (Surface area , Pore volume, Methylene blue value , % passing 15& 35 micron ,Circularity, AR, roundness , solidity, maximum aggregate size).The results

	Surface Area	Pore volume	MBV	% Passing 15 micron	% Passing 34 micron	Circ.	Ar	Round	Solidity	Maximum Aggregate Size
$ G^* _{52}$	0.191	0.281	-0.632	0.789	0.831	-0.439	0.162	-0.100	-0.487	-0.818
$ G^* _{58}$	0.217	0.293	-0.611	0.801	0.841	-0.447	0.187	-0.131	-0.495	-0.820
$ G^* _{64}$	0.167	0.278	-0.696	0.766	0.809	-0.429	0.083	-0.017	-0.466	-0.786
$ G^* _{70}$	0.157	0.274	-0.697	0.755	0.801	-0.435	0.086	-0.012	-0.477	-0.786
$ G^* _{76}$	0.177	0.305	-0.715	0.773	0.818	-0.475	0.085	-0.011	-0.514	-0.786

show that generally poor correlation was found between complex modulus and surface area, pore volume, roundness, Aspect ratio .On the other hand, maximum aggregate size , % passing 34 and 15 micron show relatively higher correlation with complex modulus , compared to other filler properties .

Table 12 Correlation Matrix between Mastic Complex Modulus and Filler properties

Furthermore, Figure 47 shows the scatter plots for $|G^*|$ at 64 vs. filler properties.

Although there are a high correlation between %passing 34&15 micron but there no pattern, as a result we cannot rely on those properties in building the prediction model.

In contrast, we can see a pattern between the MBV, solidity and $|G^*|$ so we can adopt them in the prediction model.

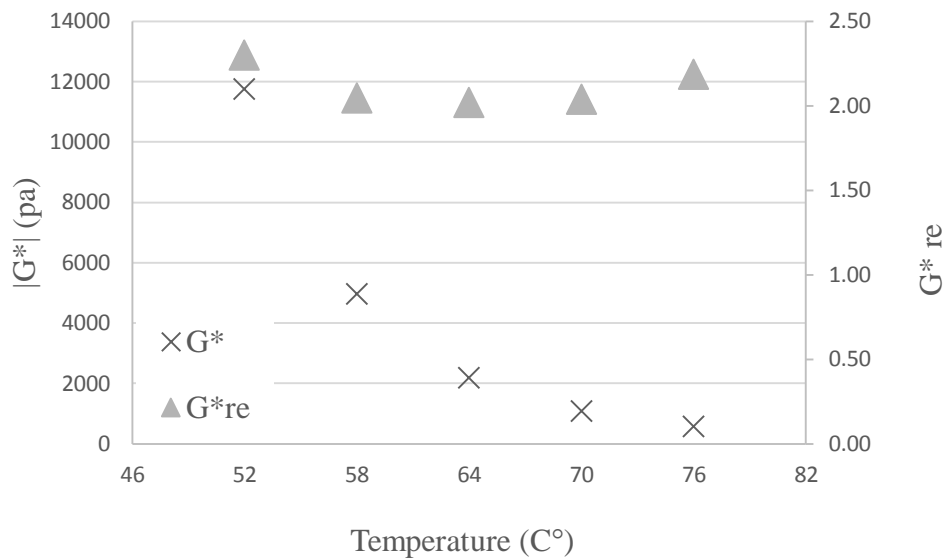


Figure 44 |G*| & |G*|re for Gabbro.

Figure 44 shows that the value of $|G^*|$ decrease with the temperature but when we normalize the value of $|G^*|$ to $|G^*|_{re}$ the effect of filler will arise, as we can see that the effect of filler is nearly constant and that accepted because the stiffness of filler will not change with temperature and the change in the $|G^*|$ of mastics is due the asphalt viscoelastic behavior.

Moreover, Figure 45 shows that the mastics and binder complex modulus decrease with increasing temperature in parallel, they have the same slope but different intercept, as a result the intercept is the sum of the filler stiffness and binder-filler interaction stiffness.

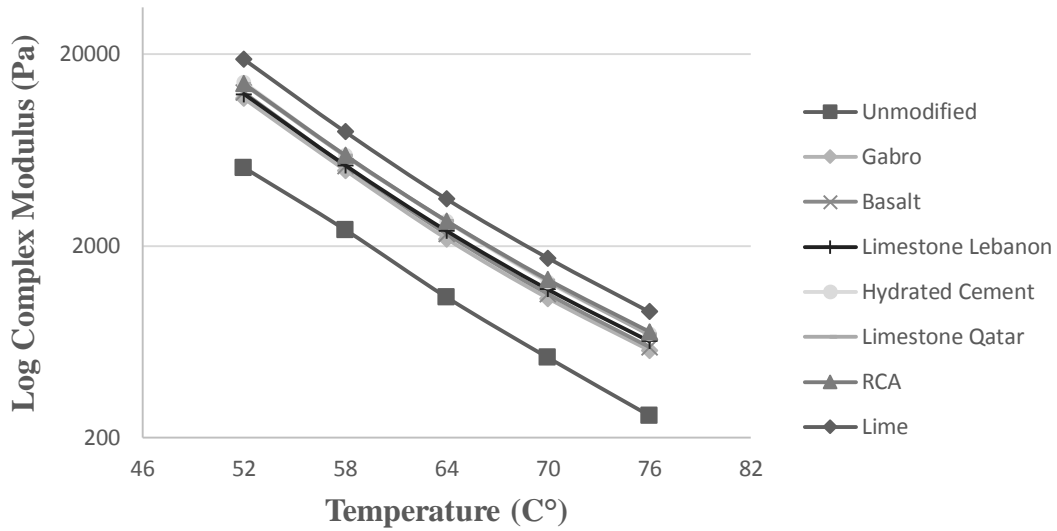


Figure 45 Log complex modulus vs temperature.

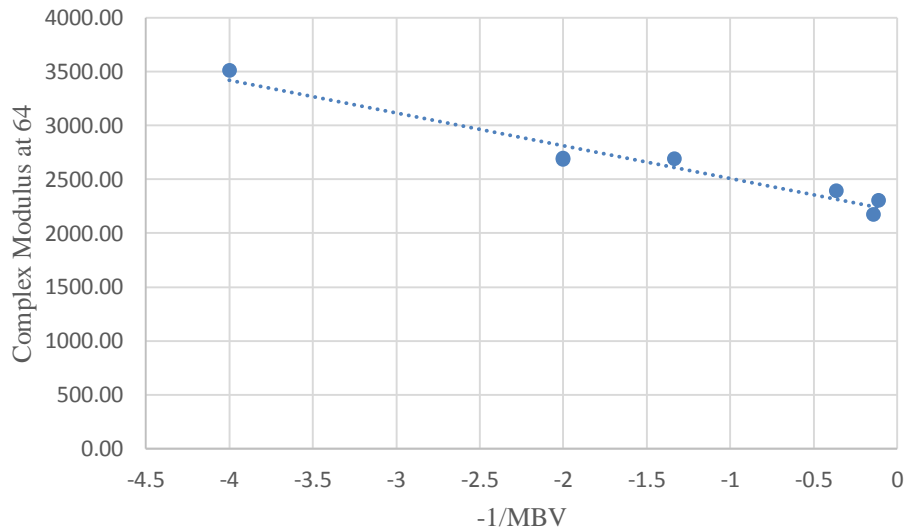


Figure 46 MBV linearity transformation.

The scatter plots illustrate nonlinear relation between $|G^*|$ and MBV, as a result linearity transformation was done for the MBV values as shown in Figure 46

Table 13 shows the corresponding stepwise regression equations for the complex modulus. A high R-square and small p-value indicate low variance in estimating the regression coefficients. It is clear that MBV significantly affect the complex modulus.

This is suggesting that asphalt mastic could also be affected by filler chemical properties.

Table 13 Stepwise regression models for |G*|

	Regression models	Adjusted R-square	P-value
 G* at 58	G* binder at 58 + 2498.27 + 669.8/MBV	0.924	0.0003512
 G* at 64	G* binder at 64 + 1127.16 + 304.91/MBV	0.9367	0.0002211
 G* at 70	G* binder at 70 + 556.17 +150.82/MBV	0.9264	0.0003232
 G* at 76	G* binder at 76 + 315.8965+ 77.457/MBV	0.9406	0.0001882

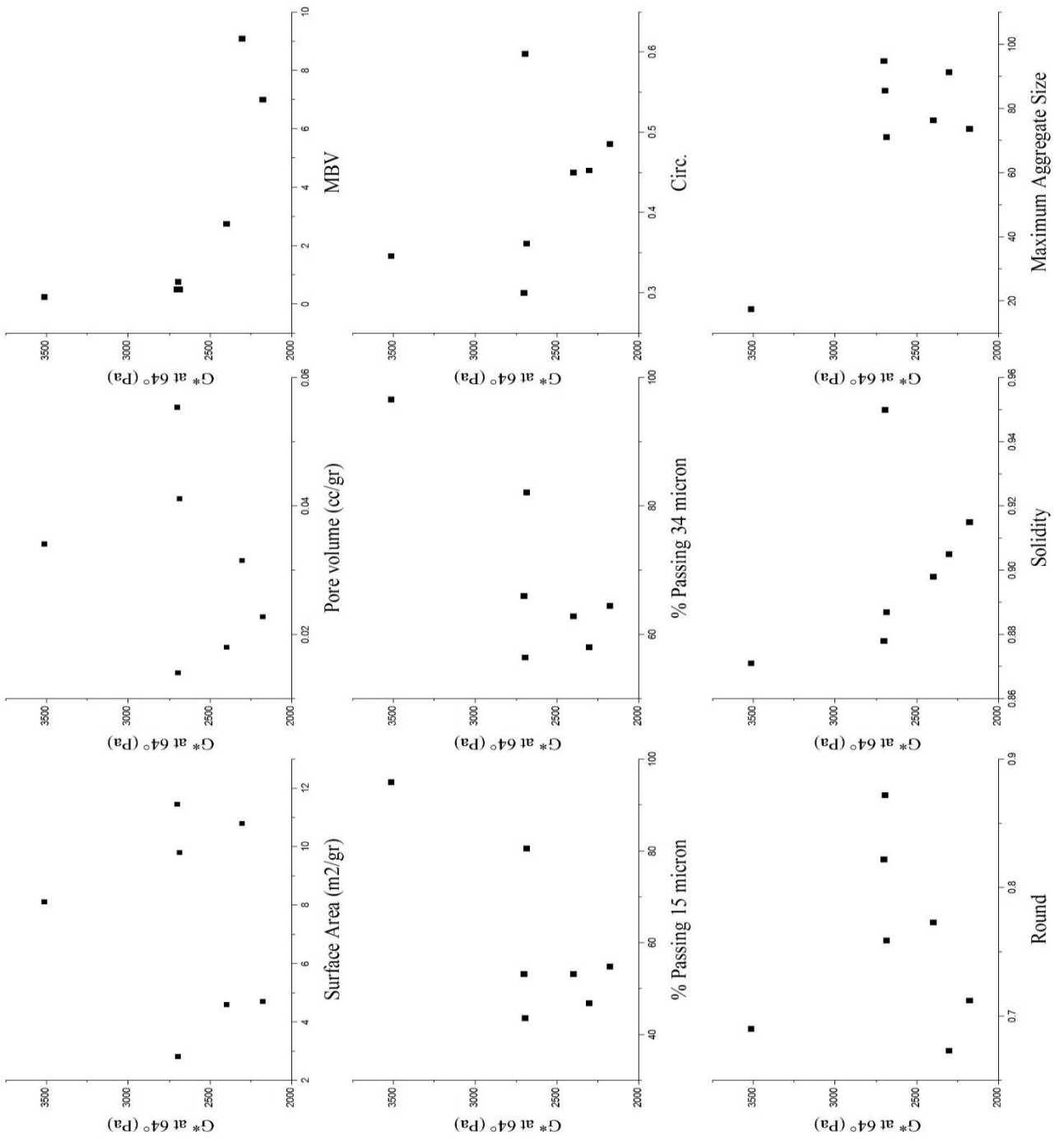


Figure 47 Scatter plots for $|G^*|$ at 64 vs filler properties

4.4.3 Multiple Stress Creep Recovery (MSCR)

The relative Jnr ratio was calculated by dividing the Jnr of the mastic on the Jnr of binder, table shows the relative Jnr ratio for the mastics. The Jnr re can be used as an indication for the influence of the filler on the Mastic properties.

Table 14 Average values of Jnr & Jnr re for different fillers

	jnr0.1	jnr0.1re	jnr3.2	jnr3.2re
G	2.95	0.31	3.36	0.31
B	2.28	0.24	2.39	0.22
LL	2.78	0.29	2.93	0.27
HC	1.49	0.16	1.58	0.15
LQ	1.98	0.21	2.34	0.22
RCA	1.51	0.16	1.37	0.13
L	1.19	0.12	1.13	0.11

One-way ANOVA was conducted between Jnr0.1re and Jnr3.2re , the result shows high p value >0.05 , as a consequence, there no statistical difference between the two values ,we can conclude that the filler dissipated the loading and help the influenced asphalt which covers the filler particle surface in carrying the load.

Table 15 Correlation Matrix between Jnr 0.1&3.2 and Filler properties

	Surface Area	Pore Volume	MBV	% Passing 15 micron	% Passing 34 micron	Circ.	Ar	Round	Solidity	Maximum Aggregate
Jnr0.1	-0.539	-0.637	0.687	-0.633	-0.668	0.582	0.126	-0.118	0.497	0.412
Jnr3.2	-0.630	-0.716	0.659	-0.629	-0.669	0.691	0.058	-0.066	0.614	0.394

The scatter plots for Jnr0.1, Jnr3.2 vs. filler properties were used for investigating the change of Jnr with filler properties, MBV and solidity show a good pattern that we can adopt them in Jnr prediction model.

A multiple regression analysis using a fully stepwise procedure was conducted to consider the effect of the filler properties on mastic and rutting potential of mixtures.

Table 16 shows the selected variables and the corresponding stepwise regression equations for the Jnr. A high R-square and small p-value indicate low variance in estimating the regression coefficients. The Jnr indicates permanent deformation potential of mastic during repeated loading, hence the relative Jnr ration reflects the filler stiffening effect. It is clear that MBV significantly affect the Jnr. This is suggests that the permanent deformation potential of asphalt mastic could also be affected by filler chemical properties.

Table 16 Stepwise regression models for Jnr

	Regression models	Adjusted R-square	P-value
Jnr0.1	2.6355– 0.4288/MBV	0.7539	0.007005
Jnr 3.2	2.583 – 0.462/MBV	0.7185	0.009931

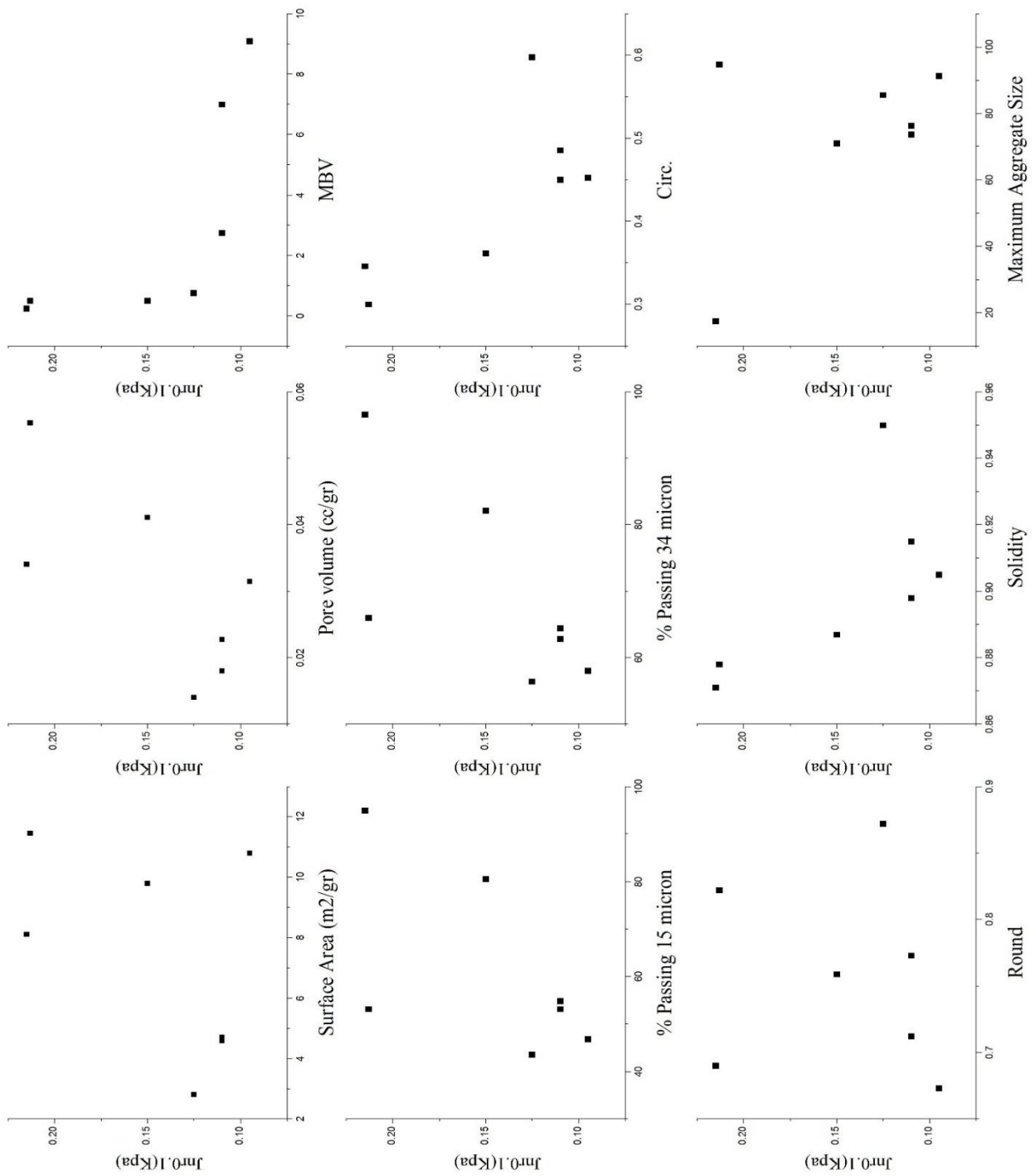


Figure 48 Scatter plots for Jnr0.1vs filler properties.

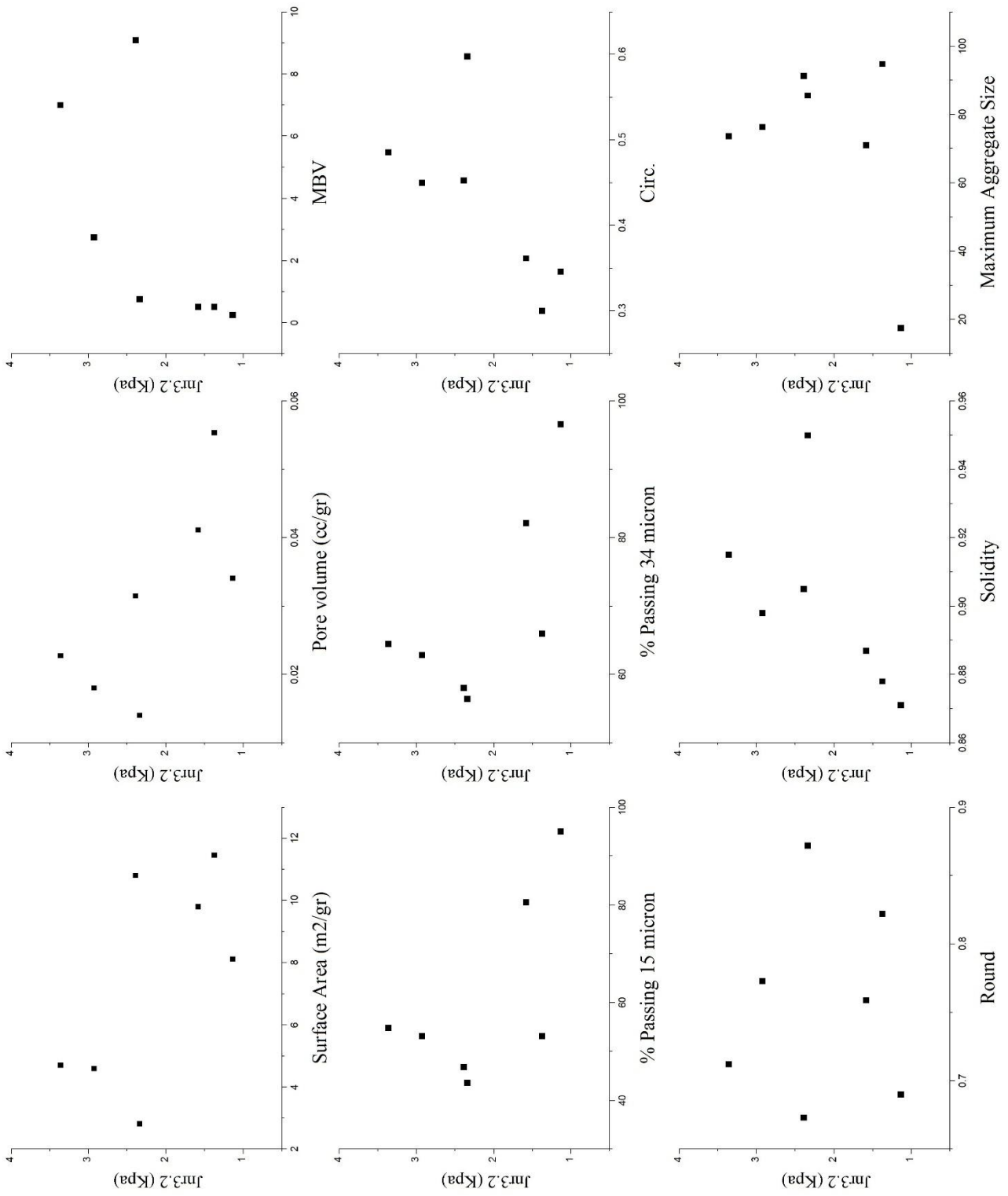


Figure 49 Scatter plots for Jnr3.2vs filler properties.

4.4.4 Rotational Viscometer

The relative viscosity was also calculated (mastic to binder) as an indicator of filler reactivity with binder. The ANOVA analysis shows that the filler type has statistically significant influence ($p\text{-value} < 0.05$) on the viscosity result. Table 17 shows the viscosity and the calculated relative viscosity for mastics.

Table 17 Average RV & RVre for Mastics

	RV at 120	RVre at 120	RV at 135	RVre at 135	RV at 150	RVre at 150	RV at 165	RVre at 165	RV at 180	RVre at 180
G	2.56	3.38	1.16	3.43	0.58	3.41	0.31	3.20	0.18	2.92
B	2.39	3.15	1.07	3.16	0.53	3.09	0.28	2.89	0.16	2.58
LL	2.61	3.45	1.13	3.34	0.55	3.24	0.29	2.99	0.17	2.75
HC	3.56	4.70	1.75	5.19	0.83	4.88	0.43	4.38	0.25	4.17
LQ	3.20	4.22	1.37	4.05	0.63	3.71	0.34	3.45	0.18	2.92
RCA	4.78	6.31	2.12	6.28	1.03	6.08	0.55	5.64	0.32	5.38
L	5.49	7.25	2.46	7.28	1.18	6.94	0.61	6.24	0.34	5.67

The Pearson correlation test was also conducted to analyze the relationship between viscosity and filler properties. Table 18 presents the correlation matrix between Mastic viscosity and filler properties (Surface area , Pore volume, Methylene blue value , % passing 15& 35 micron ,Circularity, AR, roundness , solidity, maximum aggregate size).The results show that generally poor correlation was found between viscosity and roundness, aspect ratio, surface area .On the other hand, maximum aggregate size , %

passing 34 and 15 micron show relatively higher correlation with complex modulus , compared to other filler properties .

Table 18 Correlation Matrix between Rational Viscosity and Filler properties

	Surface Area	Pore Volume	MBV	% Passing 15 micron	% Passing 34 micron	Circ.	Ar	Round	Solidity	Maximum Aggregate Size
RV at 120	0.380	0.599	-0.711	0.673	0.740	-0.669	-0.020	0.070	-0.626	-0.591
RV at 135	0.434	0.647	-0.712	0.736	0.794	-0.716	0.002	0.030	-0.669	-0.601
RV at 150	0.458	0.670	-0.679	0.733	0.792	-0.746	0.039	-0.006	-0.701	-0.598
RV at165	0.462	0.682	-0.673	0.701	0.764	-0.745	0.020	0.014	-0.692	-0.570
RV at180	0.516	0.741	-0.660	0.696	0.757	-0.803	0.023	0.004	-0.743	-0.526

Furthermore, Figure 50 and Figure 51 show the scatter plots for viscosity at 135°C and 165°C vs. filler properties. Although, there is a high correlation between percentage passing 34 &15 micron but there no pattern, as a result we cannot rely on those properties. In contrast, a pattern was found between the MBV and viscosity at 135°C but at 165 °C the effect of filler disappears due the high viscosity of binder which dominant the viscosity result. Furthermore, the circularity and solidity of filler strongly correlate with the viscosity of mastic, that be explained by existence resistance of the flow of binder between the filler particle which is controlled by the surface texture and shape of filler particle, in other word the smooth surface will give lower viscosity than the rough surface. Finally, weak correlation and no pattern were found between the viscosity and the other filler properties.

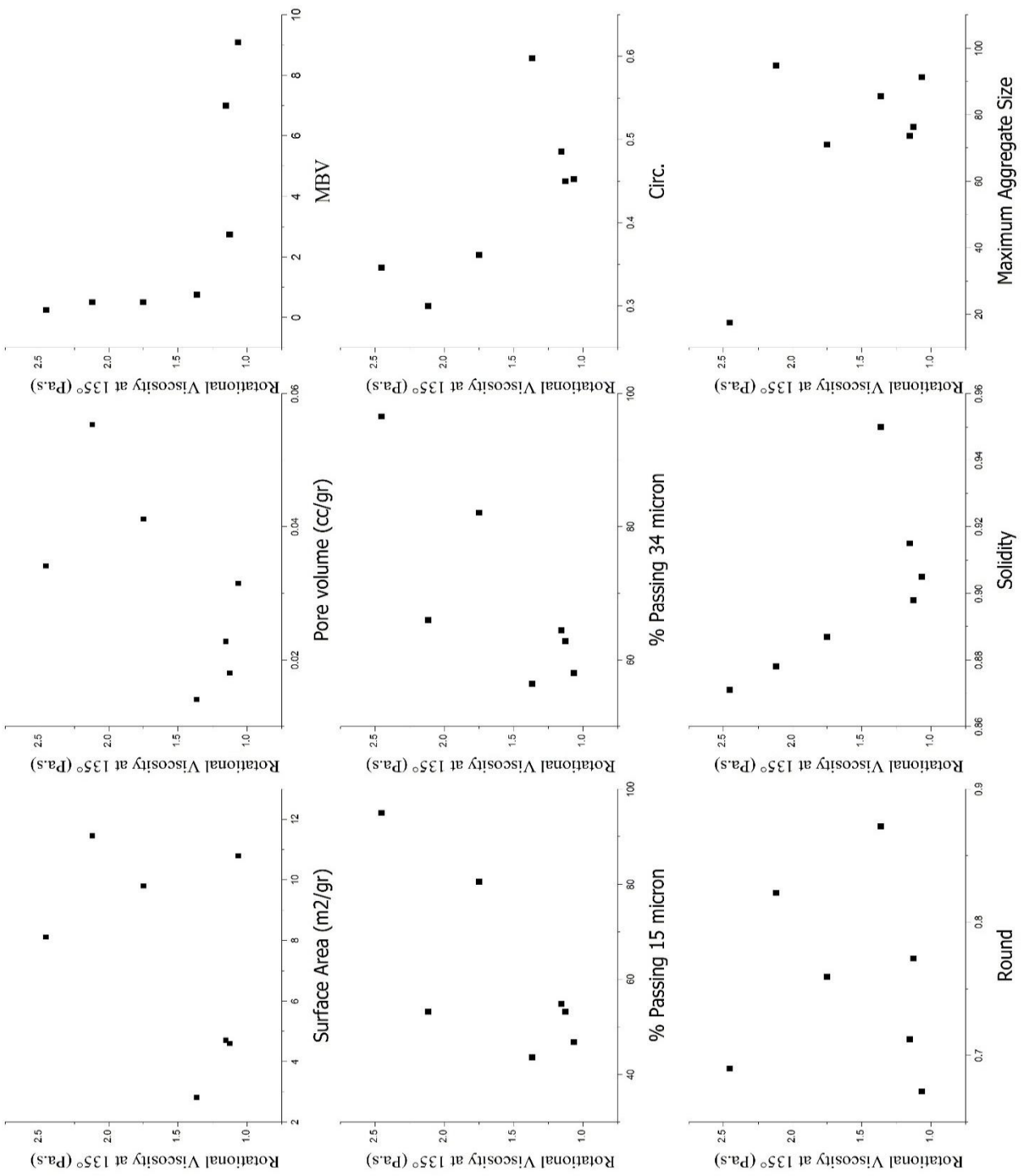


Figure 50 Scatter plots for RV 135 vs filler properties

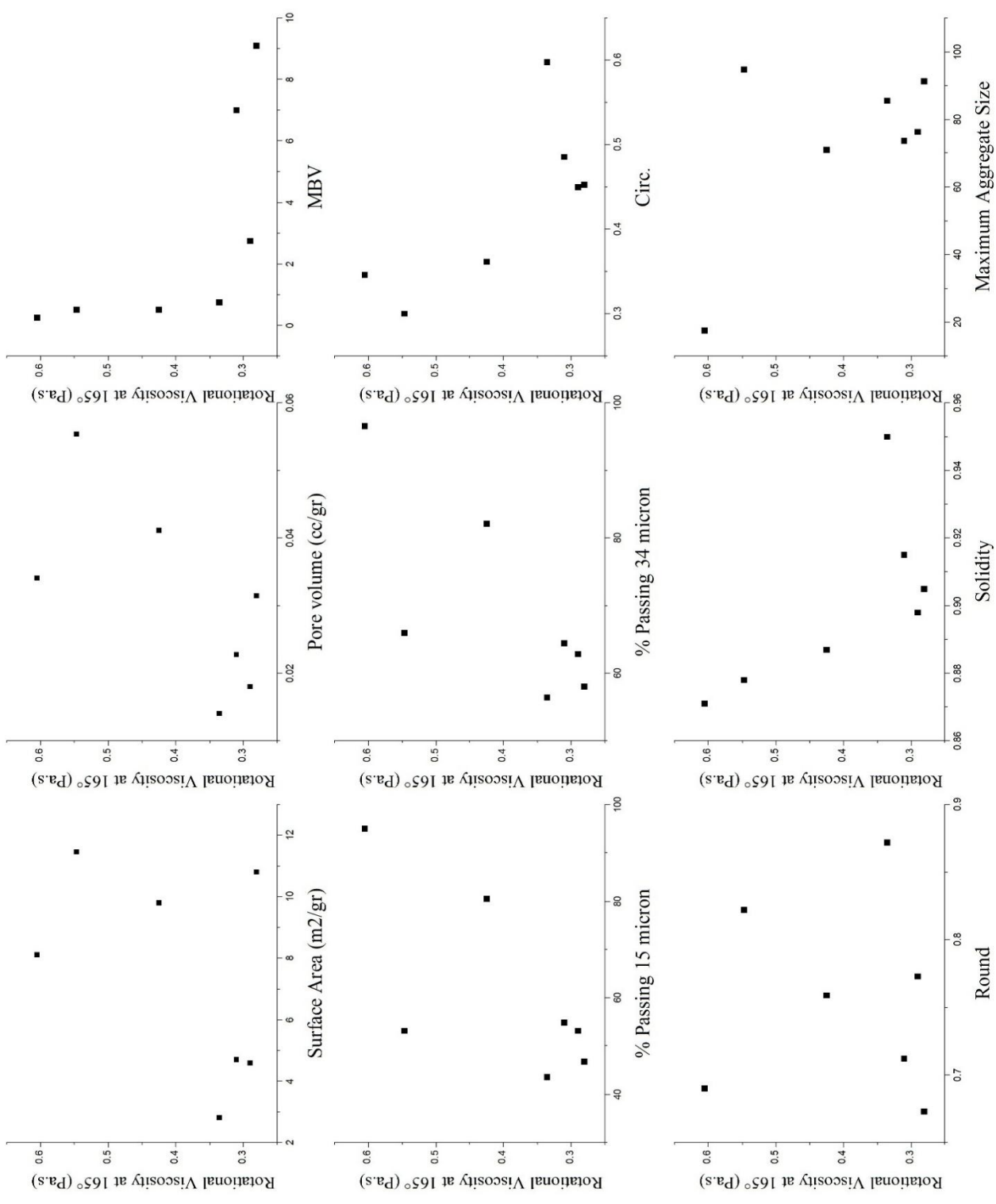


Figure 51 Scatter plots for RV 165 vs filler properties

CHAPTER 5

CONCLUSIONS AND FUTURE WORK

5.1 Conclusions

This study evaluates the performance of different types of mineral and by-product filler in asphalt pavement. Seven types of fillers namely Gabbro, Basalt, Limestone Lebanon, Limestone Qatar, Lime, Hydrated Cement, Recycled Concrete Aggregate were investigated. Scanning electron microscope, X-ray diffraction, surface analyzer, Hydrometer test results were used to characterize the fillers. Dynamic shear rheometer, Multiple stress creep recovery, Rotational Viscosity test results were used to evaluate the effect of different fillers on mastic performance. Furthermore, ultrasonic accelerated moisture conditioning experiment was conducted to evaluate water susceptibility. Based on the investigation conducted in this study, the conclusions are summarized as follows:

- For all the filler-asphalt mastics studied, the stiffness and viscosity are increased by the following factors, two or more of them may operate simultaneously:
 - a. Increase in the fineness of the filler or decrease in the particle size of the filler
 - b. Increase in calcite content of the filler
- The stiffness and rotational viscosity for all the fillers positively correlated with particle size distribution and maximum aggregate size, and negatively with the methylene blue value.
- The non-recoverable creep compliance positively correlated with Methylene blue value, and negatively with particle size distribution.

- The use of RCA as a filler improves the complex shear modulus and improves the non-recoverable creep compliance.
- Lime mastic has the highest $|G^*|$ value compared to other filler sources test. In addition, Limestone Lebanon has the highest value for the natural mineral filler
- An increase in $|G^*|/\sin(\delta)$ was observed with mixes with lime have greater tendency to improve rutting compared to all fillers tested.
- Lime Mastic has the best rutting and fatigue resistance out of all tested mastic samples.
- The replacement of Gabbro and Basalt by the Recycled Concrete Aggregate has a positive effect on mastic performance, as result for the mix performance.
- Superpave design properly showed the difference in optimum asphalt content between different asphalt mixes with different filler.
- The use of lime filler in the mixes decrease the moisture damage, while the use of Gabbro filler increases the moisture damage.
- Results and tests and calculations showed that one of the most significant features of all the fillers is MBV, which has a considerable influence on the properties of the mastics.

5.2 Recommendations and future work

Although Lime has the best overall Mastic performances but with higher asphalt content, recycled concrete aggregate is also an alternative of mineral filler, especially Gabbro and Basalt, in asphalt concrete mixes. Recycled concrete aggregate has similar properties of Hydrated Cement. This provide us with green, recycled and good performance materials in spite of the small quantity in hot asphalt mixes around 5% of

total weight of mix. Thus the idea of incorporating RCA in asphalt concrete is a valid concept towards producing more sustainable asphalt concrete mixes.

In addition, the performance of mastic may not be statistically significant, since only one asphalt binder was tested. The best approach from a statistical point of view is to test more samples to assess the significance of the results with different binders. There is a possibility that the variations in obtained test values of binder with different fillers are within the repeatability of the test methods and not due to differences in the properties of the samples.

However, several areas are still to be further investigated. The following are the recommended areas for future research:

- Investigating more asphalt mixes using only RCA filler in order to better understand the effect of RCA filler on the mix. The findings from this study might allow the adoption of the use of RCA as filler in asphalt concrete.
- Conducting further testing on the application of Ultrasound Accelerated Moisture Conditioning experiment with different mixes to test the reliability of the experiment.
- Furthermore, relating the Ultrasound Accelerated Moisture Conditioning testing results with AASHTO T 283 results and trying to get a limit for the weight lost.
- Investigating different sources of RCA in order to ensure that the source doesn't affect the obtained results and still can provide results better than the natural filler.

REFERENCES

- Al-Abdulwahhab, H. I. (1981). The effects of baghouse fines and mineral fillers on asphalt mix properties in the Eastern Province of Saudi Arabia. *Civil Engineering*.
- Bahia, H. U., Faheem, A., & Hintz, C. (2011). *Test Methods and Specification Criteria for Mineral Filler Used in Hot Mix Asphalt*: Transportation Research Board.
- Besson, F. S. (1923). *City pavements*: McGraw-Hill.
- Chen, J.-S., & Peng, C.-H. (1998). Analyses of Tensile Failure Properties of Asphalt-Mineral Filler Mastics. *Journal of Materials in Civil Engineering*, 10(4), 256-262. doi: doi:10.1061/(ASCE)0899-1561(1998)10:4(256)
- Cho, D.-W., & Bahia, H. U. (2010). New parameter to evaluate moisture damage of asphalt-aggregate bond in using dynamic shear rheometer. *Journal of Materials in Civil Engineering*, 22(3), 267-276.
- Delaporte, B., Di Benedetto, H., Chaverot, P., & Gauthier, G. (2007). Linear viscoelastic properties of bituminous materials: from binders to mastics (with discussion). *Journal of the Association of Asphalt Paving Technologists*, 76.
- Einstein, A. (1956). *Investigations on the Theory of the Brownian Movement*: Courier Corporation.
- Faheem, A. F., & Bahia, H. U. (2010). Modelling of asphalt mastic in terms of filler-bitumen interaction. *Road Materials and Pavement Design*, 11(sup1), 281-303.
- Hansen, T. C. (2004). *Recycling of demolished concrete and masonry* (Vol. 6): CRC Press.
- Kallas, B., & Krieger, H. (1960). *Effects of consistency of asphalt cements and types of mineral filler on the compaction of asphalt concrete*. Paper presented at the Proceedings, Association of Asphalt Paving Technologists.
- Kallas, B., & Puzinauskas, V. (1961). *A study of mineral fillers in asphalt paving mixtures*. Paper presented at the Proceedings of the Association of Asphalt Paving Technologists.
- Kallas, B., Puzinauskas, V., & Krieger, H. (1962). Mineral fillers in asphalt paving mixtures. *Highway Research Board Bulletin*(329).
- Lesueur, D., Petit, J., & Ritter, H.-J. (2013). The mechanisms of hydrated lime modification of asphalt mixtures: a state-of-the-art review. *Road Materials and Pavement Design*, 14(1), 1-16.
- Little, D. N., & Petersen, J. C. (2005). Unique effects of hydrated lime filler on the performance-related properties of asphalt cements: physical and chemical interactions revisited. *Journal of Materials in Civil Engineering*, 17(2), 207-218.
- Liu, S., Ma, C., Cao, W., & Fang, J. (2010). Influence of aluminate coupling agent on low-temperature rheological performance of asphalt mastic. *Construction and Building Materials*, 24(5), 650-659. doi: <http://dx.doi.org/10.1016/j.conbuildmat.2009.11.004>
- Macnaughton, M. (1924). *Laboratory Investigation of a New Theory of Sheet Asphalt Mixtures*. Paper presented at the Proceedings of the Tenth Annual Conference on Highway Engineering, University of Michigan.
- McCann, M., Anderson-Sprecher, R., Thomas, K. P., & Huang, S.-C. (2006). *Comparison of moisture damage in hot mix asphalt using ultrasonic accelerated moisture conditioning and tensile strength test results*. Paper presented at the

- Airfield and Highway Pavements. The 2006 Airfield and Highway Pavement Specialty Conference.
- McLeod, N. W. (1956). *Relationships between density, bitumen content, and voids properties of compacted bituminous paving mixtures*. Paper presented at the Highway Research Board Proceedings.
- Miller, J., & Traxler, R. (1932). *Some of the Fundamental Physical Characteristics of Mineral Filler Intend, d for Asphalt Paving Mixtures*. Paper presented at the Proceedings of the Association of Asphalt Paving Technologists.
- Mills-Beale, J., & You, Z. (2010). The mechanical properties of asphalt mixtures with recycled concrete aggregates. *Construction and Building Materials*, 24(3), 230-235.
- Paranavithana, S., & Mohajerani, A. (2006). Effects of recycled concrete aggregates on properties of asphalt concrete. *Resources, Conservation and Recycling*, 48(1), 1-12.
- Park, T. (2003). Application of construction and building debris as base and subbase materials in rigid pavement. *Journal of Transportation Engineering*, 129(5), 558-563.
- Poon, C.-S., Qiao, X., & Chan, D. (2006). The cause and influence of self-cementing properties of fine recycled concrete aggregates on the properties of unbound sub-base. *Waste Management*, 26(10), 1166-1172.
- Rahal, K. (2007). Mechanical properties of concrete with recycled coarse aggregate. *Building and environment*, 42(1), 407-415.
- Richardson, C. (1905). *The modern asphalt pavement*: J. Wiley & sons.
- Rigden, P. (1947). The use of fillers in bituminous road surfacings. A study of filler-binder systems in relation to filler characteristics. *Journal of the Society of Chemical Industry*, 66(9), 299-309.
- Shashidhar, N., & Romero, P. (1998). Factors Affecting the Stiffening Potential of Mineral Fillers. *Transportation Research Record: Journal of the Transportation Research Board*, 1638, 94-100. doi: doi:10.3141/1638-11
- Traxler, R. N. (1961). *Asphalt: Its composition, properties, and uses*: Reinhold Pub. Corp.
- Tunncliff, D. G. (1962). A review of mineral filler. *Journal of the Association of Asphalt Paving Technologists*, 31, 118-150.
- Wong, Y. D., Sun, D. D., & Lai, D. (2007). Value-added utilisation of recycled concrete in hot-mix asphalt. *Waste Management*, 27(2), 294-301.
- Yi-qiu, T., Li, Z.-H., Zhang, X.-Y., & Dong, Z.-J. (2010). Research on high-and low-temperature properties of asphalt-mineral filler mastic. *Journal of Materials in Civil Engineering*.
- Yusoff, N. I. M., Shaw, M. T., & Airey, G. D. (2011). Modelling the linear viscoelastic rheological properties of bituminous binders. *Construction and Building Materials*, 25(5), 2171-2189.
- Zeng, M., & Wu, C. (2008). Effects of Type and Content of Mineral Filler on Viscosity of Asphalt Mastic and Mixing and Compaction Temperatures of Asphalt Mixture. *Transportation Research Record: Journal of the Transportation Research Board*, 2051, 31-40. doi: doi:10.3141/2051-05

APPENDIX – A

EXPERIMENTAL PROCEDURES

Image analysis for SEM images using ImageJ software:

- 1) Open the *ImageJ* software. You can download *ImageJ* for free on your own computer by going to: <http://rsb.info.nih.gov/ij/download.html>
- 2) In *ImageJ* use the file menu to open an image
- 3) On the toolbar of *ImageJ* select the line tool. Hold down the shift key and draw a straight line along the length of the scale bar of the image being as precise as possible. This is going to be the known distance that we use as a standard to set the measurements.
- 4) Select **analyze**, then **set scale**. For the known distance type in the distance of your scale bar, and then enter the units (microns in our case).
- 5) Select a region of interest by choosing the box tool, to the far left of the line drawing tool, and draw a box around the area of interest. Only include in the box the particles you want to analyze.
- 6) Under the **Image** tab select **crop**
- 7) Under the **Image** tab select **adjust** then **threshold**
- 8) Adjust the threshold by sliding the bars so that only the particles you wish to analyze are selected. You may need to slide the top bar all the way to the left and then adjust the lower bar to do this, then choose **apply**.
- 9) On the ImageJ toolbar, select the red arrows that indicate that there are more tools, and select **drawing tools**. Use the **eraser tool** to erase any particles you do not wish to measure. For example, you will want to erase particles that are stuck

together because that will count as one particle. Don't worry about the small noise dots. These can be excluded using a size limit explained next.

- 10) Under **analyze** select **analyze particles**. Check display results and other settings you wish to use. Then take the measurements.
- 11) Under the **analyze** tab select **set measurements** and check the shape descriptor and feret's diameter.
- 12) The measurements will show up in a chart. You can then cut and paste these measurements into excel in order to analyze the data and create graphs.

Modified DSR testing procedures:

- 1) Sample setting and trimming @85 °C
- 2) Wet conditioning temperature @40 °C (60 °C for particular purposes)
- 3) Oscillation load for conditioning time @ 1% shear strain, 1.6 Hz (or 10 rad/s) frequency, and 9-minute interval
- 4) Stress sweep test @200 points from 10 Pa to 50,000 Pa with ramp-log profile, and 10 Hz frequency

UAMC testing procedures:

- 1) Locate the highest intensity of sonication using the aluminum foil test which use series of aluminum foil sheets the most intense zones of sonication inside the bath can be quite accurately identified. As consequence of cavitation, the aluminum foils are perforated. The maximum perforation occurs at maximum intensity. Obviously, the sieve should be located at the point where the maximum sonochemical effect achieved.
- 2) Prepare the loose mix following the format of AASHTO T-209.
- 3) Cure the sample for 2 hours at 149 C.

- 4) Remove the sample from the oven and stored at room temperature until the sample cooled to room temperature.
- 5) Sieve the sample on number 16# sieve the sample.
- 6) Batch the sample according to mix gradation.
- 7) Weight the sample before conditioning.
- 8) Place the sample in a glass dish containing distilled water heated at 60 C.
- 9) Place the submerged sample in a vacuum oven to maintain the 60 °C temperature and degassed at – 0.8 bar for 15 minutes.
- 10) Remove the sample from the oven and use the syringe for expelling the retained air bubbles on the sample.
- 11) Transfer the sample to the sieve that is already in water bath and make sure to keep the water level over the sample to avoid the formation of air bubbles again.
- 12) Turn on the ultrasound the required frequency.
- 13) Dry the sample with air and weight the sample and record it as weight after conditioning.
- 14) Calculate the percentage of weight lost.

APPENDIX – B

PHOTOGRAPHS



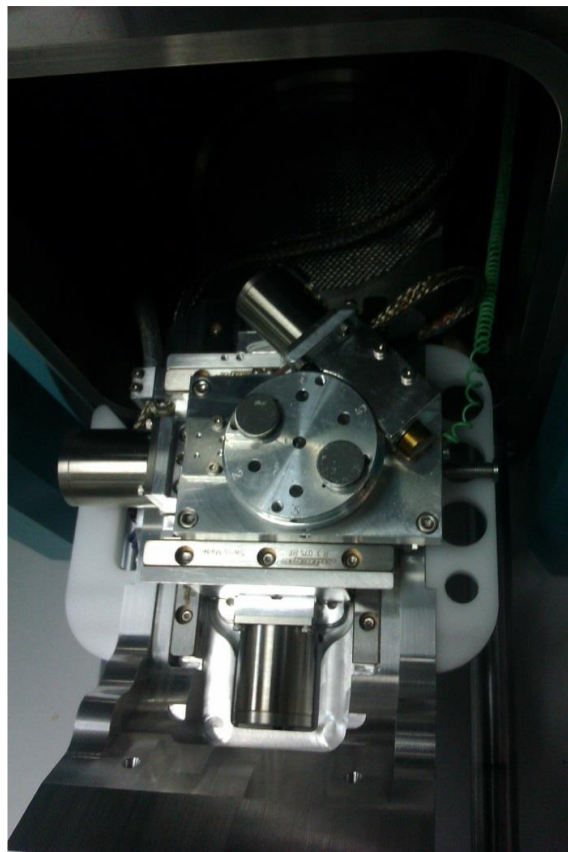
B 1 Surface Area Measurement Machine (BET)



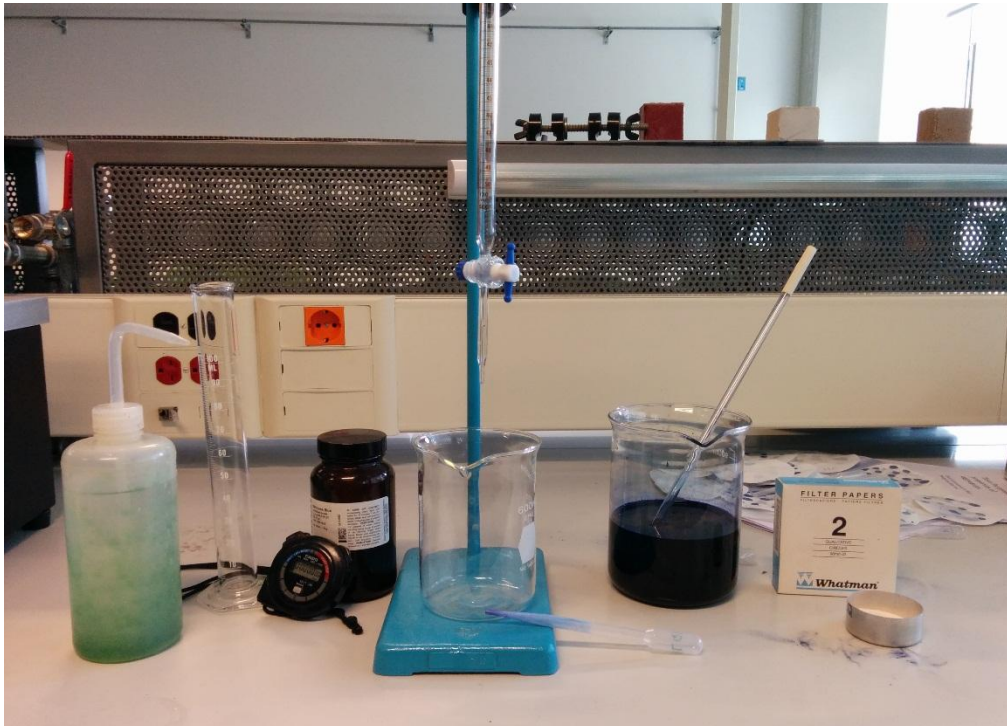
B 2 X-Ray Diffractometer



B 3 Scanning Electron Microscope used at CRSL



B 4 Filler Sample Placed in SEM machine



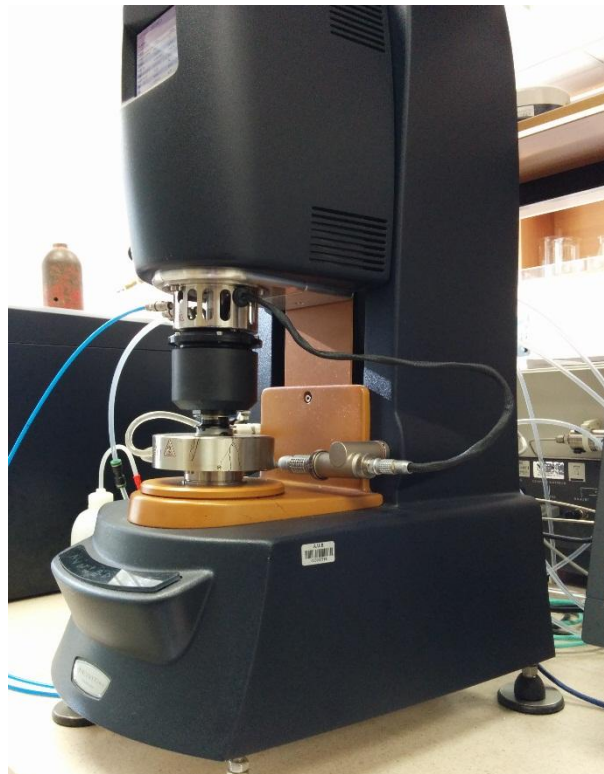
B 5 Methylene Blue Value Experiment



B 6 Mixer Used to Prepare the Mastic (Filler + Binder)



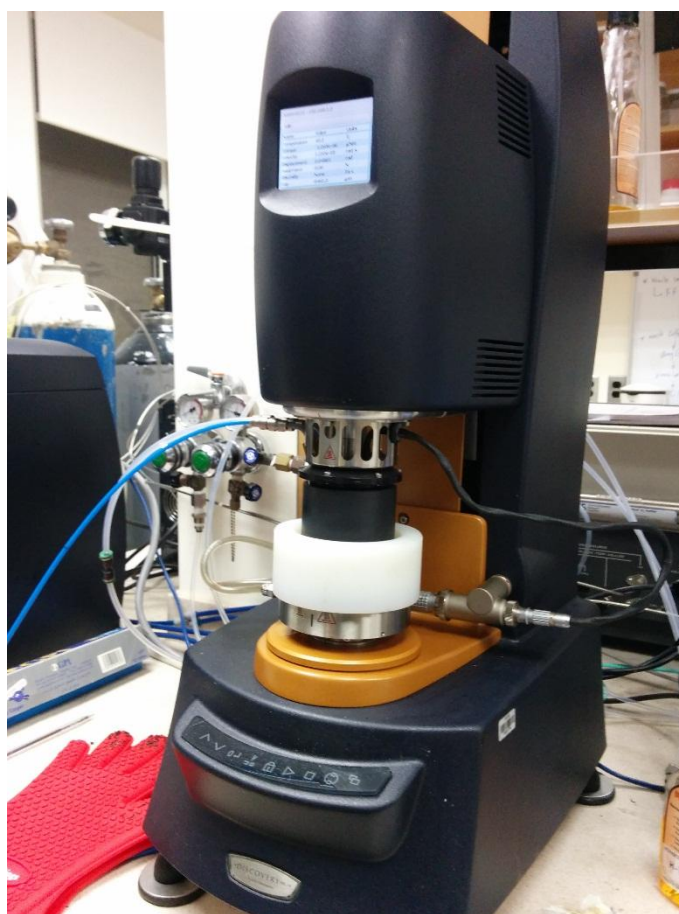
B 7 Crusher Used



B 8 DSR Machine



B 9 Viscosity Meter



B 10 Modified DSR Equipment



B 11 Vacuum Oven Used at CRSL



B 12 Ultrasonic Accelerated Moisture Conditioning Equipment

APPENDIX-C

RAW DATA

Unmodified									
Temperature	Angular frequency	Complex modulus	sin(delta)	G* /sindelta	Phase angle	Tan(delta)	Complex viscosity	Storage modulus	Loss modulus
°C	rad/s	Pa			°		Pa.s	Pa	Pa
52	10	5104.440	0.996	5.124	84.885	11.580	510.444	442.028	5084.565
58	10	2420.330	0.999	2.424	86.999	19.081	242.033	126.740	2417.005
64	10	1078.000	1.000	1.078	88.267	33.826	107.800	32.273	1077.510
70	10	522.700	1.000	0.523	88.895	54.516	52.270	9.916	522.602
76	10	261.153	1.000	0.261	89.302	84.249	26.115	3.128	261.133
Lime Qatar									
Temperature	Angular frequency	Complex modulus	sin(delta)	G* /sindelta	Phase angle	Tan(delta)	Complex viscosity	Storage modulus	Loss modulus
°C	rad/s	Pa			°		Pa.s	Pa	Pa
52	10	13914.500	0.997	13.952	85.780	13.555	1391.450	1024.098	13876.750
58	10	5889.475	0.998	5.899	86.816	17.984	588.947	327.288	5880.370
64	10	2693.425	0.999	2.696	87.644	24.372	269.343	110.965	2691.130
70	10	1315.185	1.000	1.316	88.331	34.383	131.519	38.381	1314.620
76	10	688.907	1.000	0.689	88.889	51.626	68.891	13.350	688.778
Hydrated Cement									
Temperature	Angular frequency	Complex modulus	sin(delta)	G* /sindelta	Phase angle	Tan(delta)	Complex viscosity	Storage modulus	Loss modulus
°C	rad/s	Pa			°		Pa.s	Pa	Pa

52	10	14225.900	0.998	14.252	86.560	16.641	1422.590	853.958	14200.250
58	10	5934.800	0.999	5.940	87.539	23.297	593.480	255.173	5929.305
64	10	2684.470	1.000	2.686	88.275	33.536	268.447	81.135	2683.230
70	10	1298.175	1.000	1.298	88.827	50.085	129.818	26.748	1297.890
76	10	696.219	1.000	0.696	89.149	68.718	69.622	10.378	696.140
Gabbro									
Temperature	Angular frequency	Complex modulus	sin(delta)	G* /sindelta	Phase angle	Tan(delta)	Complex viscosity	o	Loss modulus
°C	rad/s	Pa			°		Pa.s	Pa	Pa
52	10	11737.300	0.998	11.764	86.151	14.908	1173.730	790.601	11710.550
58	10	4951.960	0.999	4.958	87.144	20.293	495.196	248.545	4945.640
64	10	2176.160	0.999	2.177	88.062	30.352	217.616	74.317	2174.860
70	10	1065.180	1.000	1.065	88.745	47.223	106.518	23.512	1064.910
76	10	570.610	1.000	0.571	89.158	69.081	57.061	8.415	570.548
Basalt									
Temperature	Angular frequency	Complex modulus	sin(delta)	G* /sindelta	Phase angle	Tan(delta)	Complex viscosity	Storage modulus	Loss modulus
°C	rad/s	Pa			°		Pa.s	Pa	Pa
52	10	12585.800	0.998	12.612	86.294	15.465	1258.580	815.465	12559.300
58	10	5234.165	0.999	5.240	87.328	21.591	523.416	245.096	5228.380
64	10	2304.130	1.000	2.305	88.224	32.710	230.413	71.743	2302.995
70	10	1121.205	1.000	1.121	88.925	54.456	112.120	21.138	1121.005
76	10	593.189	1.000	0.593	89.419	100.07 3	59.319	6.037	593.158
Lime									
Temperature	Angular frequency	Complex modulus	sin(delta)	G* /sindelta	Phase angle	Tan(delta)	Complex viscosity	Storage modulus	Loss modulus
°C	rad/s	Pa			°		Pa.s	Pa	Pa

52	10	18792.450	0.998	18.835	86.164	14.913	1879.245	1257.180	18750.350
58	10	7875.955	0.999	7.886	87.149	20.081	787.596	391.643	7866.210
64	10	3513.600	0.999	3.516	87.931	27.680	351.360	126.829	3511.310
70	10	1730.645	1.000	1.731	88.501	38.227	173.065	45.240	1730.050
76	10	908.506	1.000	0.909	88.848	50.030	90.851	18.220	908.322
RCA 1									
Temperature	Angular frequency	Complex modulus	sin(delta)	G* /sindelta	Phase angle	Tan(delta)	Complex viscosity	Storage modulus	Loss modulus
°C	rad/s	Pa			°		Pa.s	Pa	Pa
52	10	14050.650	0.998	14.075	86.636	17.014	1405.065	824.477	14026.400
58	10	5945.665	0.999	5.951	87.625	24.133	594.566	246.320	5940.555
64	10	2700.060	1.000	2.701	88.395	36.020	270.006	75.398	2699.000
70	10	1333.455	1.000	1.334	88.872	53.639	133.346	25.973	1333.190
76	10	713.382	1.000	0.713	89.089	74.094	71.338	11.198	713.281
Lime Lebanon									
Temperature	Angular frequency	Complex modulus	sin(delta)	G* /sindelta	Phase angle	Tan(delta)	Complex viscosity	Storage modulus	Loss modulus
°C	rad/s	Pa			°		Pa.s	Pa	Pa
52	10	12370.150	0.998	12.395	86.370	15.762	1237.015	783.249	12345.300
58	10	5261.840	0.999	5.267	87.422	22.215	526.183	236.590	5256.515
64	10	2398.030	1.000	2.399	88.214	32.112	239.803	74.634	2396.865
70	10	1188.865	1.000	1.189	88.708	44.446	118.887	26.742	1188.560
76	10	639.210	1.000	0.639	88.910	52.617	63.921	12.145	639.095

<u>Filler Type</u>	<u>Replicate No.</u>	<u>Creep Stress level</u>	<u>R0.1 & R3.2</u>	<u>% difference in recovery between 0.100kPa and 3.200kPa " Rdiff "</u>	<u>Average non-recoverable creep compliance, kPa-1</u>
Unmodified	1	0.1	1.738340098	94.52043142	9.74768
		3.2	0.095253538		10.89604906
	2	0.1	1.618852575	92.2938581	9.42638
		3.2	0.124751077		10.56711313
Basalt	1	0.1	6.870774271	96.15578999	2.20217
		3.2	0.264126993		2.295635313
	2	0.1	2.566167821	95.46866951	2.35303
		3.2	0.116281545		2.483064688
Gabbro	1	0.1	7.050990678	94.06294388	2.362
		3.2	0.418621274		2.6614625
	2	0.1	5.674587123	96.88510781	3.53268
		3.2	0.176757271		4.056885
Lime Qatar	1	0.1	10.97681509	91.84846714	2.04168
		3.2	0.894778689		2.360113125
	2	0.1	8.611220331	89.96510711	1.9114
		3.2	0.864126737		2.3194125
Hydrated cement	1	0.1	4.406125248	91.38712851	1.48038
		3.2	0.379493905		1.47991625
	2	0.1	4.216874995	86.11364944	1.50429
		3.2	0.585570044		1.677459688
Limestone Lebanon	1	0.1	6.224752013	92.18705001	2.65333
		3.2	0.486336761		2.953217813
	2	0.1	8.240016536	94.36450527	2.91167
		3.2	0.464365698		2.899429063
RCA 1	1	0.1	5.087659758	86.51814162	1.45223
		3.2	0.685911083		1.335767813
	2	0.1	1.08328591	75.97864627	1.57618
		3.2	0.26021994		1.410806875
Lime	1	0.1	12.57542304	85.21125774	1.11389
		3.2	1.859746902		1.181069063
	2	0.1	14.20302265	89.044589	1.26923
		3.2	1.555999505		1.082611563

Sample		Temperature (oC)				
		120	135	150	165	180
Unmodified	1	0.760	0.340	0.170	0.100	0.060
	2	0.760	0.330	0.170	0.090	0.060
	3	0.750	0.340	0.170	0.100	0.060
	Average	0.757	0.337	0.170	0.097	0.060
Lime Qatar	1	3.230	1.450	0.650	0.330	0.180
	2	3.160	1.280	0.610	0.340	0.170
	Average	3.195	1.365	0.630	0.335	0.175
Lime	1	5.280	2.400	1.120	0.590	0.330
	2	5.700	2.510	1.240	0.620	0.350
	Average	5.490	2.455	1.180	0.605	0.340
Gabbro	1	2.460	1.100	0.550	0.290	0.160
	2	2.660	1.210	0.610	0.330	0.190
	Average	2.560	1.155	0.580	0.310	0.175
Basalt	1	2.740	1.230	0.600	0.330	0.180
	2	2.030	0.900	0.450	0.230	0.130
	Average	2.385	1.065	0.525	0.280	0.155
Lime Lebanon	1	2.770	1.170	0.570	0.300	0.170
	2	2.450	1.080	0.530	0.280	0.160
	Average	2.610	1.125	0.550	0.290	0.165
Hydrated cement	1	3.550	1.760	0.830	0.420	0.250
	2	3.560	1.740	0.830	0.430	0.250
	Average	3.555	1.750	0.830	0.425	0.250
RE1	1	5.260	2.370	1.180	0.630	0.380
	2	5.030	2.250	1.100	0.580	0.340
	3	4.040	1.730	0.820	0.430	0.250
	Average	4.777	2.117	1.033	0.547	0.323

TukeyHSD results to compare the surface area of different fillers								
	MeanDiff	SEM	q Value	Prob	Alpha	Sig	LCL	UCL
B G	6.10333	0.85751	10.06569	5.81E-05	0.05	1	3.20401	9.00266
LQ G	-0.97	0.85751	1.59974	0.90845	0.05	0	-3.8693	1.92933
LQ B	-7.07333	0.85751	11.66542	9.89E-06	0.05	1	-9.9727	-4.174
LL G	-0.80333	0.85751	1.32487	0.96012	0.05	0	-3.7027	2.09599
LL B	-6.90667	0.85751	11.39055	1.33E-05	0.05	1	-9.806	-4.0073
LL LQ	0.16667	0.85751	0.27487	0.99999	0.05	0	-2.7327	3.06599
L G	3.41333	0.85751	5.62931	0.0163	0.05	1	0.51401	6.31266
L B	-2.69	0.85751	4.43638	0.07778	0.05	0	-5.5893	0.20933
L LQ	4.38333	0.85751	7.22904	1.93E-03	0.05	1	1.48401	7.28266
L LL	4.21667	0.85751	6.95418	0.00278	0.05	1	1.31734	7.11599

HC G	5.1	0.85751	8.41098	4.25E-04	0.05	1	2.20067	7.99933
HC B	-1.00333	0.85751	1.65471	0.89486	0.05	0	-3.9027	1.89599
HC LQ	6.07	0.85751	10.01071	6.19E-05	0.05	1	3.17067	8.96933
HC LL	5.90333	0.85751	9.73585	8.52E-05	0.05	1	3.00401	8.80266
HC L	1.68667	0.85751	2.78167	0.47122	0.05	0	-1.2127	4.58599
RCA G	6.76667	0.80213	11.93018	7.48E-06	0.05	1	4.0546	9.47874
RCA B	0.66333	0.80213	1.16951	0.97804	0.05	0	-2.0487	3.3754
RCA LQ	7.73667	0.80213	1.36E+01	1.30E-06	0.05	1	5.0246	10.4487
RCA LL	7.57	0.80213	13.34653	1.75E-06	0.05	1	4.85793	10.2821
RCA L	3.35333	0.80213	5.9122	0.01115	0.05	1	0.64126	6.0654
RCA HC	1.66667	0.80213	2.93847	0.41131	0.05	0	-1.0454	4.37874

TukeyHSD results to compare the pore size of different fillers								
	MeanDiff	SEM	q Value	Prob	Alpha	Sig	LCL	UCL
B G	0.01277	0.00426	4.23404	0.10405	0.05	0	-0.00179	0.02732
LQ G	-0.00652	0.00426	2.16328	0.72442	0.05	0	-0.02108	0.00804
LQ B	-0.01929	0.00426	6.39732	0.00669	0.05	1	-0.03385	- 0.00473
LL G	-0.00637	0.00426	2.11196	0.74437	0.05	0	-0.02093	0.00819
LL B	-0.01913	0.00426	6.346	0.00715	0.05	1	-0.03369	- 0.00457
LL LQ	1.55E-04	0.00426	0.05132	1	0.05	0	-0.0144	0.01471
L G	0.01164	0.00426	3.86129	0.16091	0.05	0	-0.00292	0.0262
L B	-0.00112	0.00426	0.37276	0.99996	0.05	0	-0.01568	0.01343
L LQ	0.01816	0.00426	6.02456	0.01081	0.05	1	0.0036	0.03272
L LL	0.01801	0.00426	5.97325	0.01154	0.05	1	0.00345	0.03257
HC G	0.01842	0.00426	6.10951	0.00969	0.05	1	0.00386	0.03298
HC B	0.00565	0.00426	1.87547	0.82923	0.05	0	-0.0089	0.02021
HC LQ	0.02494	0.00426	8.27279	6.48E-04	0.05	1	0.01038	0.0395
HC LL	0.02479	0.00426	8.22147	6.90E-04	0.05	1	0.01023	0.03935
HC L	0.00678	0.00426	2.24822	0.69058	0.05	0	-0.00778	0.02134
RCA G	0.03264	0.00426	10.82637	3.70E-05	0.05	1	0.01808	0.0472
RCA B	0.01988	0.00426	6.59233	0.00521	0.05	1	0.00532	0.03443
RCA LQ	0.03916	0.00426	12.98965	4.35E-06	0.05	1	0.0246	0.05372
RCA LL	0.03901	0.00426	12.93833	4.57E-06	0.05	1	0.02445	0.05357
RCA L	0.021	0.00426	6.96509	0.00325	0.05	1	0.00644	0.03556

RCA HC	0.01422	0.00426	4.71686	0.05755	0.05	0	-3.38E-04	0.02878
TukeyHSD results to compare the solidity index for different fillers								
	MeanDiff	SEM	q Value	Prob	Alpha	Sig	LCL	UCL
B G	-0.00592	0.01175	0.71255	0.99859	0.05	0	-0.04319	0.03135
LQ G	0.03498	0.01175	4.21032	0.07667	0.05	0	-0.00229	0.07225
LQ B	0.0409	0.01175	4.92287	0.02446	0.05	1	0.00363	0.07817
LL G	-0.01418	0.01175	1.70676	0.88563	0.05	0	-0.05145	0.02309
LL B	-0.00826	0.01175	0.9942	0.99132	0.05	0	-0.04553	0.02901
LL LQ	-0.04916	0.01175	5.91708	0.00425	0.05	1	-0.08643	-0.01189
L G	-0.04252	0.01175	5.11786	0.01756	0.05	1	-0.07979	-0.00525
L B	-0.0366	0.01175	4.40531	0.05679	0.05	0	-0.07387	6.71E-04
L LQ	-0.0775	0.01175	9.32818	7.19E-06	0.05	1	-0.11477	-0.04023
L LL	-0.02834	0.01175	3.41111	0.23094	0.05	0	-0.06561	0.00893
HC G	-0.02502	0.01175	3.0115	0.36393	0.05	0	-0.06229	0.01225
HC B	-0.0191	0.01175	2.29895	0.66774	0.05	0	-0.05637	0.01817
HC LQ	-0.06	0.01175	7.22182	3.75E-04	0.05	1	-0.09727	-0.02273
HC LL	-0.01084	0.01175	1.30474	0.96566	0.05	0	-0.04811	0.02643
HC L	0.0175	0.01175	2.10636	0.74847	0.05	0	-0.01977	0.05477
RCA G	-0.03422	0.01175	4.11885	0.08794	0.05	0	-0.07149	0.00305
RCA B	-0.0283	0.01175	3.40629	0.23231	0.05	0	-0.06557	0.00897
RCA LQ	-0.0692	0.01175	8.32917	4.63E-05	0.05	1	-0.10647	-0.03193
RCA LL	-0.02004	0.01175	2.41209	0.6181	0.05	0	-0.05731	0.01723
RCA L	0.0083	0.01175	0.99902	0.9911	0.05	0	-0.02897	0.04557
RCA HC	-0.0092	0.01175	1.10735	0.9848	0.05	0	-0.04647	0.02807

TukeyHSD results to compare the roundness index for different fillers								
	MeanDiff	SEM	q Value	Prob	Alpha	Sig	LCL	UCL
B G	-0.03904	0.05641	0.97881	0.99201	0.05	0	-0.21797	0.13989
LQ G	0.15986	0.05641	4.00801	0.10349	0.05	0	-0.01907	0.33879
LQ B	0.1989	0.05641	4.98682	0.02196	0.05	1	0.01997	0.37783
LL G	0.06044	0.05641	1.51535	0.93127	0.05	0	-0.11849	0.23937
LL B	0.09948	0.05641	2.49416	0.5817	0.05	0	-0.07945	0.27841
LL LQ	-0.09942	0.05641	2.49266	0.58237	0.05	0	-0.27835	0.07951
L G	-0.02136	0.05641	0.53554	0.99972	0.05	0	-0.20029	0.15757
L B	0.01768	0.05641	0.44327	0.99991	0.05	0	-0.16125	0.19661
L LQ	-0.18122	0.05641	4.54355	0.04562	0.05	1	-0.36015	-0.00229
L LL	-0.0818	0.05641	2.05089	0.77036	0.05	0	-0.26073	0.09713
HC G	0.04826	0.05641	1.20997	0.97624	0.05	0	-0.13067	0.22719
HC B	0.0873	0.05641	2.18878	0.7147	0.05	0	-0.09163	0.26623

HC LQ	-0.1116	0.05641	2.79803	0.44942	0.05	0	-0.29053	0.06733
HC LL	-0.01218	0.05641	0.30538	0.99999	0.05	0	-0.19111	0.16675
HC L	0.06962	0.05641	1.74551	0.87468	0.05	0	-0.10931	0.24855
RCA G	0.1124	0.05641	2.81809	0.44105	0.05	0	-0.06653	0.29133
RCA B	0.15144	0.05641	3.7969	0.13953	0.05	0	-0.02749	0.33037
RCA LQ	-0.04746	0.05641	1.18992	0.97813	0.05	0	-0.22639	0.13147
RCA LL	0.05196	0.05641	1.30274	0.96591	0.05	0	-0.12697	0.23089
RCA L	0.13376	0.05641	3.35363	0.24766	0.05	0	-0.04517	0.31269
RCA HC	0.06414	0.05641	1.60812	0.91091	0.05	0	-0.11479	0.24307

TukeyHSD results to compare the circularity index for different fillers								
	MeanDiff	SEM	q Value	Prob	Alpha	Sig	LCL	UCL
B G	-0.03764	0.03479	1.52996	0.92828	0.05	0	-	0.07273
LQ G	0.11328	0.03479	4.60452	0.04136	0.05	1	0.00291	0.22365
LQ B	0.15092	0.03479	6.13449	0.00286	0.05	1	0.04055	0.26129
LL G	-0.0394	0.03479	1.6015	0.91247	0.05	0	-	0.07097
LL B	-0.00176	0.03479	0.07154	1	0.05	0	-	0.10861
LL LQ	-0.15268	0.03479	6.20603	0.0025	0.05	1	0.26305	0.04231
L G	-0.1395	0.03479	5.6703	0.00665	0.05	1	-	0.02913
L B	-0.10186	0.03479	4.14033	0.08518	0.05	0	-	0.00851
L LQ	-0.25278	0.03479	10.27482	1.30E-06	0.05	1	-	0.14241
L LL	-0.1001	0.03479	4.06879	0.0947	0.05	0	-	0.01027
HC G	-0.12644	0.03479	5.13944	0.01692	0.05	1	-	0.01607
HC B	-0.0888	0.03479	3.60948	0.17953	0.05	0	-	0.02157
HC LQ	-0.23972	0.03479	9.74397	3.36E-06	0.05	1	-	0.12935
HC LL	-0.08704	0.03479	3.53794	0.19696	0.05	0	-	0.02333
HC L	0.01306	0.03479	0.53085	0.99974	0.05	0	-	0.12343
RCA G	-0.18734	0.03479	7.61486	1.78E-04	0.05	1	-	0.07697
RCA B	-0.1497	0.03479	6.0849	0.00313	0.05	1	-	0.03933

RCA LQ	-0.30062	0.03479	12.21939	7.42E-08	0.05	1	-	-
RCA LL	-0.14794	0.03479	6.01336	0.00357	0.05	1	-	-
RCA L	-0.04784	0.03479	1.94457	0.81004	0.05	0	-	-
RCA HC	-0.0609	0.03479	2.47542	0.59002	0.05	0	-	-

TukeyHSD results to compare the viscosity for different fillers at 120° C								
	MeanDiff	SEM	q Value	Prob	Alpha	Sig	LCL	UCL
G U	1.8	0.23463	10.84948	8.69E-04	0.05	1	0.872	2.728
B U	1.625	0.23463	9.79467	0.00175	0.05	1	0.697	2.553
B G	-0.175	0.23463	1.05481	0.992	0.05	0	-1.103	0.753
LL U	1.85	0.23463	11.15085	7.17E-04	0.05	1	0.922	2.778
LL G	0.05	0.23463	0.30137	1	0.05	0	-0.878	0.978
LL B	0.225	0.23463	1.35618	0.96895	0.05	0	-0.703	1.153
LQ U	2.435	0.23463	14.67693	9.84E-05	0.05	1	1.50656	3.36344
LQ G	0.635	0.23463	3.82745	0.24377	0.05	0	-0.293	1.563
LQ B	0.81	0.23463	4.88227	0.09526	0.05	0	0	2
LQ LL	0.585	0.23463	3.52608	0.31409	0.05	0	-0.343	1.513
L U	4.73	0.23463	28.51002	4.85E-07	0.05	1	3.802	5.658
L G	2.93	0.23463	17.66054	2.46E-05	0.05	1	2.002	3.858
L B	3.105	0.23463	18.71535	1.58E-05	0.05	1	2.177	4.033
L LL	2.88	0.23463	17.35916	2.80E-05	0.05	1	1.952	3.808
L LQ	2.295	0.23463	13.83308	1.52E-04	0.05	1	1.367	3.223
HC U	2.795	0.23463	16.84683	3.51E-05	0.05	1	1.867	3.723
HC G	0.995	0.23463	5.99735	0.035	0.05	1	0.067	1.923
HC B	1.17	0.23463	7.05216	0.01414	0.05	1	0.242	2.098
HC LL	0.945	0.23463	5.69598	0.04573	0.05	1	0.017	1.873
HC LQ	0.36	0.23463	2.1699	0.77355	0.05	0	-0.568	1.288
HC L	-1.935	0.23463	11.66319	5.22E-04	0.05	1	-2.863	-1.007
RCA U	4.385	0.23463	26.43053	9.76E-07	0.05	1	3.457	5.313

RCA G	2.585	0.23463	15.58106	6.30E-05	0.05	1	1.657	3.513
RCA B	2.76	0.23463	16.63587	3.86E-05	0.05	1	1.832	3.688
RCA LL	2.535	0.23463	15.27968	7.28E-05	0.05	1	1.607	3.463
RCA LQ	1.95	0.23463	11.7536	4.94E-04	0.05	1	1.022	2.878
RCA L	-0.345	0.23463	2.07948	0.80401	0.05	0	-1.273	0.583
RCA HC	1.59	0.23463	9.58371	0.00203	0.05	1	0.662	2.518

TukeyHSD results to compare the viscosity for different fillers at 135° C								
	MeanDiff	SEM	q Value	Prob	Alpha	Sig	LCL	UCL
G U	0.82	0.10753	10.78457	9.06E-04	0.05	1	0.3945	1.2455
B U	0.73	0.10753	9.6009	0.00201	0.05	1	0.3045	1.1555
B G	-0.09	0.10753	1.18367	0.9848	0.05	0	- 0.5155	0.3355
LL U	0.79	0.10753	10.39002	0.00117	0.05	1	0.3645	1.2155
LL G	-0.03	0.10753	0.39456	0.99998	0.05	0	- 0.4555	0.3955
LL B	0.06	0.10753	0.78912	0.99859	0.05	0	- 0.3655	0.4855
LQ U	1.03	0.10753	13.54648	1.77E-04	0.05	1	0.6045	1.4555
LQ G	0.21	0.10753	2.7619	0.55641	0.05	0	- 0.2155	0.6355
LQ B	0.3	0.10753	3.94558	0.22012	0.05	0	- 0.1255	0.7255
LQ LL	0.24	0.10753	3.15646	0.4207	0.05	0	- 0.1855	0.6655
L U	2.12	0.10753	27.88207	6.00E-07	0.05	1	1.6945	2.5455
L G	1.3	0.10753	17.09749	3.15E-05	0.05	1	0.8745	1.7255
L B	1.39	0.10753	18.28117	1.89E-05	0.05	1	0.9645	1.8155
L LL	1.33	0.10753	17.49205	2.64E-05	0.05	1	0.9045	1.7555
L LQ	1.09	0.10753	14.33559	1.17E-04	0.05	1	0.6645	1.5155
HC U	1.415	0.10753	18.60997	1.65E-05	0.05	1	0.9895	1.8405
HC G	0.595	0.10753	7.82539	0.00754	0.05	1	0.1695	1.0205
HC B	0.685	0.10753	9.00906	0.00306	0.05	1	0.2595	1.1105
HC LL	0.625	0.10753	8.21995	0.00554	0.05	1	0.1995	1.0505
HC LQ	0.385	0.10753	5.06349	0.08083	0.05	0	- 0.0405	0.8105
HC L	-0.705	0.10753	9.2721	0.00253	0.05	1	- 1.1305	- 0.2795
RCA U	1.975	0.10753	25.97504	1.14E-06	0.05	1	1.5495	2.4005
RCA G	1.155	0.10753	15.19047	7.61E-05	0.05	1	0.7295	1.5805

RCA B	1.245	0.10753	16.37414	4.35E-05	0.05	1	0.8195	1.6705
RCA LL	1.185	0.10753	15.58502	6.28E-05	0.05	1	0.7595	1.6105
RCA LQ	0.945	0.10753	12.42856	3.32E-04	0.05	1	0.5195	1.3705
RCA L	-0.145	0.10753	1.90703	0.85726	0.05	0	- 0.5705	0.2805
RCA HC	0.56	0.10753	7.36507	0.01093	0.05	1	0.1345	0.9855

TukeyHSD results to compare the viscosity for different fillers at 150° C								
	MeanDiff	SEM	q Value	Prob	Alpha	Sig	LCL	UCL
G U	0.41	0.05596	10.36191	0.00119	0.05	1	0.18857	0.63143
B U	0.355	0.05596	8.97E+00	0.00315	0.05	1	0.13357	0.57643
B G	-0.055	0.05596	1.39001	0.96487	0.05	0	- 0.27643	0.16643
LL U	0.38	0.05596	9.60E+00	0.002	0.05	1	0.15857	0.60143
LL G	-0.03	0.05596	0.75819	0.9989	0.05	0	- 0.25143	0.19143
LL B	0.025	0.05596	0.63182	0.99966	0.05	0	- 0.19643	0.24643
LQ U	0.46	0.05596	1.16E+01	5.34E-04	0.05	1	0.23857	0.68143
LQ G	0.05	0.05596	1.26365	0.97844	0.05	0	- 0.17143	0.27143
LQ B	0.105	0.05596	2.65366	0.5963	0.05	0	- 0.11643	0.32643
LQ LL	0.08	0.05596	2.02184	0.82258	0.05	0	- 0.14143	0.30143
L U	1.01	0.05596	25.52569	1.32E-06	0.05	1	0.78857	1.23143
L G	0.6	0.05596	1.52E+01	7.71E-05	0.05	1	0.37857	0.82143
L B	0.655	0.05596	1.66E+01	4.01E-05	0.05	1	0.43357	0.87643
L LL	0.63	0.05596	1.59E+01	5.36E-05	0.05	1	0.40857	0.85143
L LQ	0.55	0.05596	1.39E+01	1.47E-04	0.05	1	0.32857	0.77143
HC U	0.66	0.05596	1.67E+01	3.78E-05	0.05	1	0.43857	0.88143
HC G	0.25	0.05596	6.32E+00	0.02642	0.05	1	0.02857	0.47143
HC B	0.305	0.05596	7.70825	0.00828	0.05	1	0.08357	0.52643
HC LL	0.28	0.05596	7.07643	0.01386	0.05	1	0.05857	0.50143
HC LQ	0.2	0.05596	5.05459	0.08149	0.05	0	- 0.02143	0.42143
HC L	-0.35	0.05596	8.84554	0.00346	0.05	1	- 0.57143	- 0.12857

RCA U	0.97	0.05596	2.45E+01	1.86E-06	0.05	1	0.74857	1.19143
RCA G	0.56	0.05596	1.42E+01	1.29E-04	0.05	1	0.33857	0.78143
RCA B	0.615	0.05596	1.55E+01	6.41E-05	0.05	1	0.39357	0.83643
RCA LL	0.59	0.05596	1.49E+01	8.74E-05	0.05	1	0.36857	0.81143
RCA LQ	0.51	0.05596	1.29E+01	2.55E-04	0.05	1	0.28857	0.73143
RCA L	-0.04	0.05596	1.01092	0.99374	0.05	0	- 0.26143	0.18143
RCA HC	0.31	0.05596	7.83462	0.00749	0.05	1	0.08857	0.53143

TukeyHSD results to compare the viscosity for different fillers at 165° C								
	MeanDiff	SEM	q Value	Prob	Alpha	Sig	LCL	UCL
G U	0.215	0.03132	9.70652	0.00186	0.05	1	0.09104	0.33896
B U	0.185	0.03132	8.35E+00	0.00501	0.05	1	0.06104	0.30896
B G	-0.03	0.03132	1.3544	0.96916	0.05	0	- 0.15396	0.09396
LL U	0.195	0.03132	8.80E+00	0.00356	0.05	1	0.07104	0.31896
LL G	-0.02	0.03132	0.90293	0.99679	0.05	0	- 0.14396	0.10396
LL B	0.01	0.03132	4.51E-01	0.99996	0.05	0	- 0.11396	0.13396
LQ U	0.24	0.03132	10.83519	8.77E-04	0.05	1	0.11604	0.36396
LQ G	0.025	0.03132	1.13E+00	0.98829	0.05	0	- 0.09896	0.14896
LQ B	0.055	0.03132	2.48E+00	0.65998	0.05	0	- 0.06896	0.17896
LQ LL	0.045	0.03132	2.0316	0.81949	0.05	0	- 0.07896	0.16896
L U	0.51	0.03132	23.02477	3.10E-06	0.05	1	0.38604	0.63396
L G	0.295	0.03132	1.33E+01	2.01E-04	0.05	1	0.17104	0.41896
L B	0.325	0.03132	14.67265	9.87E-05	0.05	1	0.20104	0.44896
L LL	0.315	0.03132	1.42E+01	1.24E-04	0.05	1	0.19104	0.43896
L LQ	0.27	0.03132	1.22E+01	3.81E-04	0.05	1	0.14604	0.39396
HC U	0.33	0.03132	1.49E+01	8.80E-05	0.05	1	0.20604	0.45396

HC G	0.115	0.03132	5.19E+00	0.07197	0.05	0	- 0.00896	0.23896
HC B	0.145	0.03132	6.54626	0.0217	0.05	1	0.02104	0.26896
HC LL	0.135	0.03132	6.09479	0.03212	0.05	1	0.01104	0.25896
HC LQ	0.09	0.03132	4.0632	0.19861	0.05	0	- 0.03396	0.21396
HC L	-0.18	0.03132	8.12639	0.00596	0.05	1	- 0.30396	- 0.05604
RCA U	0.51	0.03132	23.02477	3.10E-06	0.05	1	0.38604	0.63396
RCA G	0.295	0.03132	1.33E+01	2.01E-04	0.05	1	0.17104	0.41896
RCA B	0.325	0.03132	14.67265	9.87E-05	0.05	1	0.20104	0.44896
RCA LL	0.315	0.03132	1.42E+01	1.24E-04	0.05	1	0.19104	0.43896
RCA LQ	0.27	0.03132	1.22E+01	3.81E-04	0.05	1	0.14604	0.39396
RCA L	0	0.03132	0.00E+00	1	0.05	0	- 0.12396	0.12396
RCA HC	0.18	0.03132	8.12639	0.00596	0.05	1	0.05604	0.30396

TukeyHSD results to compare the viscosity for different fillers at 180° C

	MeanDiff	SEM	q Value	Prob	Alpha	Sig	LCL	UCL
G U	0.115	0.01871	8.69318	0	0.05	1	0.04097	0.18903
B U	0.095	0.01871	7.18132	0.013	0.05	1	0.02097	0.16903
B G	-0.02	0.01871	1.51186	0.947	0.05	0	- 0.09403	0.05403
LL U	0.105	0.01871	7.93725	0.007	0.05	1	0.03097	0.17903
LL G	-0.01	0.01871	0.75593	0.999	0.05	0	- 0.08403	0.06403
LL B	0.01	0.01871	0.75593	0.999	0.05	0	- 0.06403	0.08403
LQ U	0.115	0.01871	8.69318	0.004	0.05	1	0.04097	0.18903
LQ G	0	0.01871	0	1.000	0.05	0	- 0.07403	0.07403
LQ B	0.02	0.01871	1.51186	0.947	0.05	0	- 0.05403	0.09403
LQ LL	0.01	0.01871	0.75593	0.999	0.05	0	- 0.06403	0.08403
L U	0.28	0.01871	21.16601	0.000	0.05	1	0.20597	0.35403
L G	0.165	0.01871	12.47283	0.000	0.05	1	0.09097	0.23903
L B	0.185	0.01871	13.98469	0.000	0.05	1	0.11097	0.25903
L LL	0.175	0.01871	13.22876	0.000	0.05	1	0.10097	0.24903
L LQ	0.165	0.01871	12.47283	0.000	0.05	1	0.09097	0.23903
HC U	0.19	0.01871	14.36265	0.000	0.05	1	0.11597	0.26403

HC G	0.075	0.01871	5.66947	0.047	0.05	1	0.00097	0.14903
HC B	0.095	0.01871	7.18132	0.013	0.05	1	0.02097	0.16903
HC LL	0.085	0.01871	6.4254	0.024	0.05	1	0.01097	0.15903
HC LQ	0.075	0.01871	5.66947	0.047	0.05	1	0.00097	0.14903
HC L	-0.09	0.01871	6.80336	0.017	0.05	1	- 0.16403	-0.01597
RCA U	0.3	0.01871	22.67787	0.000	0.05	1	0.22597	0.37403
RCA G	0.185	0.01871	13.98469	0.000	0.05	1	0.11097	0.25903
RCA B	0.205	0.01871	15.49654	0.000	0.05	1	0.13097	0.27903
RCA LL	0.195	0.01871	14.74061	0.000	0.05	1	0.12097	0.26903
RCA LQ	0.185	0.01871	13.98469	0.000	0.05	1	0.11097	0.25903
RCA L	0.02	0.01871	1.51186	0.947	0.05	0	- 0.05403	0.09403
RCA HC	0.11	0.01871	8.31522	0.00515	0.05	1	0.03597	0.18403

TukeyHSD results to compare the complex modulus for different fillers at 52° (10 rad/sec)								
	MeanDiff	SEM	q Value	Prob	Alpha	Sig	LCL	UCL
G U	6632.86	752.9966	12.45727	3.26E-04	0.05	1	3653.182	9612.538
B U	7481.36	752.9966	14.05085	1.36E-04	0.05	1	4501.682	10461.04
B G	848.5	752.9966	1.59358	0.93271	0.05	0	-2131.18	3828.178
LL U	7265.71	752.9966	13.64583	1.68E-04	0.05	1	4286.032	10245.39
LL G	632.85	752.9966	1.18856	0.98445	0.05	0	-2346.83	3612.528
LL B	-215.65	752.9966	0.40502	0.99998	0.05	0	-3195.33	2764.028
LQ U	8810.06	752.9966	16.5463	4.02E-05	0.05	1	5830.382	11789.74
LQ G	2177.2	752.9966	4.08903	0.19415	0.05	0	-802.478	5156.878
LQ B	1328.7	752.9966	2.49545	0.65535	0.05	0	-1650.98	4308.378
LQ LL	1544.35	752.9966	2.90047	0.50667	0.05	0	-1435.33	4524.028
L U	13688.01	752.9966	25.70764	1.24E-06	0.05	1	10708.33	16667.69
L G	7055.15	752.9966	13.25038	2.08E-04	0.05	1	4075.472	10034.83
L B	6206.65	752.9966	11.6568	5.24E-04	0.05	1	3226.972	9186.328
L LL	6422.3	752.9966	12.06181	4.11E-04	0.05	1	3442.622	9401.978
L LQ	4877.95	752.9966	9.16135	0.00274	0.05	1	1898.272	7857.628
HC U	9121.46	752.9966	17.13114	3.10E-05	0.05	1	6141.782	12101.14

HC G	2488.6	752.9966	4.67387	0.11504	0.05	0	-491.078	5468.278
HC B	1640.1	752.9966	3.08029	0.44534	0.05	0	-1339.58	4619.778
HC LL	1855.75	752.9966	3.48531	0.32475	0.05	0	-1123.93	4835.428
HC LQ	311.4	752.9966	0.58484	0.99979	0.05	0	-2668.28	3291.078
HC L	-4566.55	752.9966	8.5765	0.00422	0.05	1	-7546.23	-1586.87
RCA U	8946.21	752.9966	16.802	3.58E-05	0.05	1	5966.532	11925.89
RCA G	2313.35	752.9966	4.34474	0.15471	0.05	0	-666.328	5293.028
RCA B	1464.85	752.9966	2.75116	0.56034	0.05	0	-1514.83	4444.528
RCA LL	1680.5	752.9966	3.15617	0.42079	0.05	0	-1299.18	4660.178
RCA LQ	136.15	752.9966	0.25571	1	0.05	0	-2843.53	3115.828
RCA L	-4741.8	752.9966	8.90564	0.00331	0.05	1	-7721.48	-1762.12
RCA HC	-175.25	752.9966	0.32914	1	0.05	0	-3154.93	2804.428

TukeyHSD results to compare the complex modulus for different fillers at 58° (10 rad/sec)								
	MeanDiff	SEM	q Value	Prob	Alpha	Sig	LCL	UCL
G U	2531.63	276.9229	12.92874	2.49E-04	0.05	1	1435.82	3627.44
B U	2813.835	276.9229	14.36993	1.15E-04	0.05	1	1718.025	3909.645
B G	282.205	276.9229	1.44119	0.95803	0.05	0	-813.605	1378.015
LL U	2841.51	276.9229	14.51127	1.07E-04	0.05	1	1745.7	3937.32
LL G	309.88	276.9229	1.58252	0.93481	0.05	0	-785.93	1405.69
LL B	27.675	276.9229	0.14133	1	0.05	0	-1068.13	1123.485
LQ U	3469.145	276.9229	17.71653	2.40E-05	0.05	1	2373.335	4564.955
LQ G	937.515	276.9229	4.78778	0.10377	0.05	0	-158.295	2033.325
LQ B	655.31	276.9229	3.34659	0.36308	0.05	0	-440.5	1751.12
LQ LL	627.635	276.9229	3.20526	0.40536	0.05	0	-468.175	1723.445
L U	5455.625	276.9229	27.86125	6.05E-07	0.05	1	4359.815	6551.435
L G	2923.995	276.9229	14.93251	8.65E-05	0.05	1	1828.185	4019.805
L B	2641.79	276.9229	13.49132	1.83E-04	0.05	1	1545.98	3737.6
L LL	2614.115	276.9229	13.34999	1.97E-04	0.05	1	1518.305	3709.925
L LQ	1986.48	276.9229	10.14473	0.00138	0.05	1	890.67	3082.29
HC U	3514.47	276.9229	17.948	2.17E-05	0.05	1	2418.66	4610.28
HC G	982.84	276.9229	5.01925	0.08414	0.05	0	-112.97	2078.65
HC B	700.635	276.9229	3.57806	0.3009	0.05	0	-395.175	1796.445

HC LL	672.96	276.9229	3.43673	0.33781	0.05	0	-422.85	1768.77
HC LQ	45.325	276.9229	0.23147	1	0.05	0	-1050.48	1141.135
HC L	-1941.16	276.9229	9.91326	0.00162	0.05	1	-3036.96	-845.345
RCA U	3525.335	276.9229	18.00348	2.12E-05	0.05	1	2429.525	4621.145
RCA G	993.705	276.9229	5.07474	0.08001	0.05	0	-102.105	2089.515
RCA B	711.5	276.9229	3.63355	0.28732	0.05	0	-384.31	1807.31
RCA LL	683.825	276.9229	3.49222	0.32292	0.05	0	-411.985	1779.635
RCA LQ	56.19	276.9229	0.28696	1	0.05	0	-1039.62	1152
RCA L	-1930.29	276.9229	9.85777	0.00168	0.05	1	-3026.1	-834.48
RCA HC	10.865	276.9229	0.05549	1	0.05	0	-1084.94	1106.675

TukeyHSD results to compare the complex modulus for different fillers at 64° (10 rad/sec)								
	MeanDiff	SEM	q Value	Prob	Alpha	Sig	LCL	UCL
G U	1098.16	152.034	10.21504	0.00132	0.05	1	496.5473	1699.773
B U	1226.13	152.034	11.40541	6.12E-04	0.05	1	624.5173	1827.743
B G	127.97	152.034	1.19037	0.98432	0.05	0	-473.643	729.5827
LL U	1320.03	152.034	12.27886	3.62E-04	0.05	1	718.4173	1921.643
LL G	221.87	152.034	2.06383	0.80912	0.05	0	-379.743	823.4827
LL B	93.9	152.034	0.87345	0.99737	0.05	0	-507.713	695.5127
LQ U	1615.425	152.034	15.02661	8.25E-05	0.05	1	1013.812	2217.038
LQ G	517.265	152.034	4.81158	0.10156	0.05	0	-84.3477	1118.878
LQ B	389.295	152.034	3.62121	0.2903	0.05	0	-212.318	990.9077
LQ LL	295.395	152.034	2.74775	0.56158	0.05	0	-306.218	897.0077
L U	2435.6	152.034	22.65585	3.53E-06	0.05	1	1833.987	3037.213
L G	1337.44	152.034	12.44081	3.29E-04	0.05	1	735.8273	1939.053
L B	1209.47	152.034	11.25044	6.74E-04	0.05	1	607.8573	1811.083
L LL	1115.57	152.034	10.37698	0.00118	0.05	1	513.9573	1717.183
L LQ	820.175	152.034	7.62923	0.00882	0.05	1	218.5623	1421.788
HC U	1606.47	152.034	14.94332	8.60E-05	0.05	1	1004.857	2208.083
HC G	508.31	152.034	4.72828	0.10952	0.05	0	-93.3027	1109.923
HC B	380.34	152.034	3.53791	0.31105	0.05	0	-221.273	981.9527
HC LL	286.44	152.034	2.66445	0.59229	0.05	0	-315.173	888.0527
HC LQ	-8.955	152.034	0.0833	1	0.05	0	-610.568	592.6577
HC L	-829.13	152.034	7.71253	0.00825	0.05	1	-1430.74	-227.517

RCA U	1622.06	152.034	15.08833	8.01E-05	0.05	1	1020.447	2223.673
RCA G	523.9	152.034	4.8733	0.09604	0.05	0	-77.7127	1125.513
RCA B	395.93	152.034	3.68292	0.27566	0.05	0	-205.683	997.5427
RCA LL	302.03	152.034	2.80947	0.53913	0.05	0	-299.583	903.6427
RCA LQ	6.635	152.034	0.06172	1	0.05	0	-594.978	608.2477
RCA L	-813.54	152.034	7.56751	0.00927	0.05	1	-1415.15	-211.927
RCA HC	15.59	152.034	0.14502	1	0.05	0	-586.023	617.2027

TukeyHSD results to compare the complex modulus for different fillers at 70° (10 rad/sec)

	MeanDiff	SEM	q Value	Prob	Alpha	Sig	LCL	UCL
G U	542.48	75.47729	10.16442	0.00136	0.05	1	243.8093	841.1507
B U	598.505	75.47729	11.21415	6.89E-04	0.05	1	299.8343	897.1757
B G	56.025	75.47729	1.04974	0.99222	0.05	0	-242.646	354.6957
LL U	666.165	75.47729	12.4819	3.21E-04	0.05	1	367.4943	964.8357
LL G	123.685	75.47729	2.31748	0.72115	0.05	0	-174.986	422.3557
LL B	67.66	75.47729	1.26774	0.97807	0.05	0	-231.011	366.3307
LQ U	792.485	75.47729	14.84875	9.02E-05	0.05	1	493.8143	1091.156
LQ G	250.005	75.47729	4.68433	0.11396	0.05	0	-48.6657	548.6757
LQ B	193.98	75.47729	3.63459	0.28707	0.05	0	-104.691	492.6507
LQ LL	126.32	75.47729	2.36685	0.70309	0.05	0	-172.351	424.9907
L U	1207.945	75.47729	22.6332	3.56E-06	0.05	1	909.2743	1506.616
L G	665.465	75.47729	12.46878	3.24E-04	0.05	1	366.7943	964.1357
L B	609.44	75.47729	11.41904	6.07E-04	0.05	1	310.7693	908.1107
L LL	541.78	75.47729	10.1513	0.00138	0.05	1	243.1093	840.4507
L LQ	415.46	75.47729	7.78445	0.00779	0.05	1	116.7893	714.1307
HC U	775.475	75.47729	14.53003	1.06E-04	0.05	1	476.8043	1074.146
HC G	232.995	75.47729	4.36561	0.15185	0.05	0	-65.6757	531.6657
HC B	176.97	75.47729	3.31588	0.37199	0.05	0	-121.701	475.6407
HC LL	109.31	75.47729	2.04814	0.8142	0.05	0	-189.361	407.9807
HC LQ	-17.01	75.47729	0.31872	1	0.05	0	-315.681	281.6607
HC L	-432.47	75.47729	8.10317	0.00607	0.05	1	-731.141	-133.799
RCA U	810.755	75.47729	15.19107	7.61E-05	0.05	1	512.0843	1109.426
RCA G	268.275	75.47729	5.02665	0.08358	0.05	0	-30.3957	566.9457
RCA B	212.25	75.47729	3.97692	0.21419	0.05	0	-86.4207	510.9207

RCA LL	144.59	75.47729	2.70917	0.57575	0.05	0	-154.081	443.2607
RCA LQ	18.27	75.47729	0.34232	0.99999	0.05	0	-280.401	316.9407
RCA L	-397.19	75.47729	7.44213	0.01026	0.05	1	-695.861	-98.5193
RCA HC	35.28	75.47729	0.66104	0.99954	0.05	0	-263.391	333.9507

TukeyHSD results to compare the complex modulus for different fillers at 76° (10 rad/sec)								
	MeanDiff	SEM	q Value	Prob	Alpha	Sig	LCL	UCL
G U	309.4575	29.82868	14.67175	9.87E-05	0.05	1	191.4226	427.4924
B U	332.036	29.82868	15.74222	5.84E-05	0.05	1	214.0011	450.0709
B G	22.5785	29.82868	1.07047	0.9913	0.05	0	-95.4564	140.6134
LL U	378.0575	29.82868	17.92416	2.20E-05	0.05	1	260.0226	496.0924
LL G	68.6	29.82868	3.25241	0.3909	0.05	0	-49.4349	186.6349
LL B	46.0215	29.82868	2.18193	0.76939	0.05	0	-72.0134	164.0564
LQ U	427.754	29.82868	20.28033	9.48E-06	0.05	1	309.7191	545.7889
LQ G	118.2965	29.82868	5.60858	0.04945	0.05	1	0.2616	236.3314
LQ B	95.718	29.82868	4.5381	0.13004	0.05	0	-22.3169	213.7529
LQ LL	49.6965	29.82868	2.35617	0.70702	0.05	0	-68.3384	167.7314
L U	647.353	29.82868	30.69178	2.21E-07	0.05	1	529.3181	765.3879
L G	337.8955	29.82868	16.02003	5.12E-05	0.05	1	219.8606	455.9304
L B	315.317	29.82868	14.94956	8.58E-05	0.05	1	197.2821	433.3519
L LL	269.2955	29.82868	12.76762	2.73E-04	0.05	1	151.2606	387.3304
L LQ	219.599	29.82868	10.41145	0.00116	0.05	1	101.5641	337.6339
HC U	435.066	29.82868	20.627	7.51E-06	0.05	1	317.0311	553.1009
HC G	125.6085	29.82868	5.95525	0.03632	0.05	1	7.5736	243.6434
HC B	103.03	29.82868	4.88478	0.09504	0.05	0	-15.0049	221.0649
HC LL	57.0085	29.82868	2.70284	0.57809	0.05	0	-61.0264	175.0434
HC LQ	7.312	29.82868	0.34667	0.99999	0.05	0	-110.723	125.3469
HC L	-212.287	29.82868	10.06478	0.00146	0.05	1	-330.322	-94.2521
RCA U	452.2295	29.82868	21.44074	5.61E-06	0.05	1	334.1946	570.2644
RCA G	142.772	29.82868	6.76899	0.01794	0.05	1	24.7371	260.8069
RCA B	120.1935	29.82868	5.69852	0.04563	0.05	1	2.1586	238.2284
RCA LL	74.172	29.82868	3.51658	0.31655	0.05	0	-43.8629	192.2069

RCA LQ	24.4755	29.82868	1.16041	0.98636	0.05	0	-93.5594	142.5104
RCA L	-195.124	29.82868	9.25104	0.00257	0.05	1	-313.158	-77.0886
RCA HC	17.1635	29.82868	0.81374	0.9983	0.05	0	-100.871	135.1984

TukeyHSD results to compare the Jnr 0.1 for different fillers at 64° C								
	MeanDiff	SEM	q Value	Prob	Alpha	Sig	LCL	UCL
G U	-6.63969	0.31822	29.50734	3.42E-07	0.05	1	-	-
B U	-7.30943	0.31822	32.48373	1.04E-07	0.05	1	-	-
B G	-0.66974	0.31822	2.97638	0.48028	0.05	0	-	-
LL U	-6.80453	0.31822	30.23991	2.62E-07	0.05	1	-	-
LL G	-0.16484	0.31822	0.73256	0.99912	0.05	0	-	-
LL B	0.5049	0.31822	2.24382	0.74766	0.05	0	-	-
LQ U	-7.61049	0.31822	33.82166	4.96E-08	0.05	1	-	-
LQ G	-0.9708	0.31822	4.31432	0.15898	0.05	0	-	-
LQ B	-0.30106	0.31822	1.33794	0.97101	0.05	0	-	-
LQ LL	-0.80596	0.31822	3.58175	0.29998	0.05	0	-	-
L U	-8.39547	0.31822	37.31018	0	0.05	1	-	-
L G	-1.75578	0.31822	7.80283	0.00768	0.05	1	-	-
L B	-1.08604	0.31822	4.82645	0.1002	0.05	0	-	-
L LL	-1.59094	0.31822	7.07027	0.01393	0.05	1	-	-
L LQ	-0.78498	0.31822	3.48852	0.3239	0.05	0	-	-
HC U	-8.09469	0.31822	35.97351	0	0.05	1	-	-
HC G	-1.45501	0.31822	6.46617	0.02325	0.05	1	-	-
HC B	-0.78527	0.31822	3.48978	0.32356	0.05	0	-	-
HC LL	-1.29016	0.31822	5.7336	0.04422	0.05	1	-	-
HC LQ	-0.48421	0.31822	2.15185	0.77975	0.05	0	-	-

HC L	0.30078	0.31822	1.33667	0.97115	0.05	0	- 0.95847	1.56002
RCA U	-8.07282	0.31822	35.87632	1.42E-09	0.05	1	- 9.33207	- 6.81358
RCA G	-1.43314	0.31822	6.36897	0.02528	0.05	1	- 2.69238	- 0.17389
RCA B	-0.7634	0.31822	3.39259	0.35001	0.05	0	- 2.02264	0.49585
RCA LL	-1.26829	0.31822	5.63641	0.04823	0.05	1	- 2.52754	- 0.00905
RCA LQ	-0.46233	0.31822	2.05466	0.8121	0.05	0	- 1.72158	0.79691
RCA L	0.32265	0.31822	1.43386	0.95906	0.05	0	-0.9366	1.58189
RCA HC	0.02187	0.31822	0.09719	1	0.05	0	- 1.23737	1.28111

TukeyHSD results to compare the Jnr 3.2 for different fillers at 64° C								
	MeanDiff	SEM	q Value	Prob	Alpha	Sig	LCL	UCL
G U	-7.37241	0.36325	28.70276	4.54E-07	0.05	1	- 8.80981	- 5.93501
B U	-8.34223	0.36325	32.47854	1.04E-07	0.05	1	- 9.77963	- 6.90483
B G	-0.96982	0.36325	3.77578	0.25479	0.05	0	- 2.40722	0.46757
LL U	-7.80526	0.36325	30.38796	2.48E-07	0.05	1	- 9.24266	- 6.36786
LL G	-0.43285	0.36325	1.6852	0.91385	0.05	0	- 1.87025	1.00455
LL B	0.53697	0.36325	2.09058	0.80035	0.05	0	- 0.90042	1.97437
LQ U	-8.39182	0.36325	32.6716	9.45E-08	0.05	1	- 9.82922	- 6.95442
LQ G	-1.01941	0.36325	3.96884	0.21571	0.05	0	- 2.45681	0.41799
LQ B	-0.04959	0.36325	0.19306	1	0.05	0	- 1.48699	1.38781
LQ LL	-0.58656	0.36325	2.28364	0.7334	0.05	0	- 2.02396	0.85084
L U	-9.59974	0.36325	37.37436	0	0.05	1	- 11.0371	- 8.16234
L G	-2.22733	0.36325	8.67161	0.00393	0.05	1	- 3.66473	- 0.78994
L B	-1.25751	0.36325	4.89582	0.0941	0.05	0	- 2.69491	0.17989
L LL	-1.79448	0.36325	6.9864	0.01494	0.05	1	- 3.23188	- 0.35709

L LQ	-1.20792	0.36325	4.70277	0.11207	0.05	0	- 2.64532	0.22948
HC U	-9.06785	0.36325	35.30358	1.16E-08	0.05	1	- 10.5053	- 7.63045
HC G	-1.69544	0.36325	6.60082	0.02071	0.05	1	- 3.13284	- 0.25805
HC B	-0.72562	0.36325	2.82503	0.53353	0.05	0	- 2.16302	0.71178
HC LL	-1.26259	0.36325	4.91562	0.09242	0.05	0	- 2.69999	0.1748
HC LQ	-0.67603	0.36325	2.63198	0.60436	0.05	0	- 2.11343	0.76137
HC L	0.53189	0.36325	2.07079	0.80686	0.05	0	- 0.90551	1.96929
RCA U	-9.35829	0.36325	36.43435	0	0.05	1	- 10.7957	-7.9209
RCA G	-1.98589	0.36325	7.73159	0.00813	0.05	1	- 3.42328	- 0.54849
RCA B	-1.01606	0.36325	3.9558	0.21817	0.05	0	- 2.45346	0.42134
RCA LL	-1.55304	0.36325	6.04639	0.03352	0.05	1	- 2.99043	- 0.11564
RCA LQ	-0.96648	0.36325	3.76275	0.25764	0.05	0	- 2.40387	0.47092
RCA L	0.24145	0.36325	0.94002	0.99591	0.05	0	- 1.19595	1.67885
RCA HC	-0.29044	0.36325	1.13077	0.98817	0.05	0	- 1.72784	1.14696

TukeyHSD results to compare the UAMC result for 2 hours conditioning								
	MeanDiff	SEM	q Value	Prob	Alpha	Sig	LCL	UCL
B G	-0.27406	0.05603	6.91755	0.01759	0.05	1	-0.49615	-0.05197
LL G	-0.22542	0.05603	5.68994	0.04664	0.05	1	-0.44751	-0.00334
LL B	0.04864	0.05603	1.22761	0.96701	0.05	0	-0.17345	0.27072
LQ G	-0.03544	0.05603	0.89444	0.99296	0.05	0	-0.25752	0.18665
LQ B	0.23862	0.05603	6.02311	0.03554	0.05	1	0.01654	0.46071
LQ LL	0.18999	0.05603	4.7955	0.09872	0.05	0	-0.0321	0.41207
L G	-0.24542	0.05603	6.19476	0.03096	0.05	1	-0.46751	-0.02334
L B	0.02864	0.05603	0.72279	0.99772	0.05	0	-0.19345	0.25072
L LL	-0.02	0.05603	0.50482	0.99969	0.05	0	-0.24209	0.20209
L LQ	-0.20999	0.05603	5.30032	0.06447	0.05	0	-0.43207	0.0121
HC G	-0.23042	0.05603	5.81615	0.04206	0.05	1	-0.45251	-0.00834
HC B	0.04364	0.05603	1.1014	0.98013	0.05	0	-0.17845	0.26572
HC LL	-0.005	0.05603	0.12621	1	0.05	0	-0.22709	0.21709
HC LQ	-0.19499	0.05603	4.92171	0.0887	0.05	0	-0.41707	0.0271

HC L	0.015	0.05603	0.37862	0.99994	0.05	0	-0.20709	0.23709
RCA G	-0.05161	0.05603	1.30271	0.95695	0.05	0	-0.2737	0.17048
RCA B	0.22245	0.05603	5.61484	0.04962	0.05	1	3.61E-04	0.44454
RCA LL	0.17381	0.05603	4.38723	0.13966	0.05	0	-0.04827	0.3959
RCA LQ	-0.01617	0.05603	0.40827	0.99991	0.05	0	-0.23826	0.20591
RCA L	0.19381	0.05603	4.89205	0.09095	0.05	0	-0.02827	0.4159
RCA HC	0.17881	0.05603	4.51343	0.12546	0.05	0	-0.04327	0.4009

TukeyHSD results to compare the UAMC result for 3 hours conditioning								
	MeanDiff	SEM	q Value	Prob	Alpha	Sig	LCL	UCL
B G	-0.21836	0.04862	6.35126	0.02733	0.05	1	-0.41108	-0.02563
LL G	-0.05232	0.04862	1.52191	0.91722	0.05	0	-0.24505	0.1404
LL B	0.16603	0.04862	4.82935	0.09592	0.05	0	-0.02669	0.35876
LQ G	0.02449	0.04862	0.71241	0.99789	0.05	0	-0.16823	0.21722
LQ B	0.24285	0.04862	7.06367	0.01575	0.05	1	0.05012	0.43557
LQ LL	0.07682	0.04862	2.23432	0.69852	0.05	0	-0.11591	0.26954
L G	-0.10232	0.04862	2.97624	0.43678	0.05	0	-0.29505	0.0904
L B	0.11603	0.04862	3.37502	0.3228	0.05	0	-0.07669	0.30876
L LL	-0.05	0.04862	1.45433	0.93114	0.05	0	-0.24272	0.14272
L LQ	-0.12682	0.04862	3.68865	0.25082	0.05	0	-0.31954	0.06591
HC G	-0.17232	0.04862	5.01231	0.08215	0.05	0	-0.36505	0.0204
HC B	0.04603	0.04862	1.33895	0.95146	0.05	0	-0.14669	0.23876
HC LL	-0.12	0.04862	3.4904	0.29454	0.05	0	-0.31272	0.07272
HC LQ	-0.19682	0.04862	5.72472	0.04533	0.05	1	-0.38954	-0.00409
HC L	-0.07	0.04862	2.03607	0.76902	0.05	0	-0.26272	0.12272
RCA G	0.05996	0.04862	1.74394	0.86149	0.05	0	-0.13277	0.25268
RCA B	0.27831	0.04862	8.0952	0.00743	0.05	1	0.08559	0.47104
RCA LL	0.11228	0.04862	3.26585	0.35151	0.05	0	-0.08044	0.305
RCA LQ	0.03546	0.04862	1.03153	0.98555	0.05	0	-0.15726	0.22819
RCA L	0.16228	0.04862	4.72018	0.10524	0.05	0	-0.03044	0.355
RCA HC	0.23228	0.04862	6.75625	0.01991	0.05	1	0.03956	0.425

TukeyHSD results to compare the UAMC result for 4 hours conditioning								
	MeanDiff	SEM	q Value	Prob	Alpha	Sig	LCL	UCL
B G	-1.08781	0.04055	37.94032	2.73E-07	0.05	1	-1.24853	-0.92708
LL G	-0.83208	0.04055	29.02102	1.88E-06	0.05	1	-0.9928	-0.67135
LL B	0.25573	0.04055	8.9193	0.00425	0.05	1	0.09501	0.41645
LQ G	-0.48637	0.04055	16.96341	7.25E-05	0.05	1	-0.64709	-0.32564

LQ B	0.60144	0.04055	20.97691	1.74E-05	0.05	1	0.44072	0.76217
LQ LL	0.34571	0.04055	12.05761	6.70E-04	0.05	1	0.18499	0.50643
L G	-1.44708	0.04055	50.47085	0	0.05	1	-1.6078	-1.28635
L B	-0.35927	0.04055	12.53053	5.25E-04	0.05	1	-0.51999	-0.19855
L LL	-0.615	0.04055	21.44983	1.50E-05	0.05	1	-0.77572	-0.45428
L LQ	-0.96071	0.04055	33.50744	6.87E-07	0.05	1	-1.12143	-0.79999
HC G	-0.95708	0.04055	33.38074	7.06E-07	0.05	1	-1.1178	-0.79635
HC B	0.13073	0.04055	4.55958	0.12063	0.05	0	-0.02999	0.29145
HC LL	-0.125	0.04055	4.35972	0.14296	0.05	0	-0.28572	0.03572
HC LQ	-0.47071	0.04055	16.41733	9.01E-05	0.05	1	-0.63143	-0.30999
HC L	0.49	0.04055	17.09011	6.90E-05	0.05	1	0.32928	0.65072
RCA G	-0.68891	0.04055	24.02765	6.74E-06	0.05	1	-0.84963	-0.52819
RCA B	0.3989	0.04055	13.91267	2.67E-04	0.05	1	0.23817	0.55962
RCA LL	0.14317	0.04055	4.99337	0.08348	0.05	0	-0.01756	0.30389
RCA LQ	-0.20254	0.04055	7.06424	0.01574	0.05	1	-0.36327	-0.04182
RCA L	0.75817	0.04055	26.4432	3.56E-06	0.05	1	0.59744	0.91889
RCA HC	0.26817	0.04055	9.35309	0.00321	0.05	1	0.10744	0.42889

TukeyHSD results to compare the UAMC result for 5 hours conditioning								
	MeanDiff	SEM	q Value	Prob	Alpha	Sig	LCL	UCL
B G	-0.31153	0.05074	8.68316	0.00497	0.05	1	-0.51266	-0.11041
LL G	-0.7723	0.05074	21.52574	1.46E-05	0.05	1	-0.97342	-0.57118
LL B	-0.46077	0.05074	12.84258	4.48E-04	0.05	1	-0.66189	-0.25964
LQ G	-0.71665	0.05074	19.97459	2.51E-05	0.05	1	-0.91777	-0.51553
LQ B	-0.40511	0.05074	11.29143	0.00101	0.05	1	-0.60624	-0.20399
LQ LL	0.05565	0.05074	1.55114	0.91074	0.05	0	-0.14547	0.25677
L G	-1.6073	0.05074	44.79906	0	0.05	1	-1.80842	-1.40618
L B	-1.29577	0.05074	36.1159	3.97E-07	0.05	1	-1.49689	-1.09464
L LL	-0.835	0.05074	23.27332	8.43E-06	0.05	1	-1.03612	-0.63388
L LQ	-0.89065	0.05074	24.82447	5.36E-06	0.05	1	-1.09177	-0.68953
HC G	-0.7973	0.05074	22.22254	1.16E-05	0.05	1	-0.99842	-0.59618

HC B	-0.48577	0.05074	13.53938	3.19E-04	0.05	1	-0.68689	-0.28464
HC LL	-0.025	0.05074	0.69681	0.99813	0.05	0	-0.22612	0.17612
HC LQ	-0.08065	0.05074	2.24795	0.69355	0.05	0	-0.28177	0.12047
HC L	0.81	0.05074	22.57652	1.04E-05	0.05	1	0.60888	1.01112
RCA G	-0.65139	0.05074	18.15565	4.61E-05	0.05	1	-0.85251	-0.45027
RCA B	-0.33985	0.05074	9.47249	0.00297	0.05	1	-0.54098	-0.13873
RCA LL	0.12091	0.05074	3.37009	0.32406	0.05	0	-0.08021	0.32203
RCA LQ	0.06526	0.05074	1.81895	0.83954	0.05	0	-0.13586	0.26638
RCA L	0.95591	0.05074	26.64341	3.38E-06	0.05	1	0.75479	1.15703
RCA HC	0.14591	0.05074	4.0669	0.18313	0.05	0	-0.05521	0.34703